Characterizing Bupropion Metabolism, Pharmacokinetics and Drug-Drug Interaction Liability

Jennifer E. Sager

A dissertation

submitted in partial fulfillment of the

requirements for the degree of

Doctor of Philosophy

University of Washington

2016

Reading Committee:

Nina Isoherranen, Chair

Kent Kunze

Bhagwat Prasad

Program Authorized to Offer Degree:

Pharmaceutics

University of Washington

Abstract

Characterizing bupropion metabolism, pharmacokinetics and drug-drug interaction liability

Jennifer E. Sager

Chair of the Supervisory Committee:
Associate Professor, Nina Isoherranen
Pharmaceutics

Bupropion is a norepinephrine and dopamine reuptake inhibitor that is currently indicated for use as an antidepressant (Wellbutrin), a smoking cessation aid (Zyban) and a weight loss therapy in combination with naltrexone (Contrave). Bupropion is also the preferred sensitive in vivo CYP2B6 substrate recommended by the FDA (U.S. Food and Drug Administration Center for Drug Evaluation and Research (CDER), 2012). Efavirenz, the only other CYP2B6 sensitive substrate, is a time dependent inhibitor (Bumpus et al., 2006) and inducer (Kharasch et al., 2012) of CYP2B6, both of which limit its usefulness. Yet, despite its numerous clinical and research applications, there are many gaps in our knowledge of bupropion pharmacokinetics. First of all, bupropion elimination pathways have yet to be fully characterized. Secondly, bupropion causes strong in vivo CYP2D6 inhibition, yet the source of the interaction has not been identified. The

goal of this project was to characterize the metabolism of bupropion and elucidate the quantitative aspects of CYP2D6 interaction. Finally, using our knowledge of bupropion metabolism, changes in CYP2B6 and CYP2C19 activity during pregnancy were assessed by evaluating the changes in bupropion PK during pregnancy.

Because less than 30% of the bupropion dose is reportedly recovered as bupropion, OH-bupropion, threohydrobupropion and erythrohydrobupropion and their conjugates (Welch et al., 1987), additional metabolites were isolated from human urine and characterized via MS/MS, NMR and UV to allow for full characterization of bupropion elimination. Three novel metabolites 4-OH-bupropion, erythro-4-OH-hydrobupropion, and threo-4'-OH-hydrobupropion were isolated and identified. The relative contribution of each elimination pathway was assessed through in vitro incubations in human liver S9 fractions or recombinant P450. CYP2B6 and CYP2C19 were found to be quantitatively minor elimination pathways, contributing to only 23 and 5% of total bupropion clearance. The majority of bupropion is cleared via reduction to threohydrobupropion (66%) and erythrohydrobupropion (6%).

To elucidate the cause of the bupropion-CYP2D6 interaction, the inhibition potential the individual stereoisomers of bupropion and OH-bupropion was investigated but these stereoisomers were not predicted to account for the observed magnitude of the in vivo interaction. However, bupropion and all of its metabolites were found to significantly downregulate CYP2D6 on the basis of activity and mRNA levels. Inclusion of downregulation into static predictions resulted in accurate predictions of the observed drug interaction.

To evaulate the effects of pregnancy on bupropion pharmacokinetics, plasma concentrations and urine amounts of bupropion and its metabolites were measured both during pregnancy and post partum in 5 subjects. While plasma levels of bupropion and its metabolites

remained steady, a significant two-fold change in OH-bupropion formation clearance was observed in the third trimester, when compared to postpartum. This result suggested that CYP2B6 is substantially induced in pregnancy and thus caution should be exercised when prescribing CYP2B6 substrates to pregnant women.

TABLE OF CONTENTS

LIST OF FIGURES

LIST OF TABLES

ACKNOWLEDGEMENTS

I would like to thank my advisor, Dr. Nina Isoherranen for her guidance throughout my graduate studies. Under her mentorship, I had the opportunity to take on numerous, diverse research projects that constantly challenged and inspired me. I am incredibly grateful for both the support I received when I needed help and for the freedom I was given to design experiments, and learn from my mistakes. I would also like to thank Nina for her commitment to my professional development. As I considered potential career pathways, she made every effort to allow me to learn more about various opportunities, for which I am greatly appreciative.

Additionally, I would like to thank the other members of the Isoherranen lab. I am lucky to have had the opportunity to work with so many wonderful, engaged people during my time in graduate school.

I would also like to thank Dr. Kent Kunze, Dr. Bhagwat Prasad, Dr. Jash Unadkat, and Dr. Joanne Wang for serving on my committee. Their thoughtful questions and advice helped me to optimize my study aims and recognize the broader implications of my research.

DEDICATION

I would like to dedicate this dissertation to my parents, Joe and Kathy Sager as well as my sister, Becca. Thank you for your love and support throughout the years.

Chapter 1. INTRODUCTION

1.1 BUPROPION CLINICAL INDICATIONS

Bupropion is a norepinephrine and dopamine reuptake inhibitor as well as a nicotine receptor antagonist. Bupropion was originally developed to improve the selectivity and efficacy of antidepressant treatment while minimizing the side effects associated with selective serotonin reuptake inhibitors (SSRIs) and tricyclic antidepressants (Fava et al., 2005; Horst and Preskorn, 1998; Maxwell, 1985). In 1985, Bupropion HCl (Wellbutrin) was first approved for use as a treatment for major depression, after demonstrating comparable efficacy to typical antidepressants (Chouinard, 1983; Feighner et al., 1986, 1991; Mendels et al., 1983; U.S. Food and Drug Administration Center for Drug Evaluation, 1985; Weisler et al., 1994). Bupropion is considered to be an atypical antidepressant because it exhibits its antidepressant effects through dual inhibition of norepinephrine (NE) and dopamine (DA) reuptake, which sets it apart from other classes of antidepressants. Potentially due to its unique mechanism of action, addition of bupropion to SSRI or selective norepinephrine reuptake inhibitor (SNRI) therapy has been shown to aid in the treatment of refractive depression (Fatemi et al., 1999; Garcia-Pares, 2011; Marshall et al., 1995). Bupropion is also a viable alternative for patients who cannot tolerate other antidepressants because it lacks the anticholinergic, cardiac and sexual side effects of many SSRIs and tricyclic antidepressants (Dunner et al., 1998; Maxwell, 1985).

Following the entry of Wellbutrin to the market, clinical indications for bupropion have expanded to include smoking cessation (Zyban) (U.S. Food and Drug Administration Center for Drug Evaluation, 1997; U.S. Food and Drug Administration, Center for Drug Evaluation and Research, 2014) and weight loss (Contrave) (U.S. Food and Drug Administration, Center for Drug Evaluation and Research, 2014). Due to a higher prevalence of depression among smokers vs. non-smokers (Glassman et al., 1990; Hall et al., 1990) and a link between depression and relapse following smoking cessation

(Covey et al., 1990; Hall et al., 1994), efforts were made to understand whether antidepressants could be used as smoking cessation agents (Hurt et al., 1997). Of the drugs evaluated, bupropion immediate (IR) and sustained release (SR) formulations demonstrated efficacy (Ferry and Burchette, 1994; Hurt et al., 1997; Jorenby, 1999; Wilkes, 2008). In 1997, sustained release bupropion was approved as the first non-nicotine based smoking cessation therapy (Wilkes, 2008) and continues to be marketed under the trade name Zyban.

In 2016, bupropion was also approved as a weight loss aid in combination with naltrexone (U.S. Food and Drug Administration, Center for Drug Evaluation and Research, 2014). This combination therapy has been shown to result in significant weight loss when added to a modified diet and lifestyle (Apovian, 2015; Greenway et al., 2009; Sherman et al., 2016; U.S. Food and Drug Administration, Center for Drug Evaluation and Research, 2014; Wadden et al., 2011).

1.2 BUPROPION CLINICAL PHARMACOLOGY

Bupropion is available in immediate release, sustained release and extended release oral formulations. All three formulations are bioequivalent. The absolute bioavailability is unknown since there is no intravenous (IV) formulation. However, bupropion is rapidly and extensively absorbed. Following a single oral dose of ^{14}C-bupropion, the peak concentration of bupropion in plasma was reached by 2 hours (Findlay et al., 1981; Lai and Schroeder, 1983). Additionally, approximately 88% of the dose was recovered in the urine and the 10% recovered in the feces was predominantly made up of metabolites, suggesting near complete absorbtion of the ^{14}C bupropion-HCl tablet (Schroeder, 1983; Welch et al., 1987). No gender effects are observed in PK parameters after correcting for body weight. Additionally, linear increases in AUC have been reported for doses ranging from 50-250mg in both male and female subjects (Findlay et al., 1981; U.S. Food and Drug Administration Center for Drug Evaluation, 2013a).

Bupropion is extensively metabolized. Following a single oral dose of ^{14}C-bupropion, less than 1% of the dose was recovered as unchanged bupropion in urine or feces (Schroeder, 1983) and the AUC of ^{14}C-bupropion represented only 2% of the total ^{14}C AUC (Welch et al., 1987).

Bupropion has three known primary active metabolites; OH-bupropion, threohydrobupropion and erythrohydrobupropion (Figure 1.1.). In vivo, bupropion has an elimination half-life of approximately 21 hours and reaches steady state within a week. OH-bupropion has a similar half-life to bupropion (20 hours), while threo- and erythrohydrobupropion have longer half-lives (33 and 37 hours, respecitvely) than the parent drug (U.S. Food and Drug Administration Center for Drug Evaluation, 2001). Steady state concentrations of OH-bupropion and threohydrobupropion are 5-10 fold higher than bupropion while erythrohydrobupropion concentrations are comparable to the parent (U.S. Food and Drug Administration Center for Drug Evaluation, 1985). While relatively few studies have focused on the stereoselective metabolism or disposition of bupropion, bupropion is administered as a racemeate, and undergoes stereoselective metabolism to (R,R)-and (S,S)-OH-bupropion, (R,R)- and (S,S)-threohydrobupropion and (R,S) and (S, R)-erythrohydrobupropion (Figure 1.1). While the kinetics of the individual enantiomers of threo and erythrohydrobupropion have not been studied, bupropion and OH-bupropion have been found to exhibit stereoselective disposition (Kharasch et al., 2008). (R)-Bupropion and (R,R)-OH-bupropion exposures are approximately 3- and 44-fold higher than the (S)-bupropion and (S,S)-OH-bupropion, respectively (Kharasch et al., 2008).

1.3 Bupropion Metabolism And Its Use as a CYP2B6 Probe

The formation of OH-bupropion from bupropion has been proposed to be a selective marker of CYP2B6 activity (Faucette et al., 2000; Hesse et al., 2000). This is based on historical data from P450 supersome panels, in which CYP2B6 was been reported to be the main contributor to OH-bupropion formation, with minor contribution of CYP2E1 (Faucette et al., 2000; Hesse et al., 2000). This finding was futher supported by inhibition panel studies that demonstrated that bupropion hydroxylation was exclusively inhibited by an anti-CYP2B6 antibody (Faucette et al., 2000; Hesse et al., 2000).

Additionally, formation of OH-bupropion has been found to be correlated with CYP2B6 protein content and activity (Faucette et al., 2000; Hesse et al., 2000). However, these experiements were performed at concentrations of 50µM, 500 µM and 12mM bupropion, which are all supraphysiological considering the circulating concentrations of bupropion at steady state range between 0.2 and 1µM (U.S. Food and Drug Administration Center for Drug Evaluation, 2013a). Thus it remains unclear whether bupropion hydroxylation is a reliable marker of CYP2B6 activity at physiologically relevant concentrations. It is important for this question to be addressed because bupropion is currently the preferred sensitive in vitro and in vivo CYP2B6 substrate recommended by the FDA (U.S. Food and Drug Administration Center for Drug Evaluation and Research (CDER), 2012). Efavirenz is currently the only alternative CYP2B6 probe, yet its utility is limited due to the fact that it is an inducer and time dependent inhibitor of CYP2B6 (Bumpus et al., 2006; Kharasch et al., 2012). Establishing the percent contribution of CYP2B6 to OH-bupropion formation intrinsic clearance is critical to determining if in vitro bupropion hydroxylation is a reliable measure of CYP2B6 activity. Additionally, characterization of OH-bupropion elimination is needed in order to determine whether bupropion can be used to probe in vivo CYP2B6 activity. Currently, either the racemic OH-bupropion to bupropion AUC ratio or the ratio of (S,S)-OH-bupropion to S-bupropion is used. The later has been proposed to be prefereable due to the fact that that (S,S)-OH-bupropion exhibits formation rate limited kinetics (Kharasch et al., 2008). However, the use of this AUC ratio to detect changes in CYP2B6-mediated formation clearance assumes that the metabolite clearance remains constant (Equation 1.1).

$$\frac{AUC_m}{AUC_p} = \frac{Cl_f}{CL_m} \qquad \text{Equation 1.1}$$

While the pathways involved in OH-bupropion elimination have not been fully characterized, glucuronide and sulfate conjugates have been detected in urine in greater quantities than unchanged OH-bupropion (Zhu et al., 2014). Thus, in cases where OH-bupropion metabolism may potentially be altered, use of a metabolite to parent AUC ratio is not a dependable marker of CYP2B6 activity. Instead, the in vivo OH-bupropion formation clearance may be better estimated by accounting for the ratio of the

amount of OH-bupropion ($A_{e,\ OH\text{-}bupropion}$) and its metabolites ($A_{e,\ sequential\ metabolites}$) excreted to the AUC of bupropion (Equation 1.2).

$$CL_f = \frac{A_{e,\ hydroxybupropion} + A_{e,\ sequential\ metabolites}}{AUC_{bupropion}} \qquad \text{Equation 1.2}$$

This, however, assumes that all of the subsequent metabolites can be accounted for. Deeper understanding of bupropion elimination and mass balance is therefore needed in order to evaluate the use of the various bupropion measurements as CYP2B6 probes.

Recent work has suggested a role of 11β-hydroxysteroid dehydrogenase-1 in the formation of threohydrobupropion (Connarn et al., 2015; Meyer et al., 2013; Skarydova et al., 2013) and erythrohydrobupropion. In liver S9 fractions, approximately 90% of threo- and erythrohydrobupropion formation has been reported to be inhibited by a selective 11β-hydroxysteroid dehydrogenase-1 inhibitor, carbenoxolone (Connarn et al., 2015). Some formation of threohydrobupropion formation has also been reported in intestinal S9 fractions, yet the intestinal formation has been attributed to aldoketoreductase-7 due to potent inhibition of threohydrobupropion formation by flufenamic acid (Connarn et al., 2015). Despite the recent work that has been conducted to better understand bupropion's reduction pathways, systematic kinetic studies have not been conducted to allow assessment of the fractional contribution of the reductive pathways to bupropion elimination.

CYP2C19 has also been proposed to play a role in bupropion metabolism. Involvement of CYP2C19 in the formation of OH-bupropion has been proposed based on supersome panel data (Chen et al., 2010). Yet the relative contribution is thought to be minor since OH-bupropion formation correlates with CYP2B6 activity, and inhibition with a selective CYP2B6 inhibitory antibody resulted in 92% inhibition of OH-bupropion formation (Chen et al., 2010). CYP2C19 has been suggested to be the main enzyme involved in the formation of additional, uncharacterized hydroxylation products of bupropion (Chen et al., 2010). Yet, only CYP3A4, CYP2C19 and CYP2B6 were assessed in this study, and thus it is possible that other enzymes could be involved in the formation of these additional metabolites. Despite the lack of conclusive in vitro data regarding the involvement of CYP2C19 in

bupropion metabolism, there is in vivo evidence to suggest that CYP2C19 is a relatively important elimination pathway for bupropion. In CYP2C19 intermediate metabolizers, the AUC of bupropion was found to be significantly increased (Zhu et al., 2014), with an estimated f_m of 0.13. Hence, in CYP2C19 extensive metabolizers, the percent contribution of CYP2C19 to bupropion clearance may be as high as 25%. CYP2C19 genotype was also found to impact the exposure to erythrohydrobupropion and threohydrobupropion, causing 22% and 28% increases in their steady state exposures, respectively.

1.4 The Importance of Bupropion's Metabolites in Clinical Safety and Efficacy

Much of bupropion's pharmacological acitivty and toxicity is attributed to its metabolites. Bupropion's antidepressant activity is attributed to inhibition of dopamine and norepinephrine reuptake by bupropion and its metabolites. In vitro, bupropion and its metabolites, hydroxybupropion and threohydrobupropion inhibit NE and DA reuptake (Damaj et al., 2004; Fava et al., 2005; Musso et al., 1993; Stahl et al., 2004). The inhibition appears to be enantioselective, with S-bupropion having a 2 fold lower IC_{50} for DA and NE transporters than R-bupropion (Musso et al., 1993). Furthermore, the S,S-enantiomer of hydroxybupropion was found to be a much more potent inhibitor of both dopamine and norepinephrine uptake than R,R-hydroxybupropion (Carroll et al., 2011; Damaj et al., 2004). And in fact, the S,S-hydroxybupropion IC_{50} value for the norepinephrine transporter was an order of magnitude lower than that of bupropion and the IC_{50} value for the dopamine transporter was comparable to that of bupropion in stably transfected HEK293 cell. In vitro DA and NE inhibition data is further supported by in vivo studies. Numerous studies in rodent models have demonstrated that bupropion can cause dose dependent decreases in dopamine and norephinephrine neuronal firing as well as increased synaptic and brain concentrations of dopamine and norepinephrine (Ascher et al., 1995a; Nomikos et al., 1989, 1992). In humans, notable dopamine receptor occupancy as high as 25% has been recorded

following steady state bupropion dosing (Learned-Coughlin et al., 2003; M. Árgyelán, 2006; Stahl et al., 2004).

The mechanism of bupropion's smoking cessation activity remains unclear. It is thought that bupropion may work partially through modulating addiction through altering dopamine and norepinephrine signaling. Additionally, part of the smoking cessation effects of bupropion is attributed to antagonism of nicotinic acetylcholine receptors (nAChRs). In vitro studies directly evaluating nAChR inhibition have only been performed for bupropion and the enantiomers of OH-bupropion. Threohydrobupropion and erythrohydrobupropion have been shown to partially substitute for nicotine in mouse behavioral studies, but their ability to inhibit nAChRs has not been directly tested in vitro (Bondarev et al., 2003). Bupropion and OH-bupropion are reported to be noncompetitive antagonists (Carroll et al., 2011; Damaj et al., 2004; Slemmer et al., 2000). Bupropion is the most potent inhibitor of nAChR α3-β4, with an IC_{50} 1.8 μM, while S,S-OH-bupropion and R,R-OH-bupropion have IC_{50} values of 10 and 6.5 μM, respectively. S,S-OH-bupropion has the lowest IC_{50} value (3.3 μM) for nAChR α4-β2 while bupropion (12 μM) and R,R-OH-bupropion show much weaker inhibition potency. R,R-OH-bupropion and bupropion are equally potent inhibitors of α4-β4 (IC_{50} 7.6 and 7.9 μM, respectively), while S,S-OH-bupropion has a comparatively high IC_{50} value of 28 μM) (Carroll et al., 2011; Damaj et al., 2004). In mouse models, S,S-OH-bupropion has been reported to be a more potent nicotine antagonist than R-R-OH-bupropion and bupropion (Damaj et al., 2004). In tail flick, hot-plate, motility and hypothermia assays, the AD_{50}'s of S,S-OH-bupropion (0.2, 1.0, 0.9, 1.5 mg/kg) were consistently lower than that of bupropion (1.5, 5.5. 8.2. 19.4 mg/kg) and R,R-bupropion (2.5, 10.3, >20, >20 mg/kg), respectively. The S,S- enantiomer was also more important for suppressing nicotine reward and withdrawal symptoms (Damaj et al., 2010) as well as chronic nicotine tolerance in mouse model (Grabus et al., 2012). Since bupropion and S,S,-OH-bupropion circulate at similar concentrations in humans, S,S-OH-bupropion is likely to play a larger role than bupropion in smoking cessation. However, following a single oral dose R,R-OH-bupropion has a C_{max} 18 fold higher than that of S,S-OH-bupropion. As a result, its contribution to smoking cessation outcomes may be equal to that of S,S-

OH-bupropion. In human studies, circulating OH-bupropion levels following bupropion treatment have been reported to be predictive of smoking cessation outcomes. (Zhu et al., 2012a). Yet no studies have assessed the relationship between the concentrations of the individual OH-bupropion enantiomers and rates of smoking cessation.

1.5 Bupropion Mass Balance And Uncharacterized Metabolites

Although OH-bupropion, threohydrobupropion and erythrohydrobupropion are the main circulating metabolites, the amount of these metabolites and their conjugates excreted in urine only account for 23% of the oral dose (Welch et al., 1987). Another 22% of the dose hase been reported to be excreted in urine as m-chlorohippuric acid, a glycine conjugate of m-chlorobenzoic acid (Welch et al., 1987). Yet, nearly 40% of the dose is recovered in urine as unidentified polar metabolites (Welch et al., 1987).

Additional metabolites have been detected in vitro and in vivo, and their structures have tentatively been proposed based on mass spectral data. Proposed structures of the novel metabolites are shown in Figure 1.2, along with potential formation pathways. In vitro, NADPH-dependent formation of multiple hydroxylation products from bupropion have been reported (Chen et al., 2010; Taylor, 1995). From incubation of bupropion in human liver S9 fractions, three mono-hydroxylation products and a minor dihydroxylation product have been reported (Taylor, 1995). The major metabolite, based on mass spectroscopic response, was determined to be the pharmacologically active OH-bupropion, which results from hydroxylation of the *t*-butyl group. The other two mono-hydroxylated metabolites were proposed to be the result of hydroxylation outside of the tert-butyl group. This was based on data showing the loss of 56 from the parent ion ([M+H] 256), resulting in an [M+H] 200 ion which is consistent with the loss of an intact tert-butyl group. Had the hydroxylation occurred in the *t*-butyl group, a loss of water would be required prior to the loss of an intact *t*-butyl group, resulting an [M+H] 184 ion instead of an [M+H] 200 ion . The short retention time and mass spectral fragmentation pattern suggested that one was a phenolic species while the other was proposed to result from hydroxylation on

the methyl group and the aromatic ring. Chen et al. also reported the formation of multiple hydroxylated species in vitro (Chen et al., 2010). Four monohydroxylated species were observed after incubation of bupropion in HLM (Chen et al., 2010). In addition to the t-butyl hydroxylation product, a methyl group hydroxylation and two aromatic hydroxylation products were proposed based of their mass spectral fragmentation patterns. Additionally, LC/TOFMS analysis of human urine has suggested the presence of reduced and hydroxylated metabolites, a glucuronide of a dihydroxylation product as well as conjugates of proposed aromatic hydroxylation product(s) (Petsalo et al., 2007). The structures of these analytes were tentatively proposed based on accurate mass data (Petsalo et al., 2007). The reduced and hydroxylated metabolite was proposed to be the result of reduction of the ketone and hydroxylation of the aromatic ring based on the m/z 258→184, indicating a loss of a hydroxylated t-butyl group.

To date, the structures of the reduced and hydroxylated metabolite(s) and alternative monohydroxylation products have not been systematically characterized, nor are authentic standards available. Furthermore, it is not known whether the reduced and hydroxylated metabolite(s) observed in vivo are products from OH-bupropion or from threo/erythrohydrobupropion.

1.6 BUPROPION IN PREGNANCY

Major depression and smoking cessation treatment are common among pregnant women. In a study conducted across 10 obstetrics clinics throughout Michigan, 20.4% of the pregnant women reported having elevated depressive symptoms (Marcus et al., 2003). Between 2000 and 2010 12% of women reported quitting smoking before the 3rd trimester while another 12% continued to smoke (Tong et al., 2013). Due to the adverse consequences of untreated depression and smoking on fetal development and maternal health, women are encouraged to seek treatment for depression and nicotine addiction (Coleman, 2007; Marcus et al., 2003; Tong et al., 2013; U.S. Department of Health and Human Services., 2014), While treatment can be successful without pharmacotherapies, some women need to use antidepressants and smoking cessation medications. Thus, bupropion is used during

pregnancy as an antidepressant and as a smoking cessation aid. Hospital records from a randomly selected pregnancy population indicate that approximately 0.5% of the women were exposed to bupropion during pregnancy (Alwan et al., 2010). However, little is known about bupropion disposition or pharmacodynamics in pregnant women.

Studies of bupropion in pregnant rats and rabbits did not suggest teratogenicity, however, there were slight increases in fetal malformations and decreased fetal weight when rabbits received doses equivalent to the maximum expected human dose (U.S. Food and Drug Administration Center for Drug Evaluation, 2013a). Retrospective analysis of health care data failed to identify any significant differences in the prevalence of congenital malformations between women exposed to bupropion during pregnancy and the normal population (Cole et al., 2007). Yet when malformations are stratified by type, a positive association was found between maternal bupropion use and neonatal left outflow tract heart defects (Alwan et al., 2010). In absence of adequate control studies, there is not sufficient data to determine that bupropion is safe for use during pregnancy. As a result, bupropion is categorized as a Pregnancy Category C drug, indicating that it should only be used in pregnancy if the benefits of treatment outweigh the potential risks to the developing fetus (U.S. Food and Drug Administration Center for Drug Evaluation, 2013a).

Limited in vitro and in vivo evidence suggest that bupropion pharmacokinetics is likely to be altered during human pregnancy. CYP2B6 is implicated in the formation of OH-bupropion. In vitro and in vivo data suggest that this pathway is induced during pregnancy, which could lead to increased exposure to OH-bupropion, and thus result in changes in pharmacological response and toxicity. Estrogens have been shown to play an important role in CYP2B regulation in rodent models (Koh et al., 2012; Nemoto and Sakurai, 1995; Yamada et al., 2002; Yamamoto et al., 2001). Additionally, in human hepatocytes, estradiol has been reported to induce CYP2B6 activity and mRNA expression. (Dickmann and Isoherranen, 2013). Based on concentrations of estradiol in pregnancy (Abduljalil et al., 2012; O'Leary et al., 1991; Soldin et al., 2005) and in vitro induction parameters, CYP2B6 expression is predicted to increase during pregnancy by 1.1, 1.4 and 1.9 fold in the first, second and third trimesters

(Dickmann and Isoherranen, 2013; Ke et al., 2014). The results of clinical studies with methadone and sertraline have suggested the potential for CYP2B6 induction but a study evaluating nevirapine pharmacokinetics revealed no change in nevirapine clearance in pregnancy (Capparelli et al., 2008a; Freeman et al., 2008; Pond et al., 1985). These studies are limited by the fact that the substrates all have multiple routes of elimination (Erickson et al., 1999; Obach et al., 2005; Totah et al., 2008; Wang and DeVane, 2003). Because it is unclear how each pathway is effected in pregnancy, clearance changes are not reliable markers of changes in CYP2B6 activity during pregnancy. In vivo studies with sensitive CYP2B6 substrates are needed in order to provide further evidence of the impact of pregnancy on enzyme expression and activity.

CYP2C19, which has been reported to play a role in bupropion elimination (Zhu et al., 2014), is also expected to be altered in pregnancy. A study evaluating changes in proguanil pharmacokinetics in pregnancy suggests that there may be a 60% decrease in CYP2C19 activity in T2 and T3 as compared to postpartum levels (Ke et al., 2014). However, in vivo studies with sensitive CYP2B6 and CYP2C19 substrates have not previously been conducted in order to provide further evidence of the impact of pregnancy on enzyme expression and activity.

1.7 HYPOTHESIS AND AIMS

Despite bupropion's numerous clinical and research applications, its pharmacokinetics have been incompletely characterized. Bupropion has several metabolites that have not been definitively identified, nor have their formation pathways been characterized. Furthermore, the elimination pathways of bupropion have yet to be fully characterized stereoselectively and bupropion's utility as a CYP2B6 probe has not been adequately evaluated. Finally, bupropion causes strong in vivo CYP2D6 inhibition, yet the source of the interaction has not been identified. The overall hypothesis of this thesis was that the relative contribution of the bupropion elimination pathways and the magnitude of the bupropion-CYP2D6 interaction could be elucidated through thorough characterization of bupropion's stereoselective metabolism and in vivo pharmacokinetics. We addressed this hypothesis in four aims:

Aim 1. Identify additional metabolites of bupropion from human urine and determine their quantitative importance to bupropion elimination (Chapter 2),

Aim 2. Characterize the stereoselective metabolism of bupropion via incubations in recombinant enzyme systems and human liver S9 fractions (Chapter 3)

Aim 3. Quantitatively explain the in vivo CYP2D6 inhibition by bupropion through extensive characterization of stereoselective disposition of bupropion and its metabolites, in vitro inhibition and effects of bupropion on CYP2D6 transcription (Chapter 4)

Aim 4. Assess the effects of pregnancy on CYP2C19 and CYP2B6 activity using bupropion as the probe (Chapter 5).

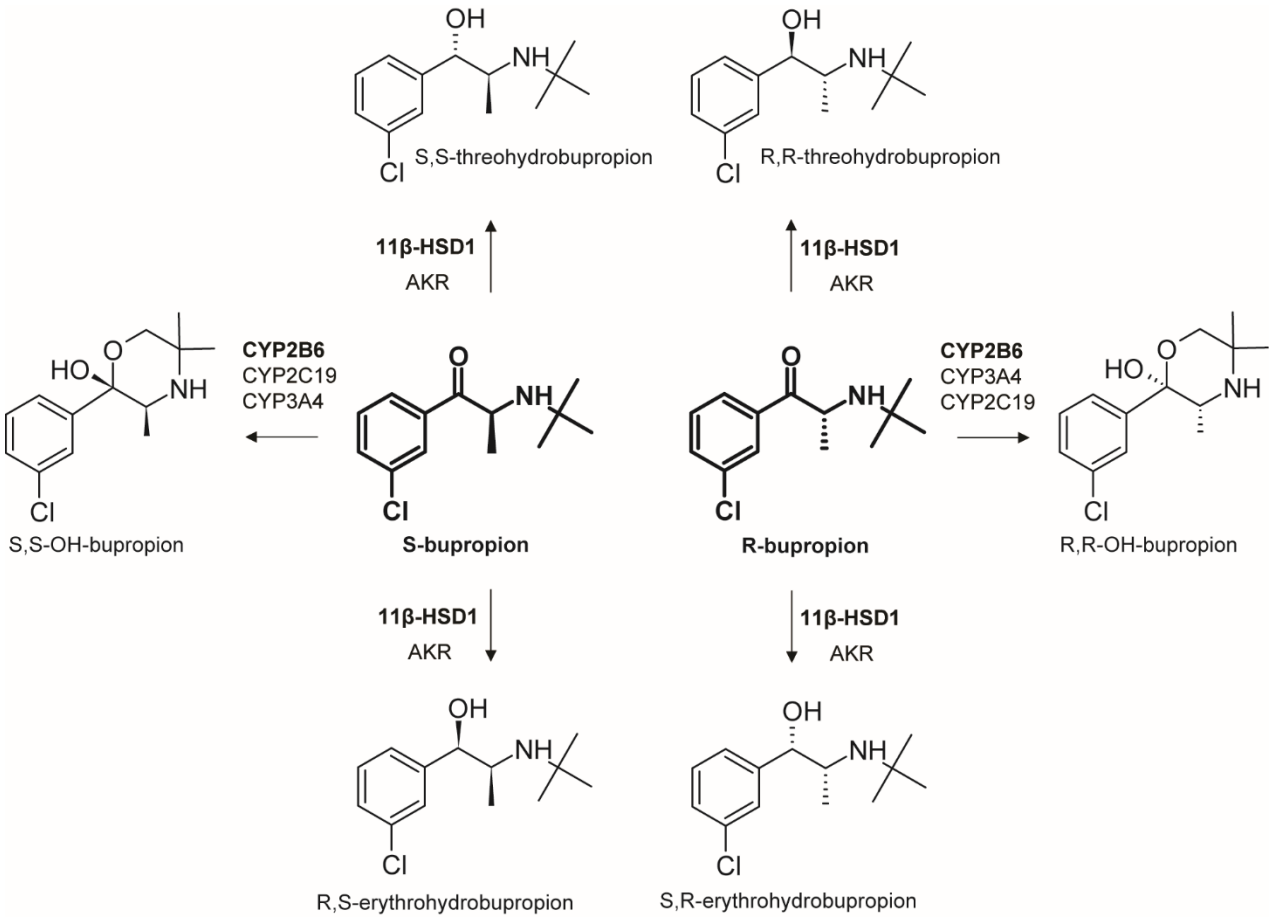

Figure 1.1. Structures of the enantiomers of bupropion and its metabolites as well as the enzymes proposed to be involved in metabolite formation. AKR is Aldoketoreductase, 11β-HSD1 is 11β-hydroxysteroid dehydrogenase.

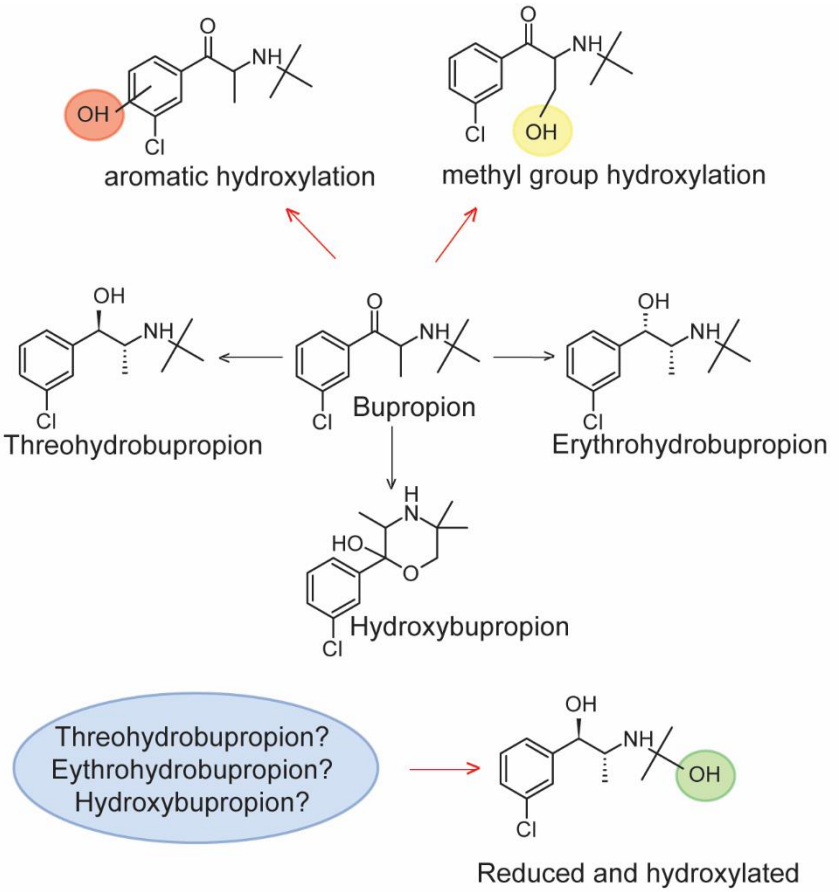

Figure 1.2. Bupropion metabolism scheme and proposed structures of new metabolites. Circles indicate proposed hydroxylation sites. The oval denotes potential precursor for the reduced and hydroxylated metabolite.

Chapter 2.

IDENTIFICATION AND STRUCTURAL CHARACTERIZATION OF THREE NEW METABOLITES OF BUPROPION IN HUMANS

This chapter was published, in part in *ACS Med. Chem. Lett.*, 2016, *7* (8), pp 791–796

2.1 ABSTRACT

Bupropion is a widely used antidepressant, smoking cessation aid and the recommended CYP2B6 probe drug. However, current understanding of bupropion elimination pathways is limited. Bupropion has three active circulating metabolites, OH-bupropion, threohydrobupropion and erythrohydrobupropion, but these metabolites and their conjugates represent only 20% of the dose recovered in urine, and the majority of the elimination pathways of bupropion result in uncharacterized metabolites. The aim of this study was to determine the structures of the uncharacterized bupropion metabolites using human clinical samples and in vitro incubations. Three metabolites, 4'-OH-bupropion, erythro-4'-OH-hydrobupropion and threo-4'-OH-hydrobupropion were detected in human liver microsomal incubations and were isolated from human urine. The structures of the metabolites were confirmed via comparison of UV absorbance, NMR spectra and mass spectral data to those of synthesized standards. In total, these metabolites represented 24% of the drug related material excreted in urine.

2.2 INTRODUCTION

Bupropion is a norepinephrine and dopamine reuptake inhibitor that is currently indicated for use as an antidepressant (Wellbutrin) (U.S. Food and Drug Administration Center for Drug Evaluation, 2013b), a smoking cessation aid (Zyban) (U.S. Food and Drug Administration Center for Drug Evaluation, 1997) and a weight loss therapy in combination with naltrexone (Contrave) (U.S. Food and Drug Administration, Center for Drug Evaluation and Research, 2014). Bupropion is also the preferred sensitive in vivo CYP2B6 probe substrate recommended by the FDA (U.S. Food and Drug Administration Center for Drug Evaluation and Research (CDER), 2012). Yet, despite its numerous clinical and research applications, the factors contributing to observed interindividual variability in bupropion disposition and in its safety and efficacy is poorly understood (Fava et al., 2005; Hill et al., 2007; Rissmiller and Campo, 2007; Woodcock et al., 2012).

In vivo, bupropion undergoes extensive metabolism, with less than 1% of the dose excreted unchanged in urine after a single oral dose (Findlay et al., 1981; Schroeder, 1983). Much of the pharmacological activity and toxicity of bupropion is attributed to the three known primary metabolites: OH-bupropion, threohydrobupropion and erythrohydrobupropion (Figure 2.1) (Ascher et al., 1995b; Bondarev et al., 2003; Carroll et al., 2011; Damaj et al., 2004, 2010; Fava et al., 2005; Musso et al., 1993; Nomikos et al., 1989; Stahl et al., 2004). All of these metabolites circulate at concentrations higher than bupropion (Benowitz et al., 2013; U.S. Food and Drug Administration Center for Drug Evaluation and Research, 2003). OH-bupropion appears to be the main contributor to the efficacy of bupropion in smoking cessation, while both OH-bupropion and threohydrobupropion are suggested to be primarily responsible for the anti-depressant activity of bupropion (Bondarev et al., 2003; Damaj et al., 2004; Jefferson et al., 2005; Zhu et al., 2012b). All three metabolites also have markedly lower LD_{50} values than bupropion (Welch et al., 1987) and cause dose dependent increases in convulsion risk in mouse models (Silverstone et al., 2008). Thus, it is possible that additional, yet unidentified metabolites of bupropion may also have pharmacological and toxicological activity and contribute to the effects of bupropion in vivo. Such metabolites and novel metabolic pathways may also contribute to the interindividual variability in bupropion efficacy and toxicity. Thus better characterization of the elimination pathways of bupropion is necessary.

Current knowledge of bupropion metabolism is incomplete. Bupropion, OH-bupropion, erythrohydrobupropion, threo-hydrobupropion and their conjugates (N- and O-glucuronides and sulfates (Gufford et al., 2016; Petsalo et al., 2007)) make up only 23% of the drug related material excreted in urine (Welch et al., 1987) with an additional 22% of the drug related material excreted as *m*-chlorohippuric acid (Welch et al., 1987). The remaining 36 % of the dose is excreted in urine as uncharacterized polar metabolites. Possible structures of some of these metabolites such as aromatic hydroylation products or products of hydroxylation of the methyl group (potential sites indicated by red arrows in Figure 2.1) have been proposed based on mass spectral data from in vitro incubations and urine samples from clinical

subjects (Petsalo et al., 2007). Furthermore, analysis of human urine samples revealed the presence of a reduced and hydroxylated metabolite (Chen et al., 2010; Petsalo et al., 2007; Taylor, 1995). However, the structures of the additional metabolites and their relative importance in circulation or overall elimination of bupropion are unknown. The goal of this study was to characterize the major unknown metabolites of bupropion and to generate synthetic standards of these metabolites for quantitative characterization of bupropion elimination pathways. In the future, these metabolites can be evaluated for their potential pharmacological and toxicological activity.

2.3 MATERIALS AND METHODS

2.3.1 Materials and General Methods

Bupropion, hydroxybupropion, threohydrobupropion, erythrohydrobupropion, bupropion-d_9, hydroxybupropion-d_6, threohydrobupropion-d_9, dextrorphan glucuronide and imipramine glucuronide were purchased from Toronto Research Chemicals (Ontario, Canada). Glacial acetic acid, hydrochloric acid, formic acid, sodium hydroxide, sodium carbonate and sodium borohydride, were purchased from Sigma-Aldrich (St. Louis, MO). NMR solvents were purchased from Cambridge Isotope Labs (Tewksbury, MA). 1-(3-Chloro-4-methoxyphenyl)propan-1-one was obtained from Atlantic Research Chemicals (Bude, Cornwall, UK). Methylene chloride and diethyl ether, optima grade acetonitrile, methanol, and water were purchased from Fisher Scientific (Waltham, MA). Human liver microsomes (HLM) and cytosolic fractions from four donors were obtained from the University of Washington Human Liver Bank (Seattle, WA). All donors were CYP2C19 and CYP2D6 extensive metabolizers. HLMs and cytosol were prepared using standard ultracentrifugation methods and pooled before use. NMR spectra were acquired using a 500 MHz Bruker NMR spectrometer. UV absorbance was measured using a Nanodrop 2000c (Thermo Scientific, Waltham, MA) and HRMS was performed on a Waters Synapt G1 QTOF (Milford, MA).

2.3.2 Clinical Study.

The study was approved by the University of Washington Institutional Review Board. Five female subjects were enrolled in the study after providing written informed consent. The subjects were taking bupropion daily for therapeutic reasons. Urine was collected over one dosing interval and a single blood sample was collected to measure steady state bupropion concentrations. Urine from one subject taking 300 mg of bupropion daily was used for metabolite isolation.

2.3.3 In vitro Incubations in Subcellular Fractions.

Incubations were performed in 100 mM potassium phosphate buffer (KPi; pH 7.4), in a final volume of 100 µl. Bupropion, hydroxybupropion (OH-bupropion), threohydrobupropion, erythrohydrobupropion, 4'-OH-bupropion or threohydrobupropion-d_9 were incubated at 10 µM concentration with 0.1 mg/mL HLM or cytosol (not for threohydrobupropion-d_9). Following a 5 min preincubation at 37 °C, reactions were initiated by adding 10 µL NADPH (1 mM, final concentration). Reactions were terminated after 20 minutes by adding an equal volume of acetonitrile containing 100 nM hydroxybupropion-d_6 internal standard.

2.3.4 Detection of Metabolites in Incubation and Urine Samples Using LC/MS/MS.

Bupropion metabolites were detected in HLM, or cytosol incubations using an API5500 QTRAP® Q-LIT mass spectrometer (AB Sciex, Foster City, CA) coupled to an Agilent 1290 UHPLC (Agilent, Santa Clara, CA). The turbo ion spray interface was operated in positive ion mode. Samples were centrifuged for 15 (incubations) or 40 (urine and plasma) minutes at 3000 g and the supernatant was transferred to a 96 well plate for LC-MS analysis. An Agilent ZORBAX XDB-C18 column (150x4.6mm, 5µm) was used to separate the analytes with an 0.8 mL/min isocratic flow of mobile phase consisting of 35% methanol with 0.4% formic acid, and 65% water with 0.04% formic acid (Connarn et al., 2015). The presence of reduced and hydroxylated metabolites, dihydroxylation products and direct hydroxylation products of bupropion were detected first by monitoring selected parent-fragment

MS/MS transitions (MRM transitions) adapted from previous studies (Chen et al., 2010; Petsalo et al., 2007). Full MS/MS fragment ion spectra were collected using the same MRM transitions as the survey scan for parallel information dependent acquisition via an enhanced product ion (EPI) scan of $[M+H]^+$ ions m/z 256, 262, 242, 258 and 267. The collision energy was set to 19 V for all MRM transitions and 40 for all EPI scans**.** The presence of metabolites in preparative HPLC fractions was initially screened using an HPLC method consisting of an Agilent ZORBAX XDB-C18 column (50 x 2.1 mm, 5µm) and a mobile phase consisting of 0.1% formic acid (A) and ACN (B). A flow rate of 0.3 mL/min was used with a gradient elution starting at 10% B, increasing to 95% B by 3.5 minutes, held at 95% until 5 minutes, then allowed to re-equilibrate to initial conditions by 7 minutes. The mass spectrometer settings were identical in this method as described above. For detection of bupropion and its metabolites, the following MRM mass transitions (*m*/*z*) were used: 240→184 (bupropion), 249→189 (bupropion-d_9), 256→238 (OH-bupropion), 262→244 (OH-bupropion-d_6), 242→168 (threo- and erythrohydrobupropion), 251→168 (threohydrobupropion-d_9), metabolites M1-M3 (256→182, 256→200), metabolites M4-M7 (258→184), and metabolites M6-d_9 and M7-d_9 (267→184 and 266→184). Proposed structures of M1-M7 are shown in Table 2.1.

2.3.5 Analysis of Bupropion Metabolites in Human Urine.

Urine samples from 5 subjects taking bupropion chronically were analyzed to identify bupropion metabolites excreted in urine. The samples were prepared by adding 140 µL 3:1 acetonitrile:methanol into 60 µL urine. To establish the importance of conjugation (O-glucuronidation, N-glucuronidation, sulfate conjugation) in the elimination of bupropion metabolites, urine was either left untreated or acidified for deconjugation. For acidified samples, 500 µL 6 N HCl was added to an equal volume of urine and the samples were incubated overnight at 90 °C. The sample was then neutralized via the addition of 6N NaOH. For the control samples, 50 µL urine was added to 150 µL water. 10 µL of the samples were protein precipitated with 190 µL 3:1 acetonitrile:methanol. Deconjugation of 100 nM dextrorphan glucuronide, imipramine N-glucuronide or 200 µM 4'-nitrocatechol sulfate spiked in blank

urine was used as positive controls for O-glucuronide, N-glucuronide and sulfate deconjugation, respectively. Samples were centrifuged at 3000 g for 40 minutes and the supernatants were transferred to a 96-well plate and analyzed by LC-MS.

2.3.6 Detection of Imipramine N-glucuronide and Dextrorphan-O-glucuronide.

An LC/MS/MS system consisting of API4500 triple quadrupole mass spectrometer (AB Sciex, Foster City, CA) coupled with an LC-20AD ultra-fast liquid chromatography system (Shimadzu Co., Kyoto, Japan) was used for detection of Imipramine N-glucuronide and dextrorphan O-glucuronide. Positive ion spray mode was used for detection of imipramine N-glucuronide while negative ion spray mode was used for the detection of dextrorphan O-glucuronide. An Agilent ZORBAX XDB-C18 column (50 x 2.1 mm, 5µm) and a mobile phase consisting of 0.1% formic acid (A) and ACN (B) were used. The flow rate was 0.3 mL/min, with a gradient elution starting at 10% B, increasing to 95% B by 3.5 minutes, held at 95% until 4 minutes, then allowed to re-equilibrate to initial conditions by 6 minutes. The retention time and m/z for dextrorphan-O-glucuronide were 1.3 min and 432→256, respectively. The retention time and m/z for imipramine- N-glucuronide were 3.1 min and 457→208, respectively.

2.3.7 Isolation and Purification of Metabolites from Urine.

Urine (500 mL) from one subject taking 300mg bupropion daily was deconjugated by adding an equal volume of 6 N HCl and incubating at 90 °C overnight. The mixture was placed on ice and titrated to pH 8.6 with 12 N NaOH. Bupropion metabolites were extracted with ethyl acetate, and the ethyl acetate extracts were evaporated using a rotary evaporator (BUCHI, Flawil, Switzerland). The residue was resuspended in 10 mL of methanol and then passed through a 0.45 µM syringe filter. The filtered sample was evaporated under nitrogen and the sample was resuspended first in 1 mL methanol followed by addition of 1 mL H_2O. Metabolite M1, and the combination of M4 and M6, were isolated from this extract using a BioLogic DuoFlow 10 System (BioRad, Hercules, CA) FPLC and an Agilent XDB-C18

PrepHT cartridge (21.2 µm x 150mm, 5µm) coupled to a XDB-C18 PrepHT 5 µm guard cartridge (Agilent Technologies, Santa Clara, CA). An isocratic method consisting of 35% methanol and 0.04% formic acid was run at a flow rate of 10 mL/min for 40 min. The injection volume was 500 µL. Fractions were collected as 10 mL fractions from 0-30 mL, 5mL fractions from 30 to 300 mL, 10 mL fractions from 300 to 400 mL using a BioFrac fraction collector from BioRad. Following collection, 998 µL 1:3 methanol:acetonitrile was added to a 2 µL aliquot of each fraction and the fractions were analyzed by LC/MS/MS for the presence of M1 (4'-OH-bupropion), and M4+M6 (erythro/threo-4'-OH-bupropion). Fractions containing analytes of interest were pooled and dried under reduced pressure using a vacuum concentrator (Speed vac, Thermo Savant). Samples were resuspended in 200 µL methanol and further purified using an Agilent XDB-C18 (4.6 µm x 150mm, 5µm) column coupled to an Agilent 1200 series HPLC with a UV detector. An isocratic mobile phase consisting of 25% MeOH with 0.04% formic acid and 75% 0.04% formic acid was used at a flow rate of 0.8 mL/min. Fractions were collected at 2.5-3.5 min (erythro/threo-4'-OH-bupropion) and 4.5-5 min (4'-OH-bupropion). The compounds were then dried under reduced pressure and resuspended in water. The pH was adjusted to 2 with optima grade formic acid and remaining contaminants removed by liquid-liquid extraction with dichloromethane. The aqueous layer was then adjusted to pH 8.6 and extracted with ethyl acetate and dried under nitrogen in a 40°C water bath. The resulting pure compounds were analyzed by UV, HRMS and NMR. Compounds were determined to be >95% pure by the HPLC method described above.

2.3.8 4'-OH-Bupropion HBr Synthesis.

This compound was synthesized by the method of Butz, et al. (Butz et al., 1981) from 1-(3-chloro-4-methoxyphenyl)-1-propanone with minor modifications. The initial bromination and amine displacement processes were carried out as described in a recent synthesis of bupropion (Perrine et al., 2000). The boron tribromide demethylation was performed as previously described (Butz et al., 1981) except the reaction mixture was treated with methanol affording the HBr salt of the product. The resulting compound was determined to be >95 percent pure using HPLC-UV.

2.3.9 Threo/erythro-4'-OH-hydrobupropion.

These compounds were synthesized using a modification of the reduction method reported by Luche (Luche, 1978). 4'-OH-bupropion HBr was suspended in 5 mL of water and the pH adjusted to 8.6 with aqueous ammonia. The free base was obtained by extracting with 5 volumes ethyl acetate and evaporation. To a solution of 4'-OH-bupropion (15 mg, 60 μmole) in methanol, $CeCl_3 \cdot 7H_2O$ (22 mg, 60 μmole). Sodium borohydride (23 mg, 600 μmole) was added in 5 portions over two hours, while stirring at room temperature. Reaction progress monitored by HPLC until no additional product formation was observed. The solvent was evaporated under nitrogen and the residue resuspended in 10 mL of water. The pH was adjusted to 8.6 with aqueous ammonia, and the product extracted with ethyl acetate (5 x 10 mL). The combined ethyl acetate extracts were evaporated under nitrogen and the product resuspended in water. The mixture of threo- and erythro-4'-OH-hydrobupropion was purified by solid phase extraction (SPE) (C18, Varian). Following loading, the SPE cartridge was rinsed with water, and the product eluted with increasing concentrations of methanol (10% increments from 10-100%). The mixture of threo- and erythro-4'-OH-hydrobupropion (1:3) eluted when washed with 50% methanol.

2.4 RESULTS

In order to identify the primary metabolites of bupropion formed in vitro, bupropion was incubated with human liver microsomes (HLM) and metabolite formation was measured using multiple reaction monitoring (MRM). Upon incubation of bupropion with HLM, NADPH dependent formation of six metabolites was observed (Figure 2.2). In addition to OH-bupropion (Figure 2.2a) and erythrohydrobupropion and threohydrobupropion (**Figure 2.2**b), three additional monohydroxylation products (M1-M3) were detected with a parent (M+H) mass of m/z 256 and a main MRM transition of m/z 256→ 182 (**Figure 2.2**c). In absence of analytical standards, relative comparisons were made based on ion abundance. On the basis of ion abundance, M1 and M2 appeared to be equally as important in bupropion metabolism, while M3 formation appeared to be minor. All three metabolites had similar

fragmentation pathways (**Figure 2.2**c and d). The main fragmentation via a loss of 56 Da was indicative of a loss of the *t*-butyl group as isobutylene, a finding in agreement with hydroxylation outside of the *t*-butyl group. However, the fragmentation patterns did not allow for the determination of the exact hydroxylation site.

In order to determine if M1-M3 were present in vivo, urine and plasma were obtained from 5 subjects taking bupropion chronically for therapeutic reasons. Samples were analyzed for the presence M1-M3 using MRM of m/z 256→ 182. For this analysis, urine was analyzed before and after acid deconjugation since sulfate and glucuronide conjugates of the unknown bupropion hydroxylation products have been reported (Petsalo et al., 2007). Metabolite M1 was detectable in plasma, urine and acid deconjugated urine from all 5 subjects (Figure 2.3) while M2 was not detected in any of the samples, despite the fact that the extent of its formation in vitro seemed to be equivalent to that of M1. Metabolite M3 was detected in the urine of 3 subjects prior to acid deconjugation, and in the acid deconjugated urine of all 5 subjects, but at much lower abundance than M1. Acid deconjugation markedly increased M1 and M3 ion abundance, suggesting an important role for conjugation in the elimination of these metabolites (Sager, 2016). Based on ion abundance in both in vitro incubations and acid deconjugated urine, M1 appeared to be the predominant unknown hydroxylation product of bupropion. To determine the structure of M1, it was extracted from acid deconjugated urine samples and purified using preparative chromatography. A sufficient quantity of M1 was isolated to allow structural characterization via NMR, UV-Vis and MS/MS spectroscopy (Figure 2.4). MS (TOF ESI+) for $C_{13}H_{19}ClNO_2^+$ $[M+H]^+$ (calc 256.1104, observed 256.1101). Max UV absorbance was 350 nM. The presence of only 3 protons in the aromatic region of the NMR spectrum suggested that M1 was a product of aromatic hydroxylation (Figure 2.4c). The hydroxylation site was assigned to the 4' position based on NMR chemical shifts and coupling constants (Figure 2.4c). The NMR spectral shifts were as follows: ^{1}H NMR (CD_3OD, 500 MHz): δ 8.20 (d, 1H, J = 3 Hz), 8.03 (d, 1H, J = 7 Hz), 7.11 (d, 1H, J = 9 Hz), 5.22 (q, 1H, J = 7 Hz), 1.61 (d, 3H, J = 7 Hz), 1.39 (s, 9H). A reference standard of 4'-OH-bupropion HBr was then synthesized and the structure of M1 confirmed by comparison of the LC

retention time, the MS/MS spectra, maximum UV absorbance (350 nm) and NMR spectrum between the isolated metabolite and the synthesized compound. For the synthetic compound, the NMR spectral shifts were as follows: ^{1}H NMR (CD_3OD, 500 MHz): δ 8.20 (d, 1H, *J* = 2 Hz), 8.04 (dd, 1H, *J* = 9, 2 Hz), 7.11 (d, 1H, *J* = 9 Hz), 5.22 (q, 1H, *J* = 7 Hz), 1.61 (d, 3H, *J* = 7 Hz), 1.39 (s, 9H).

Previous studies of bupropion metabolism have reported the presence of reduced and hydroxylated bupropion metabolites in in vitro incubations and in vivo, yet the precursor(s) for the metabolite(s) have not been identified. To evaluate the possibility of sequential metabolism of the primary bupropion metabolites, OH-bupropion, threohydrobupropion erythrohydrobupropion and 4'-OH-bupropion were incubated in HLM or human liver cytosolic fractions to confirm the formation of sequential metabolites, and determine which substrate(s) and subcellular fractions are involved in the formation of the reduced and hydroxylated metabolite(s). NADPH dependent formation of two hydroxylated metabolites from both erythrohydrobupropion (M4 and M5) and threohydrobupropion (M6 and M7) (Figure 2.5) was detected with an M+1 ion of m/z 258 and MRM transition of 258→184, following incubation of erythro- and threohydrobupropion in HLM. No NADPH dependent formation of metabolites with m/z transitions of 258→184 were observed following incubation of threohydrobupropion, erythrohydrobupropion, OH-bupropion or 4'-OH-bupropion in cytosolic fractions or following OH-bupropion incubation in HLM (data not shown). Based on ion abundance, metabolites M4 and M6 appeared to be the major hydroxylation products of erythro- and threohydrobupropion, respectively, while M5 and M7 appeared to be minor metabolites. Chromatograms and representative spectra for M4-7 are shown in Figure 2.5. While the [M+H] 258 ion of all four metabolites (M4-M8) suggested that these are hydroxylated metabolites of threo- and erythrohydrobupropion ([M+H] 242), the MS/MS fragmentation patterns (Figure 2.5) did not allow determination of the sites of hydroxylation. Due to the hydroxylation, these metabolites do not exhibit the loss of 56 Da alone; rather, they each primarily lose H_2O or $C_4H_8 + H_2O$, as shown in the proposed fragmentation pathway in Figure 2.5c. To identify the site of hydroxylation in these compounds, threohydrobupropion-d_9, containing deuteriums in the *t*-butyl group, was incubated in HLM to determine whether M6 and 7 were

hydroxylated in the *t*-butyl group, as was previously proposed (Petsalo et al., 2007). Depending on the hydroxylation site, the products were expected to differ by one Da in the M+H ion, as shown in Figure 2.5d, allowing for detection of *t*-butyl hydroxylation. Parent masses of m/z 267 for both M6 and M7 suggested no loss of *t*-butyl deuteriums (Figure 2.5e), confirming that the hydroxylation was either in the aromatic ring or in the methyl group (Figure 2.5d).

Metabolites M4, 6 and 7 were all detectable in plasma and urine from all 5 subjects (Figure 2.6). Acid deconjugation resulted in substantially greater ion abundance for M4, 6 and 7 than in untreated urine (Figure 2.6). Metabolite M5 was only detectable in urine following acid deconjugation (Figure 2.6a, Figure 2.6). Based on the ion abundances from incubations and deconjugated urine, M4 and M6 were considered to be the major contributors to the elimination of threo- and erythrohydrobupropion. To obtain structural information for M4 and M6, these two metabolites were isolated and purified from deconjugated urine as a mixture (45:55) of erythro- and threohydrobupropion. A representative chromatogram of the purified compounds is shown in Figure 2.7b. Sufficient material was purified to allow structural characterization via NMR, UV-VIS and MS/MS analysis (Figure 2.7). The presence of three protons in the aromatic region of the NMR spectrum indicated that M4 and M6 were products of aromatic ring hydroxylation. The hydroxylation site was proposed to be at the 4' position based on NMR chemical shifts and coupling constants. For erythro-4'-OH-hydrobupropion and threo-4'-OH-hydrobupropion NMR spectral shifts were as follows: ^{1}H NMR (CD_3OD, 500 MHz, CH_3OOH internal standard): δ 7.43 (d, 1H, *J* = 2 Hz), 7.22 (dd, 1H, *J* = 9, 2 Hz), 6.97 (d, 1H, *J* = 8 Hz), 4.38 (d, 0.55H, *J* = 10 Hz, threo), 1.48 (s, 9H, erythro), 1.46 (s, 9H, threo), 1.18 (d, 3H, *J* = 7 Hz, erythro), 1.16 (d, 3H, *J* = 7 Hz, threo). The ratio of threo-4'-OH- to erythro-4'-OH-hydrobupropion in the isolated sample was determined to be 55:45 based on the integration of the signal at δ 4.38 ppm, signals at δ 1.48 vs. δ 1.46, and δ 1.18 vs. δ 1.16. MS (TOF ESI+) for $C_{13}H_{21}ClNO_2^+$ $[M+H]^+$ (calc 258.1261, found 258.1266 2.008ppm). Max UV absorbance was 214 nM. A reference standard was synthesized via reduction of the 4'-OH-bupropion. Comparison of NMR chemical shifts, maximum UV absorbance, LC retention times and MS/MS fragmentation patterns between the isolated compound and the synthesized standard

confirmed the structures as erythro-4'-OH-hydrobupropion (M4) and threo-4'-OH-hydrobupropion (M6).

To establish the relative importance of the new metabolites in vivo, their concentrations were quantified in plasma and urine. The dose-normalized concentrations of 4'-OH-bupropion (M1), threo-4'-OH-hydrobupropion (M4) and erythro-4'-OH-hydrobupropion (M6) in plasma were low, 12±6 nM/g for 4'-OH-bupropion, 7±1 nM/g threo-4'-OH-hydrobupropion (M4) and 33±20 nM/g for erythro-4'-OH-hydrobupropion (M6). Concentrations of all three compounds were below the LLOQ (3.3 nM/g) in one subject. On average, 4'-hydroxybupropion (M1) concentrations were less than 0.01 percent of those of bupropion within the same subject. Circulating concentrations of threo-4'-OH-hydrobupropion (M4) and erythro-4'-OH-hydrobupropion (M6) were 1.8 and 2.2 percent of bupropion steady state average concentration. Metabolite safety is typically considered to be a concern when steady state concentrations are greater than 10% of the parent (U.S. Food and Drug Administration Center for Drug Evaluation, 2008). Thus, it may not be necessary to screen these compounds for toxicity. However, despite the low circulating concentrations of these compounds, they were abundant in urine. The overall recovery of bupropion metabolites is shown in Table 2.2. On average, 39% of the total oral dose was recovered over the steady state dosing interval. The amount of threohydrobupropion and its metabolites represented 26% of the dose, while only 5% and 6% of the dose was excreted as OH-bupropion and erythrohydrobupropion or their metabolites. On average, 4'-OH-bupropion, threo-4'-OH-hydrobupropion and erythro-4'-OH-hydrobupropion and their conjugates account for 1.9 %, 14 % and 11 % of the total oral bupropion dose excreted in urine, respectively (Table 2.2). After accounting for the fraction of threo- and erythrohydrobupropion excreted unchanged, as conjugates or as 4'-hydroxylation products, 4'hydroxylation accounts for approximately 70 and 20% of the elimination of erythro- and threohydrobupropion, respectively. As such, changes in the formation of these metabolites could have a substantial impact on the circulating levels of threo- and erythrohydrobupropion.

2.5 CONCLUSION

In conclusion, we report the identification and characterization of seven additional metabolites of bupropion including 4'OH-bupropion, erythro-4'-OH-hydrobupropion and threo-4'-OH-hydrobupropion. Our findings are in agreement with previous tentative proposals of metabolite structures based on MS data but provide exact identification of the hydroxylation sites and methods for synthesizing these metabolites. The presence of hydroxylated metabolites of erythro and threohydrobupropion, and conjugates of an aromatic hydroxylation product(s) were previously proposed based on MS data of human urine samples (Petsalo et al., 2007). Similarly multiple monohydroxylation products of bupropion were proposed based on incubation data of bupropion in human liver S9 fractions and HLM (Chen et al., 2010; Taylor, 1995). The data shown here demonstrate that 4'hydroxylation is the predominant hydroxylation pathway. This is in contrast to previous reports suggesting hydroxylation of the methyl group in addition to the aromatic hydroxylation products (Chen et al., 2010; Taylor, 1995). The synthetic standards of the new metabolites allowed determination of their quantitative importance. Quantitative analysis revealed low circulating concentrations for all three new metabolites, suggesting the risk for toxicity resulting from these metabolites is likely low. However, M4 and M6 were important elimination pathways for two active metabolites of bupropion and thus further research into the factors regulating their formation is warranted. Characterization of the formation kinetics of these metabolites along with OH-bupropion, erythrohydrobupropion and threohydrobupropion will be presented in Chapter 3.

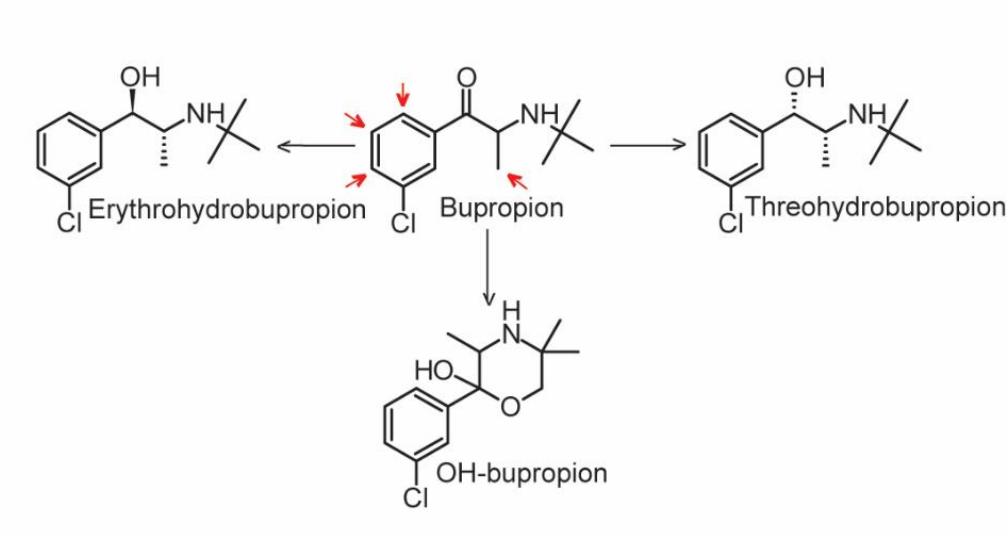

Figure 2.1. Bupropion and its active metabolites. Red arrows indicate potential additional hydroxylation sites.

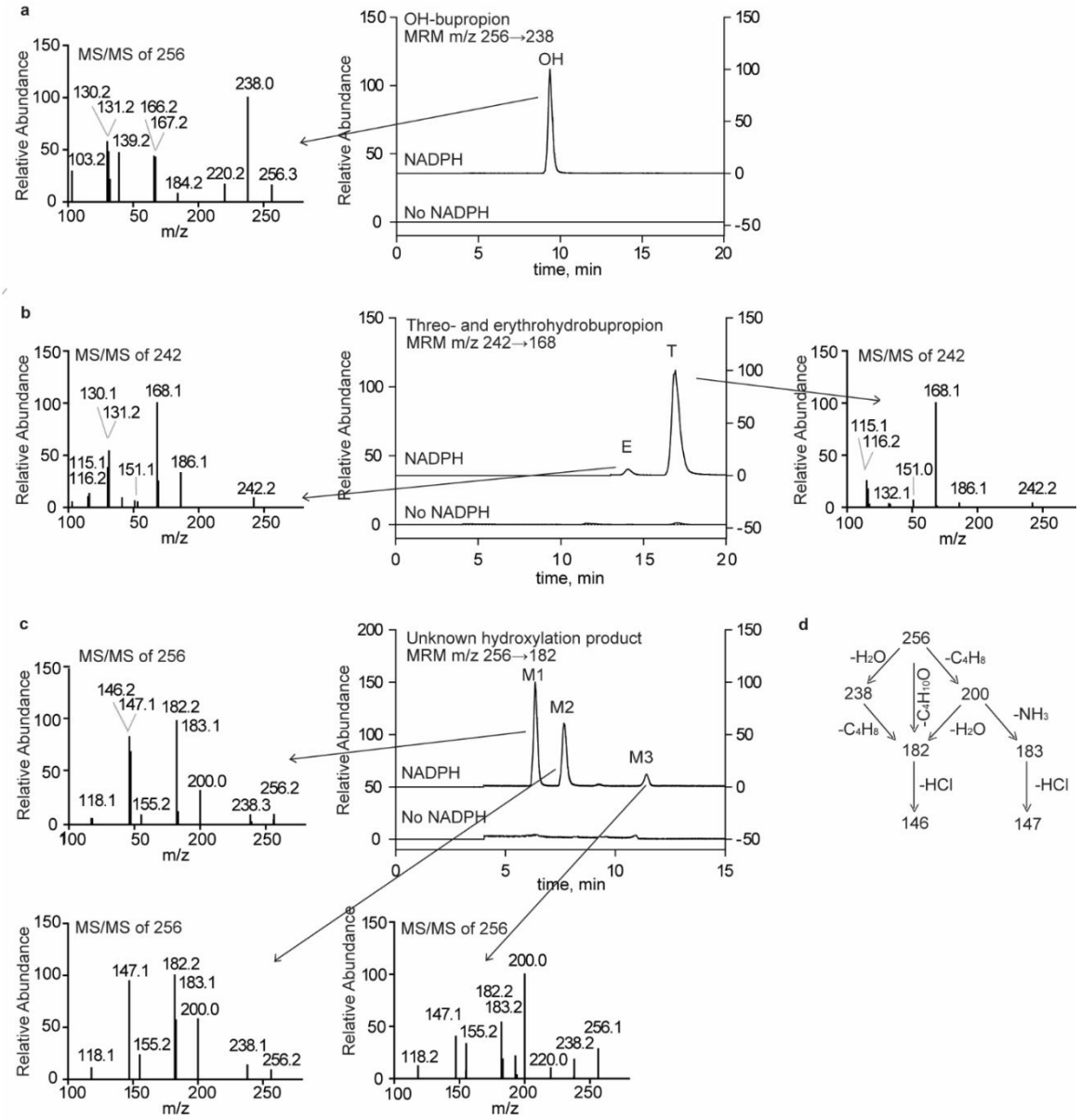

Figure 2.2. Characterization of metabolites formed in bupropion incubations. (a) A representative MRM chromatogram of m/z transition 256→238 depicting NADPH-dependent formation of OH-bupropion (OH) from bupropion incubation in HLM and MS/MS spectrum for OH-bupropion ([M+H] 256) (b) A representative MRM chromatogram of m/z transition 242→168 depicting NADPH dependent formation of erythrohydrobupropion (E) and threohydrobupropion (T) following bupropion incubation in HLM and MS/MS spectra for erythro- and threohydrobupropion ([M+H] 242). (c) Representative chromatogram of m/z transition 256→182 showing NADPH dependent formation of M1, M2 and M3 following bupropion incubation in HLM and MS/MS spectra for M1, M2 and M3 ([M+H] 256). (d) Proposed fragmentation pathways of M1-M3.

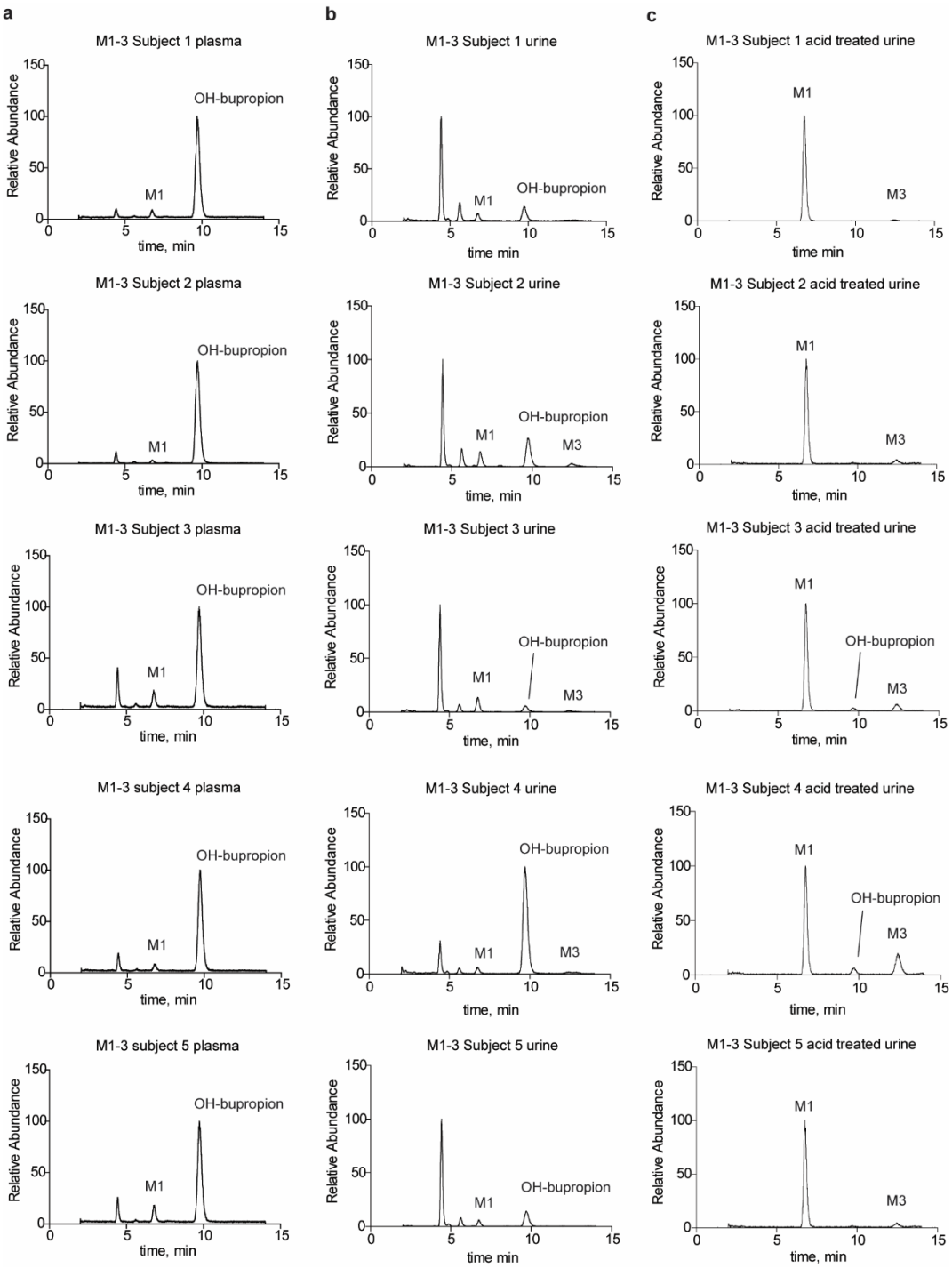

Figure 2.3. Detection of hydroxylated bupropion metabolites M1-M3 in plasma and urine of the 5 study subjects. MRM chromatograms of m/z 256→182 (M1-M3) from subject plasma (a), urine (b) and acid deconjugated urine (c). M1 was detected in the plasma and urine of all 5 subjects. M3 was not detected in plasma but was detectable in the urine of three subjects. Acid deconjugation yielded detectable levels of both M1 and M3 in the urine of all 5 subjects. The peaks eluting before M1 were likely conjugates, due to the fact that they were not detected following acid deconjugation. M2 was not detected in any of the samples.

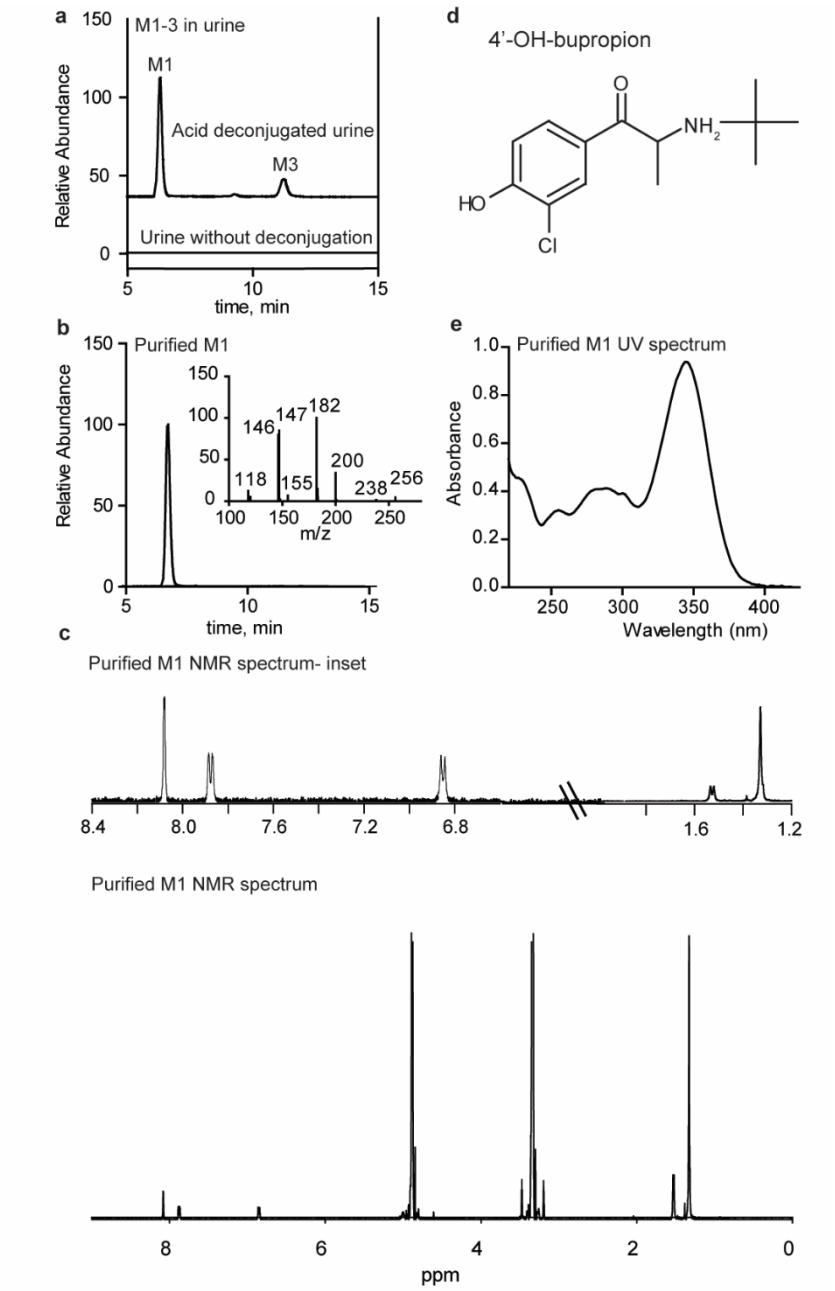

Figure 2.4. Structural characterization of isolated M1. (a) A representative MRM chromatogram of m/z transition 256→182 (M1-M3) from urine before and after acid deconjugation. (b) A representative MRM chromatogram of m/z transition 256→182 of M1 isolated from urine and an MS/MS spectrum ([M+H] 256) (c) NMR spectrum, (d) structure of 4'-OH-bupropion and (e) UV spectrum for M1 isolated from acid deconjugated urine.

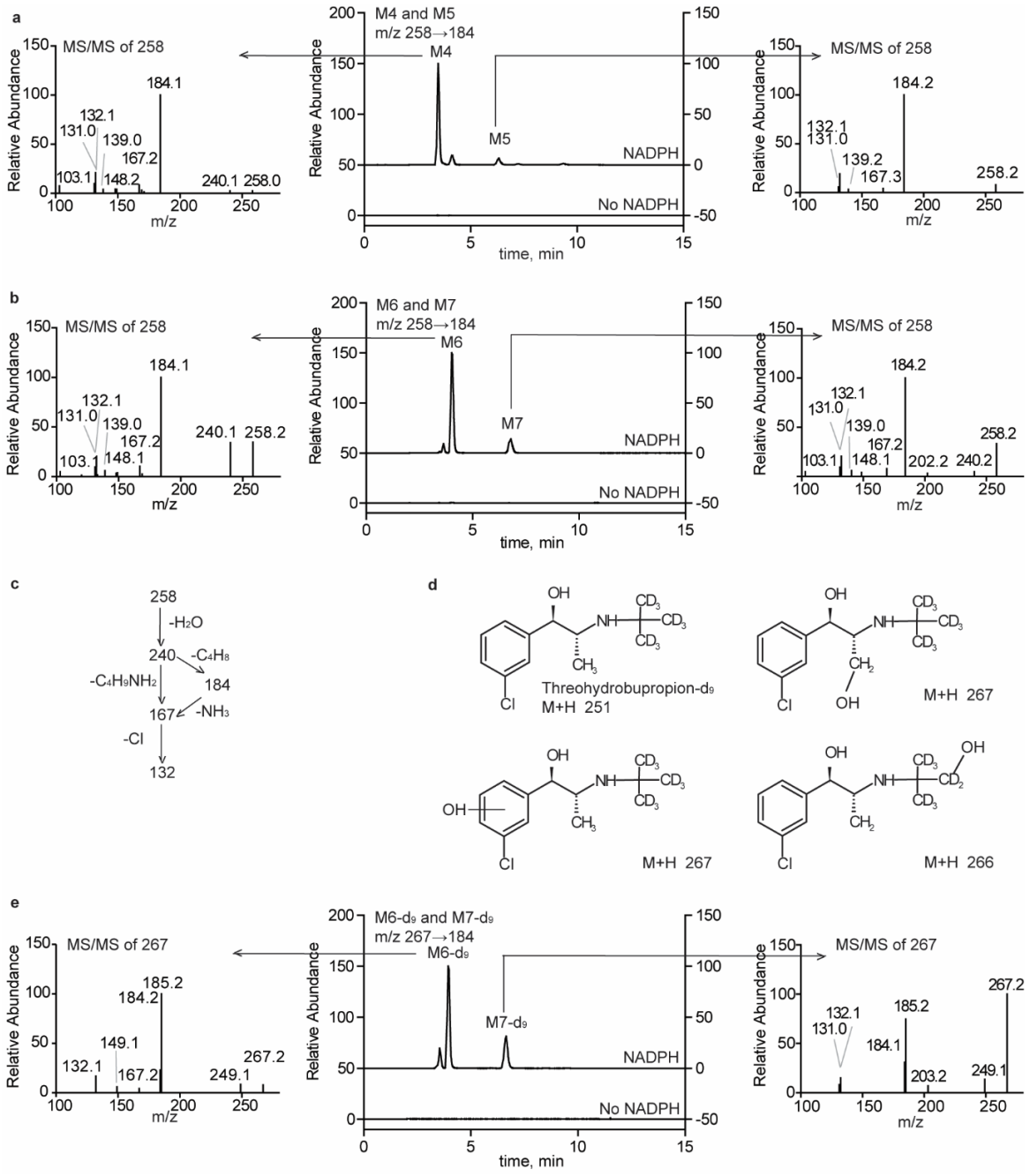

Figure 2.5. Characterization of metabolites formed in HLM incubations of erythrohydrobupropion and threohydrobupropion. A representative MRM chromatogram of m/z transition 258→184 depicting NADPH-dependent formation of metabolites M4 and M5 from erythrohydrobupropion in HLM (a) or M6 and M7 following threohydrobupropion incubation in HLM (b). Insets, MS/MS spectra. (c) Proposed fragmentation pathways of M4-7. (d) Structures and [M+H] mass of threohydrobupropion-d_9 and its potential hydroxylation products. (e) A representative MRM chromatogram of m/z transition 267→184 depicting NADPH-dependent formation of M6-d_9 and M7-d_9 following threohydrobupropion-d_9 incubation in HLM.

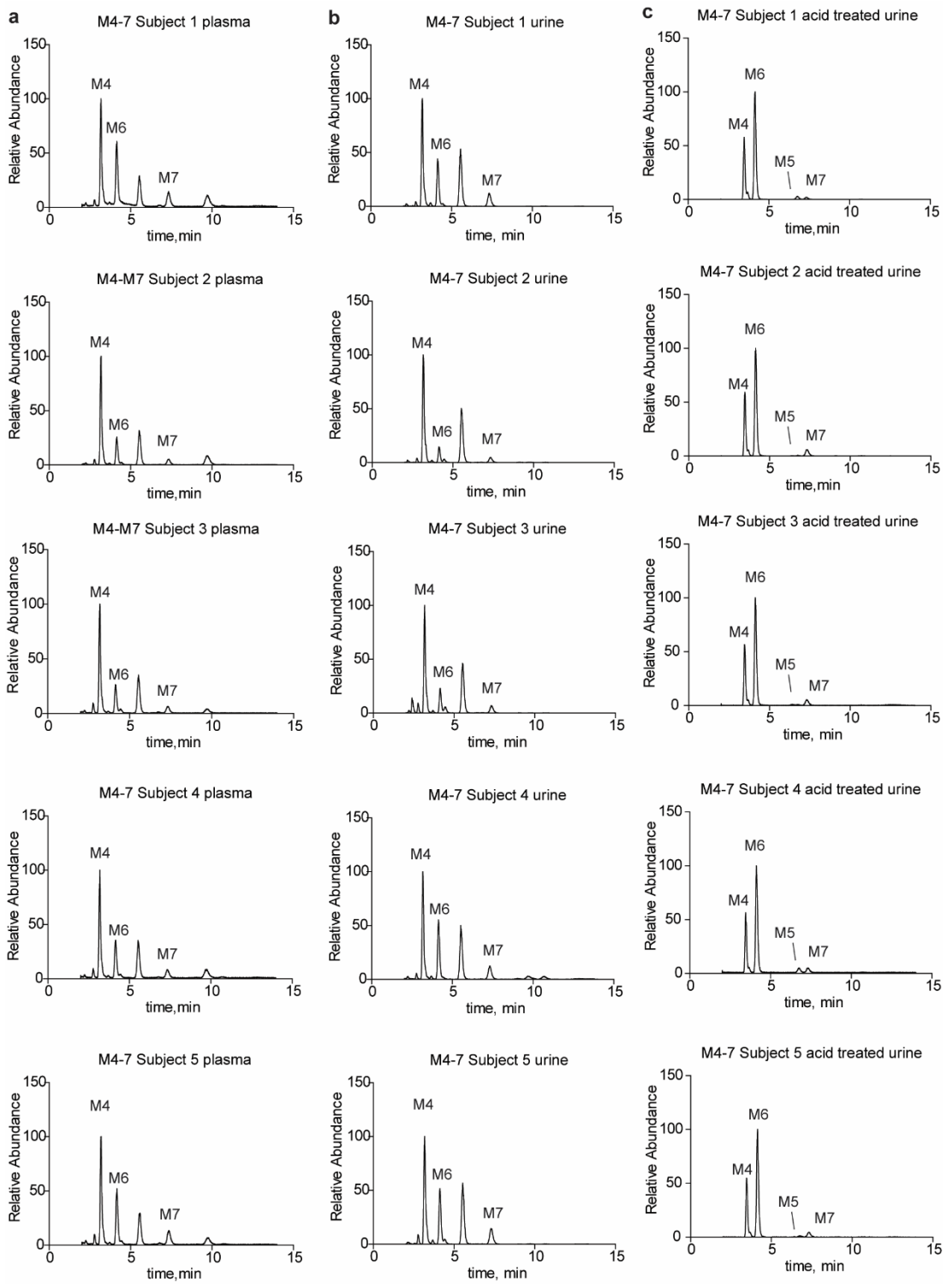

Figure 2.6. Detection of M4-M7 in plasma and urine of the 5 study subjects. MRM chromatograms of m/z 258→184 (M4-M7) from subject plasma (a), urine (b) and acid deconjugated urine (c). M4, 6 and 7 were detected in plasma and urine from all subjects. M5 was only detected following acid deconjugation. The peak eluting at 5.3 minutes was likely a conjugate, as it was not detected following acid deconjugation.

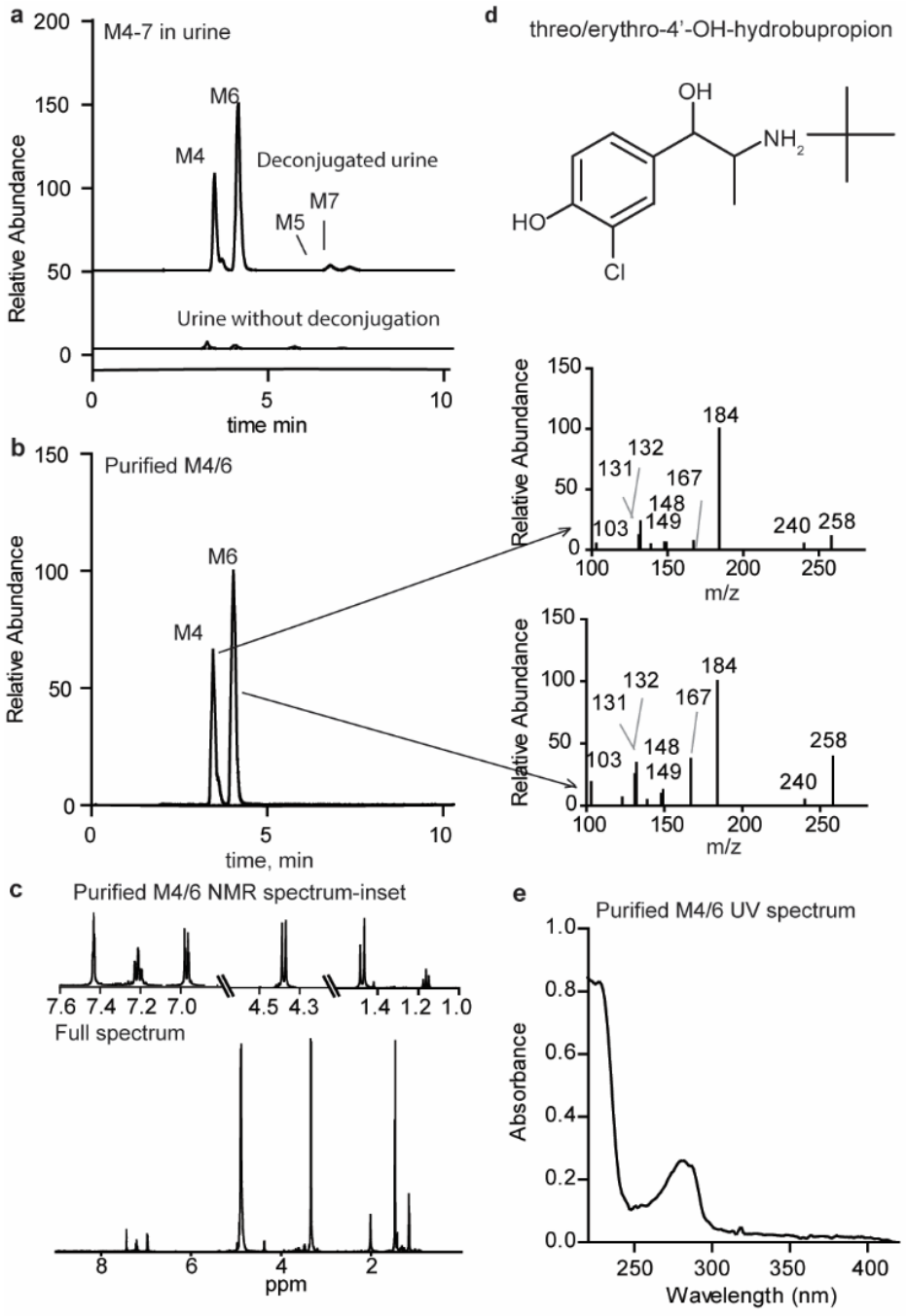

Figure 2.7. Structural characterization of M4 and M6. (a) A representative MRM chromatogram of m/z transition 258→184 (M4-M7) from urine before or after acid deconjugation. (b) A representative MRM chromatogram of m/z transition 258→184 of M4+M6 isolated from urine and MS/MS spectra of M4 and M6. (c) NMR spectrum for M4+6 isolated from acid deconjugated urine. (d) Structure of threo/erythro-4'-OH-hydrobupropion. (e) UV spectra of a mixture of metabolites M4+M6 isolated from urine.

Table 2.1. Proposed structures of metabolites M1-M7

	Potential Structures
M1, M2, M3	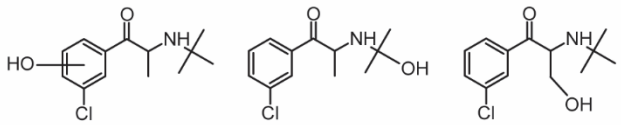
M4, M5, M6, M7	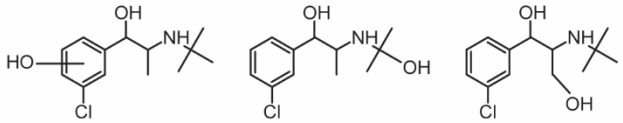

Table 2.2. The percent of the oral bupropion dose recovered in urine as bupropion and its metabolites over a steady state dosing interval

Compound	Total as free + conjugated (% of dose)	Free (µmole)*	Conjugated (µmole)*
Bupropion	1.4 ± 1.1	59 ± 71	6.5 ± 7.3
OH-bupropion	5.0± 3.2	77 ± 69	110 ± 63
Threohydrobupropion	21±14	610 ± 550	250 ± 140
Erythrohydrobupropion	1.9±1	63 ± 65	22 ±12
4'-OH-bupropion	0.8±1.0	0.3 ± 0.2	29 ± 36
Threo-4'-OH-hydrobupropion	5.3±3.5	0.9 ± 0.9	200 ± 140
Erythro-4'-OH-hydrobupropion	4.1±2.7	3.3 ± 3.2	160 ± 100
m-chlorohippuric acid	3.0 ±0.7	167 ±130	-
Total	39±15	980 ± 850	770 ± 220

*The molar amounts are normalized to the administered dose in each subject

Chapter 3.

CHARACTERIZING THE STEREOSELECTIVE METABOLISM OF BUPROPION: THE CONTRIBUTION OF CYP2B6 IS MINOR

This chapter was published, in part, in *Drug Metabolism and Disposition*

3.1 ABSTRACT

Bupropion is a widely used antidepressant, smoking cessation aid and weight loss therapy. It is administered as a racemic mixture, but the pharmacokinetics and activity of bupropion are stereoselective. Bupropion activity and side effects are attributed to bupropion and its metabolites S- and R-OH-bupropion, threohydrobupropion, and erythrohydrobupropion, yet the stereoselective metabolism in vitro and the enzymes contributing to the stereoselective disposition of bupropion have not been characterized. In addition, the predicted fraction metabolized (f_m) of 40% by CYP2B6 in bupropion clearance based on ticlopidine drug-drug interaction (DDI) (Turpeinen et al., 2005) is not in agreement with the f_m to the CYP2B6 probe metabolite OH-bupropion in vivo (16%) suggesting that the enzymes contributing to overall bupropion clearance and metabolite formation are not fully characterized. The aim of this study was to characterize the stereoselective metabolism of bupropion in vitro in order to to explain the stereoselective pharmacokinetics and the effect of DDIs and CYP2C19 pharmacogenetics on bupropion exposure. This in vitro data suggests that threohydrobupropion accounts for 50% and 82%, OH-bupropion for 34% and 12% erythrohydrobupropion 8% and 4% and 4'-OH-bupropion 7% and 2% of overall R- and S-bupropion clearance, respectively. Overall, the fm_{CYP2B6} was predicted to be 19% and the $fm_{CYP2C19}$ 5%. Importantly, ticlopidine was found to inhibit all metabolic pathways of bupropion in vitro including threo- and erythrohydrobupropion formation and 4'OH-bupropion formation by CYP2C19 , explaining the in vivo DDI. The stereoselective pharmacokinetics of bupropion were quantitatively explained by the in vitro metabolic clearances and in vivo interconversion between bupropion stereoisomers.

3.2 INTRODUCTION

Bupropion is an atypical antidepressant that is also used as a smoking cessation aid and weight loss therapy. It is administered as a racemic mixture of S- and R- bupropion, which have stereoselective

disposition and interconvert in vivo (Kharasch et al., 2008; Laizure and DeVane, 1985). The stereoisomers of bupropion also have differential pharmacological activity towards dopamine, norephinephrine and nicotinic acetylcholine receptors (Damaj et al., 2004, 2010). Bupropion's three metabolites, OH-bupropion, threohydrobupropion and erythrohydrobupropion (Figure 3.1), have also been implicated in bupropion's pharmacological activity and toxicity (Bondarev et al., 2003; Damaj et al., 2004). All three metabolites produced dose dependent increases in convulsion risk in mouse models (Silverstone et al., 2008), and in humans, dose related increases in seizure risk have been attributed to higher metabolite levels (U.S. Food and Drug Administration Center for Drug Evaluation, 2013a). High metabolite concentrations have also been attributed to side effects such as dry-mouth and insomnia (Johnston et al., 2001). For antidepressant response, trough concentrations of bupropion have been shown to be determinant of activity (Goodnick, 1992; Preskorn, 1983), and significantly lower metabolite levels have been reported in those who respond to antidepressant treatment than in non-responders (Golden, 1988). A strong dose-response relationship has also been reported for smoking cessation success (McAffee, 1998). However, in humans, OH-bupropion concentrations, instead of bupropion, are predictive of smoking cessation outcome (Zhu et al., 2012a) and much of the antidepressant and nicotine cessation activity has been attributed to S,S-OH-bupropion (Damaj et al., 2004, 2010). Whether metabolites contribute to weight loss activity has not been reported. Based on these data, processes that affect bupropion metabolism resulting in altered metabolite and parent concentrations will directly impact the safety and efficacy of bupropion.

Bupropion is metabolized to OH-bupropion, threohydrobupropion, erythrohydrobupropion (Welch et al., 1987) and 4'-OH-bupropion in vitro and in vivo (Sager et al., 2016) (Figure 1). In addition threo- and erythrohydrobupropion are hydroxylated to erythro-4'-OH-hydrobupropion and threo-4'-OH-hydrobupropion in vitro and in vivo. In vivo 67% of the dose recovered in urine over a steady state dosing interval is comprised of threohydrobupropion and its metabolites, 6% of erythrohydrobupropion and its metabolites and 5% of OH-bupropion and its conjugates (Sager et al.,

2016). An additional 3% of the dose was recovered as4'-OH-bupropion and its conjugates. In vitro OH-bupropion formation is catalyzed primarily by CYP2B6 (Faucette et al., 2000; Hesse et al., 2000), while formation of all 4'OH- metabolites has been attributed to CYP2C19 (Sager et al., 2016). OH-bupropion formation is accepted as an in vitro and in vivo probe reaction of CYP2B6 activity. However, the involvement of CYP2C19 and CYP3A4 in OH-bupropion formation at clinically relevant concentrations has also been proposed (Chen et al., 2010) and it is possible that the contributions of the individual CYP enzymes to OH-bupropion formation are stereoselective. Of note, the disposition of OH-bupropion in vivo is stereoselective with significantly different exposures to the R and S OH-bupropion (Kharasch et al., 2008). Clopidogrel and ticlopidine cause 36% and 61% increases in bupropion AUC, respectively (Turpeinen et al., 2005), which have been attributed to CYP2B6 inhibition. However, inhibition of CYP2B6 mediated formation of OH-bupropion cannot explain these DDIs due to the minor contribution of OH-bupropion to bupropion elimination, suggesting that bupropion elimination pathways are inadequately characterized especially in regards to possible CYP2C19 contribution (as suggested by 13% increase in bupropion exposure in CYP2C19 intermediate metabolizers) (Zhu et al., 2014) and inhibition of the various metabolic pathways by ticlopidine and clopidogrel. Approximately 90% of threo- and erythrohydrobupropion formation was shown be by 11β-hydroxysteroid dehydrogenase-1 (11 β –HSD-1) , with a minor contribution of cytosolic aldoketoreductase(s) (Connarn et al., 2015; Meyer et al., 2013; Skarydova et al., 2013) but the stereoselectivity in threo- and erythrohydrobupropion formation has not been explored. The aim of this study was to determine the overall contribution of CYP2B6 and CYP2C19 to bupropion stereoisomer clearance and to characterize the stereos elective metabolic pathways of broking that can explain the observed in vivo stereos elective to in bupropion clearance.

3.3 MATERIALS AND METHODS

3.3.1 Materials

Bupropion, R-bupropion, S-bupropion, OH-bupropion, R,R-OH-bupropion, S,S-OH-bupropion, threohydrobupropion, erythrohydrobupropion, bupropion-d_9, OH-bupropion-d_6 and threohydrobupropion-d_9 were purchased from Toronto Research Chemicals (Ontario, Canada). 4'-OH-bupropion, threo-4'-OH-hydrobupropion and erythro-4'-OH-hydrobupropion were synthesized as previously described (Sager et al., 2016) . Hydrochloric acid, formic acid and sodium hydroxide were purchased from Sigma-Aldrich (St. Louis, MO). Optima grade acetonitrile, methanol, water and pooled human liver microsomes (Gibco, mixed gender, n=50) were purchased from Fisher Scientific (Waltham, MA). S9 fractions (n=20, mixed gender) and recombinant enzymes were purchased from BD Biosciences (San Jose, CA). MAB-CYP2B6 inhibitory antibody was purchased from Corning.

3.3.2 LC/MS/MS Quantification Methods

Unless otherwise specified, incubations were quenched with an equal volume of acetonitrile (incubations) or 2 volumes of 1:3 methanol:acetonitrile (plasma and blood) containing 100 nM OH-bupropion-d_6 and threohydrobupropion-d_9 as internal standards. Samples were centrifuged for 15 minutes at 3000 g and the supernatant was transferred to a 96 well plate for LC-MS/MS analysis. The concentrations of bupropion, OH-bupropion, threohydrobupropion, erythrohydrobupropion, 4'-OH-bupropion, erythro-4'-OH-hydrobupropion, threo-4'-OH-hydrobupropion and ticlopidine were determined using an LC/MS/MS system consisting of an AB-Sciex API 4500 triple quadrupole mass spectrometer (AB Sciex, Foster City, CA) coupled with an LC-20AD ultra-fast liquid chromatography system (Shimadzu Co., Kyoto, Japan). The turbo ion spray interface was operated in positive ion mode. For measurement of OH-bupropion formation in supersome panels and ticlopidine concentrations, analytes were separated using an Agilent ZORBAX XDB-C18 column (50 x 2.1mm, 5µM) as

previously described (Sager et al., 2016). In S9 fraction incubations, recombinant CYP2C19 incubations, and inhibition assays, OH-bupropion, threohydrobupropion, erythrohydrobupropion, erythro-4'-OH-hydrobupropion, threo-4'-OH-hydrobupropion, and 4'-OH-bupropion were separated using an Agilent ZORBAX XDB-C18 column (150 x 4.6 mm, 5 µM) with an isocratic elution at flow rate of 0.8 mL/min with a mobile phase consisting of 35% methanol and 65% water with 0.4% formic acid according to a previously described method (Connarn et al., 2015; Sager et al., 2016). Bupropion enantiomer concentrations in plasma were determined stereoselectively using a α-acid glycoprotein column (100 x 2 mm, 5 µm) with a guard cartridge (10 x 2 mm, 5µm) (ChromTech, Apple Valley, MO). The mobile phase consisted of 20 mM ammonium formate, pH 5.7 (A) and methanol (B). A gradient elution at 0.22 mL/min starting at 10% B, increasing to 21.2% B by 25 min and 23.5% B by 34 minutes was used with re-equilibration to initial conditions by 45 min. Bupropion and its metabolites were detected using positive ion electrospray ionization using the following MRM mass transitions (*m*/*z*): 240→184 (bupropion), 249→189 (bupropion-d_9), 256→238 (OH-bupropion), 262→244 (OH-bupropion-d_6), 242→168 (threo- and erythrohydrobupropion), 251→168 (threohydrobupropion-d_9), 256→182 (4'-OH-bupropion), 258→184 (threo- and erythro-4'-OH-bupropion). Ticlopidine concentrations were detected using the MRM transition (*m/z*) 264→154 (ticlopidine). Data analysis was performed using Analyst software version 1.6.2 (AB Sciex).

3.3.3 General Incubation Conditions

All incubations were performed in 100 mM potassium phosphate buffer (pH 7.4), with a final incubation volume of 100 µL. With the exception of the IC_{50} shift experiments, all metabolite formation experiments were initiated with NADPH (1 mM) following a 5 min preincubation at 37 °C. For rCYP and inhibitor panels, all substrate concentrations were 1 µM. Activity assays were allowed to proceed for 7 minutes prior to termination of the reaction with an equal volume of acetonitrile containing 100 nM OH-bupropion-d_6 and threohydrobupropion-d_9. Reaction times were sufficiently

short to ensure that there was less than 5% interconversion of S- and R-bupropion. The metabolite formation was linear in relation to incubation time and protein content and no substrate depletion was observed in the incubations. Protein binding at all protein concentrations was determined to be negligible. All incubations were performed in triplicate alongside a control without NADPH.

3.3.4 Recombinant Cytochrome P450 Incubations

R-bupropion (1 µM or 100 µM) and S-bupropion (1 µM or 100 µM) were incubated with 5 pmol of CYP1A2, CYP2B6, CYP2C8, CYP2C9, CYP2C19, CYP2D6, CYP2E1, CYP3A4 in 100 mM potassium phosphate buffer (pH 7.4). For determination of OH-bupropion, 4'-OH-bupropion, R- or S-bupropion (6 concentrations between 1 and 20 µM for CYP2B6 and CYP3A4 or 0.5 and 48 µM for CYP2C19) were incubated with 1 pmole CYP2B6 or 5 pmole of CYP2C19 or CYP3A4). For determination of threo-4'-OH-hydrobupropion and erythro-4'-OH-hydrobupropion formation kinetics, threohydrobupropion (6 concentrations between 5 and 500 µM) and erythrohydrobupropion, (6 concentrations between 5 and 500 µM), respectively, were incubated with 5 pmol CYP2C19. Intrinsic clearance values in recombinant enzyme systems were scaled to hepatic intrinsic clearances assuming 137 pmol/mg protein for CYP3A4 (Stringer et al., 2009), 17 pmol/mg protein for CYP2C19 (Stringer et al., 2009), 14.2 pmol/mg protein for CYP2B6 (Totah et al., 2008) and 40 mg microsomal protein/ gram liver (Brown et al., 2007) 1500g was used as the liver weight, assuming 70kg body weight and 21.4g liver/kg body weight (Ito and Houston, 2005). The fractional contribution of CYP2B6, CYP2C19 and CYP3A4 to the formation of R,R- and S,S-OH-bupropion was calculated by dividing the hepatic intrinsic clearance for each enzyme by the sum of the hepatic intrinsic clearances for the enzymes forming the metabolite.

3.3.5 Inhibition of Bupropion Metabolite Formation by Specific P450 Inhibitors, a CYP2B6 Inhibitory Antibody and by Ticlopidine

To further evaluate the contribution of specific P450 enzymes to the formation of OH-bupropion, 4'-OH-bupropion, threohydrobupropion and erythrohydrobupropion, troleandomycin (CYP3A4, 50 μM), furafylline (CYP1A2, 10 μM), (+)-N-3-benzylnirvanol (CYP2C19, 2 μM), montelukast (CYP2C8, 1.5 μM), sulfaphenazole (CYP2C9, 30 μM), and quinidine (CYP2D6, 4 μM) were used in HLM incubations as previously described (Peng et al., 2011). Time dependent inhibitors troleandomycin and furafylline were preincubated for 15 minutes in the presence of NADPH prior to addition of substrate. Inhibition studies with the CYP2B6 inhibitory antibody (MAB-2B6) were conducted by pre-incubating HLM (0.5 mg/mL) with the antibody (2 μL per 100 μg HLM) or Tris buffer (control) on ice for 20 minutes. Following the pre-incubation, 100 mM KPi buffer, pH 7.4 and substrate were added and the samples preincubated for 5 minutes at 37°C. All incubations were performed at 1 μM substrate concentration. The reactions were initiated by the addition of NADPH (1 mM) and quenched after 7 min with an equal volume of acetonitrile containing 100 nM OH-bupropion-d_6 and threohydrobupropion-d_9.

To assess the potential for time-dependent inhibition of OH-bupropion, 4'-OH-bupropion, threohydrobupropion and erythrohydrobupropion formation by ticlopidine, ticlopidine (7 concentrations between 0.1 and 100 μM), was incubated with 0.5 mg/mL HLM in 100 mM Kpi buffer (100μL final) at 37° C for 30 minutes in the presence or absence of 1mM NADPH before bupropion (1 μM) or bupropion + NADPH was added. To control for ticlopidine depletion during the 30-minute preincubation, ticlopidine concentrations were measured prior to the 7-minute activity and the measured concentrations were used to determine the IC_{50} values. The magnitude of the IC_{50} shift was determined from the ratio of the IC_{50} value measured following preincubation without NADPH to that with NADPH in the preincubation. A shift ≥ 1.5 was considered to indicate the potential for irreversible inhibition (Berry and Zhao, 2008; Grimm et al., 2009).

3.3.6 Determination of in vitro Intrinsic Clearances for Bupropion Metabolites in S9 Fractions

Due to previous reports of minor cytosolic contributions to threo and erythrohydrobupropion formation (Connarn et al., 2015; Meyer et al., 2013; Skarydova et al., 2013), all incubations to assess the relative contributions of metabolite formation were performed in human liver S9 fractions. In order to determine the intrinsic formation clearance of threohydrobupropion, erythrohydrobupropion and OH-bupropion in human liver S9 fractions, R- or S- bupropion (7 concentrations between 0.4 and 16 µM) was added to KPi containing 1 mg/mL human liver S9 fractions. For determination of formation clearances at substrate concentrations below 1 µM, which was needed for the measurement of 4'-OH-bupropion CL_{int}, S9 fractions (5mg/mL) were incubated with R- or S-bupropion at 4 concentrations between 0.2 and 1 µM. S9 fraction intrinsic clearance values were scaled to hepatic intrinsic clearance using the scaling factor of 96.1 mg protein/g liver (Watanabe et al., 2009). 1500g was used as the liver weight, assuming 70kg body weight and 21.4g liver/kg body weight (Ito and Houston, 2005). The fraction of R and S bupropion metabolism (f_m) attributed to each metabolic pathway was determined from the ratio of the formation clearance of a given metabolite(s) in S9 fractions to the sum of of the S9 $CL_{int,H}$ for the respective substrate.

The fm_{CYP2B6} for R-bupropion, S-bupropion and racemic bupropion were calculated according to equations 3.1, 3.2 and 3.3, respectively,

$$fm_{CYP2B6,R-BUP} = \left(\frac{CL_{int,R,R-OH,S9}}{CL_{int,R-BUP,S9}} * \frac{CL_{int,R,R-OH,rCYP2B6}}{CL_{int,R,R-OH,rCYP}} \right) \quad \text{Equation 3.1}$$

$$fm_{CYP2B6,S-BUP} = \left(\frac{CL_{int,S,S-OH,S9}}{CL_{int,S-BUP,S9}} * \frac{CL_{int,S,S-OH,rCYP2B6}}{CL_{int,S,S-OH,rCYP}} \right) \quad \text{Equation 3.2}$$

$$fm_{CYP2B6,BUP} = \left(fm_{CYP2B6,S-BUP} * 0.5 \right) + \left(fm_{CYP2B6,R-BUP} * 0.5 \right) \quad \text{Equation 3.3}$$

in which $CL_{int,compound,S9}$ is the $CL_{int,}$ value determined for the formation of agiven metabolite in S9 fractions and $CL_{int,R\text{-}BUP,S9}$ and $CL_{int,S\text{-}BUP,S9}$ are the $\sum CL_{int,}$ values for all the detected metabolites for R-

bupropion, S-bupropion and bupropion in S9 fractions. $CL_{int,compound,rCYP2B6}$ is the intrinsic clearance to a given metabolite in rCYP2B6. $CL_{int,R,R\text{-}OH,rCYP}$ and $CL_{int,S,S\text{-}OH,rCYP}$ are the sums of the $CL_{int,H}$ for the formation of R,R-OH-bupropion, S,S-OH-bupropion by all rCYPs evaluated (CYP2C19, CYP3A4 and CYP2C19). The $fm_{CYP2C19}$ was calculated similarly according to equation 3.4, 3.5 and 3.6.

$$fm_{CYP2C19,\ R-BUP} = \frac{CL_{int,R,4'-OH,S9}}{CL_{int,R-BUP,S9}} + \left(\frac{CL_{int,R,R-OH,S9}}{CL_{int,R-BUP,S9}} * \frac{CL_{int,R,R-OH,rCYP2C19}}{CL_{int,R,R-OH,rCYP}} \right) \quad \text{Equation 3.4}$$

$$fm_{CYP2C19,\ S-BUP} = \frac{CL_{int,S,4'-OH,S9}}{CL_{int,S-BUP,\ S9}} + \left(\frac{CL_{int,S,S-OH,S9}}{CL_{int,S-BUP,\ S9}} * \frac{CL_{int,\ rCYP2C19}}{CL_{int,S,S-OH,\ rCYP}} \right) \quad \text{Equation 3.5}$$

$$fm_{CYP2C19,BUP} = (fm_{CYP2C19,R-BUP} * 0.5) + (fm_{CYP2C19,S-BUP} * 0.5) \quad \text{Equation 3.6}$$

3.3.7 Determination of unbound fractions, bupropion blood:plasma ratio and isomerization rates of R- and S-bupropion.

The protein binding of bupropion (1 µM) in plasma and in S9 fractions (5 mg/mL) and ticlopidine (4 µM) in HLM (0.5 mg/mL) was determined using ultracentrifugation as described previously (Shirasaka et al., 2013). Due to bupropion isomerization (Coles and Kharasch, 2008), racemic bupropion (0.5 µM) was used to determine the plasma protein binding of the enantiomers of bupropion, The individual enantiomers were measured by LC/MS. For determination of the isomerization rate of R- and S- bupropion in plasma, blank human plasma (100 µL) containing 500 nM R- or S-bupropion was incubated at 37°C. At 0, 15, 30, 45 and 60 minutes, plasma was quenched and placed on ice. The rate of isomerization was determined using equation 3.7, where S_0 and S_t are the substrate concentrations at time zero and t, respectively, and k is the first order rate constant for the isomerization.

$$S_t = S_0 * e^{(-kt)} \quad \text{Equation 3.7}$$

3.3.8 Simulation of the Steady State Concentration Ratios of R- and S-bupropion

To simulate the stereoselective metabolism together with the interconversion of bupropion enantiomers the steady state concentrations of R- and S-bupropion were simulated using Simbiology (Mathworks, Natick, MA). To reflect steady state conditions, a constant dosing rate of R and S bupropion (75 mg/day for each stereoisomer, to simulate a 150mg/day dose) was used with hepatic clearance values for R-bupropion ($CL_{e,R}$) and S-bupropion ($CL_{e,S}$) as predicted from the measured S9 intrinsic clearance values. To obtain estimated of $CL_{e,R}$ and $CL_{e,S}$, the $CL_{int,H}$ values reported for R- and S- bupropion were scaled to hepatic clearances for R-bupropion ($CL_{int,H,R}$) and S- bupropion ($CL_{int,H,S}$) according to Equations 3.8 and 3.9, respectively. $\sum CL_{int,H,R}$ is the sum of the $CL_{int,H}$ from R-bupropion S9 fraction incubations and $\sum CL_{int,H,S}$ is the sum of the $CL_{int,H}$ from S-bupropion S9 fraction incubations

$$CL_{e,R} = \frac{Q * fu_B * \sum CL_{int,H,R}}{Q + \left(fu_B * \sum CL_{int,H,R} \right)} \qquad \text{Equation 3.8}$$

$$CL_{e,s} = \frac{Q * fu_B * \sum CL_{int,H,s}}{Q + \left(fu_B * \sum CL_{int,H,s} \right)} \qquad \text{Equation 3.9}$$

The fraction unbound in blood (fu_B) was determined by multiplying the fraction unbound in plasma by the plasma:blood ratio. To evaluate the effect of isomerization on the ratio of R- and S-bupropion, the concentrations of R- and S- bupropion were simulated both in the absence of isomerization and in the presence of variable in vivo isomerization rates (18 rates between 0.2 and 10 L/hr). The steady state concentrations of R- and S- bupropion were described by equations 3.10 and 3.11, respectively, where C_R is the concentration of R-bupropion and C_S is the concentration of S-bupropion.

$$R_{in,R} + CL_{S-R}\left(C_s\right) = C_R\left(CL_{S-R} + CL_{e,R}\right) \qquad \text{Equation 3.10}$$

$$R_{in,S} + CL_{S-R}\left(C_R\right) = C_S\left(CL_{S-R} + CL_{e,S}\right) \qquad \text{Equation 3.11}$$

$R_{in,\,R}$ and $R_{in,\,S}$ are the steady state constant rate inputs (75 mg/day) of R and S bupropion, respectively. $CL_{e,\,R}$ (12.4 L/hr) and $CL_{e,\,S}$ (43.5 L/hr) are the hepatic clearances of R- and S-bupropion, respectively. Simulations were performed in absence of isomerization or in the presence of a reversible isomerization clearance, $CL_{S\text{-}R}$ (18 values ranging from 0.2-10 L/hr).

The f_m values for each metabolic pathway in the simulations with different isomerization rates were calculated as the ratio of the amount of a given metabolite excreted over a dosing interval to the total dose administered over that interval. The f_m for CYP2B6 based on the simulation was calculated according to equation 3.12:

$$\text{fmCYP2B6} = \frac{A_{e,R,R-OH-bupropion} * fm_{CYP2B6,R,R-OH} + Ae_{S,S-OH-bupropion} * fm_{CYP2B6,\,S,S-OH}}{Dose} \quad \text{Equation 3.12}$$

where $A_{e,R,R\text{-}OH\text{-}bupropion}$ and $A_{e,S,S\text{-}OH\text{-}bupropion}$ are the amount of R,R-OH- and S,S-OH-bupropion excreted over a given time interval. The $fm_{CYP2B6,R,R\text{-}OH}$ and $fm_{CYP2B6,S,S\text{-}OH}$ are the fraction of R,R-OH-bupropion (0.9) and S,S-OH-bupropion (0.89) formation attributed to CYP2B6 based on $CL_{int,H}$ values scaled from rCYP CL_{int} (Table 1), respectively. The fm for CYP2C19 was calculated according to equation 3.13:

$$fm_{CYP2C19} = \frac{A_{e,R,R-OH-bupropion} * fm_{CYP2C19,R,R-OH} + Ae_{S,S-OH-bupropion} * fm_{CYP2C19,\,S,S-OH} + Ae_{4'-OH-bupropion}}{Dose}$$

Equation 3.13

The $fm_{CYP2C19,R,R\text{-}OH}$ and $fm_{CYP2C19,S,S\text{-}OH}$ are the fraction of R,R-OH-bupropion (0.025) and S,S-OH-bupropion (0.095) formation attributed to CYP2C19 based on $CL_{int,H}$ values scaled from rCYP CL_{int} (Table 3.1), respectively. $Ae_{4'\text{-}OH\text{-}bupropion}$ is the total amount of 4'-OH-bupropion excreted over the dosing interval.

3.3.9 Data Analysis

The formation velocity was plotted against the substrate concentration and fit via linear or nonlinear regression in Graphpad Prism (Graphpad Software, San Diego, CA). When saturable kinetics

were observed over the substrate concentration range, the maximum metabolite formation velocity, kcat or V_{max}, and the Michaelis Menten affinity constant, $K_{m,}$ were determined using equation 3.14:

$$v = \frac{V_{max} \times [S]_0}{K_m + [S]_0} \qquad \text{Equation 3.14}$$

The metabolite intrinsic formation clearance was calculated as the ratio of the V_{max} and K_m determined in equation 1. In cases where product formation was linear over the concentration range, CL_{int} was determined from the slope using linear regression. One-way ANOVA with post-hoc Tukey test was used to test for significance of changes in metabolite formation in the P450 inhibitor panels.

3.4 RESULTS

3.4.1 Characterization of the Enzymes Involved in Bupropion Metabolite Formation

To determine the enzymes contributing to OH-bupropion stereoisomer formation, R- and S-bupropion were incubated with a panel of recombinant human CYP enzymes. At supraphysiological concentrations of R- and S-bupropion (100 μM), R,R-OH-bupropion and S,S-OH-bupropion formation was detected in CYP2B6, CYP2C19, CYP3A4 and CYP1A2 supersomes but the relative formation rates of S,S-OH-bupropion and R,R-OH-bupropion in CYP3A4, CYP1A2 and CYP2C19 supersomes were approximately 2, 0.4, and 0.1% of that in CYP2B6 supersomes (Figure 3.2A). When clinically relevant concentrations of substrate were used (1 μM), formation of R,R-OH-bupropion and S,S-OH-bupropion was only observed in CYP2B6, CYP2C19 and CYP3A4 supersomes. At this concentration CYP2B6 was still the most efficient enzyme forming R,R- and S,S-OH-bupropion, but the relative contributions of CYP2C19 and CYP3A4 were increased in comparison to the supraphysiological concentrations. At 1 μM substrate concentration, product formation rates in CYP2C19 and CYP3A4 supersomes were 10% and 2% of the rates in CYP2B6 supersomes for S-bupropion and 7 and 2% for R-bupropion, respectively (Figure 3.2B).

To further characterize the relative importance of CYP2B6 in OH-bupropion stereoisomer formation, the formation kinetics of R,R-OH-bupropion and S,S-OH-bupropion were determined in recombinant P450's (Figure 3.2D and E). The in vitro CL_{int} values are listed in Table 3.1, along with the predicted $CL_{int, H}$. Formation of R,R-and S,S-OH-bupropion in CYP3A4 and CYP2B6 supersomes was linear over the substrate concentration range, suggesting that the K_m values for CYP2B6 and CYP3A4 greatly exceed 10 µM and 20 µM, respectively. The intrinsic formation clearance of S,S-OH-bupropion was 1.8-fold higher than that of R,R-OH-bupropion in CYP2B6 supersomes but in CYP3A4 supersomes S,S-OH-bupropion formation was only 30% that of R,R-OH-bupropion . Upon incubation of R- and S-bupropion in CYP2C19 supersomes, the formation of R,R- and S,S-OH-bupropion were saturable. While both substrates had similar K_m values (9 µM for R-bupropion and 4 µM for S-bupropion), the intrinsic enzyme activity for S,S-OH-bupropion formation was 10 fold higher than that of R,R-OH-bupropion formation. Based on the extrapolated $CL_{int, H}$ values, CYP2B6 was predicted to contribute to 90 and 89% of R,R- and S,S-OH-bupropion formation, respectively (Table 3.1). CYP2C19 is predicted to form 2.5 and 9.5% of R,R- and S,S-OH-bupropion, respectively, while CYP3A4 contributes to 7.5 and 1% to the formation of R,R-OH-bupropion and S,S-OH-bupropion, respectively.

To confirm the predicted contribution of individual P450 isoforms to R,R- and S,S-OH-bupropion formation selective inhibitor panel was employed in HLMs together with an inhibitory CYP2B6 antibody. The selective monoclonal antibody (MAB-2B6) decreased the formation of R,R- and S,S-OH-bupropion by 91 and 81%, respectively, confirming that CYP2B6 is the major enzyme involved in the formation of both OH-bupropion enantiomers (Figure 3.2C). No significant inhibition was observed by any of the chemical inhibitors, a finding in agreement with the predicted minor contributions of CYP2C19 and CYP3A4 to OH-bupropion formation. Interestingly, R,R- and S,S-OH-bupropion formation in the N-benzylnirvanol treated HLMS was 11% and 20% higher than the control

($p<0.05$), respectively, and S,S-OH-bupropion formation in the presence of montelukast was 15% higher than control ($p<0.05$) suggesting activation of some P450s by these inhibitors.

In a panel of P450 supersomes, the formation of 4'-OH-bupropion was shown to be catalyzed exclusively by CYP2C19. Based on the recombinant enzyme data, the formation kinetics of 4'-OH-bupropion from S and R bupropion were characterized only in CYP2C19 supersomes, (Table 3.1 and Figure 3.3). Both R-bupropion and S-bupropion had similar affinity (K_m 5 µM for R-bupropion and 4 µM for S-bupropion) to CYP2C19, and the V_{max} for 4'-OH-formation was the same for both stereoisomers (19 pmol/min/pmol for R-bupropion and 18 pmol/min/pmol for S-bupropion). To confirm the importance of CYP2C19 in 4'-OH-bupropion formation, the effects of selective CYP inhibitors on 4'-OH-burpopion formation was determined (Figure 3.3). Following incubation of R- or S-bupropion, N-benzylnirvanol (CYP2C19 inhibitor) inhibited 84% and 82% of the 4'-OH-bupropion formation from R and S-bupropion, respectively. Minor inhibition (10%) of 4'-OH-bupropion formation was detected upon incubation of S-bupropion with MAB-CYP2B6, suggesting potentially minor involvement of CYP2B6, however, no 4'-OH-bupropion formation was observed in CYP2B6 supersomes.

Similar to 4'OH-bupropion formation, it was suggested that the formation of threo-4'-OH-hydrobupropion and erythro-4'-OH-hydrobupropion is catalyzed only by CYP2C19 (Sager et al., 2016). Hence, the formation kinetics of both metabolites were characterized in CYP2C19 supersomes following incubation of either threo- or erythrohydrobupropion and the contribution of CYP2C19 was tested using selective CYP inhibitors in HLM. Saturable kinetics were observed for both threo-4'-OH-hydrobupropion and erythro-4'-OH-hydrobupropion formation. The formation of threo-4'-OH-hydrobupropion was a higher affinity (K_m 13 µM) and higher capacity process (0.55pmol/min/pmol) than erythro-4'-OH-hydrobupropion formation (K_m 42 µM) (0.40 pmol/min/pmol). The formation clearance of threo-4'-OH-hydrobupropion was 4-fold higher than that of erythro-4'-OH-hydrobupropion. (Table 3.3 and Figure 3.4). The major role of CYP2C19 in the formation of threo-

and erythro-4'-OH-hydrobupropion was further supported by the 87% inhibition of threo-4'-OH-hydrobupropion formation and 96% inhibition of erythro-4'-OH-hydrobupropion formation by N-benzylnirvanol (Figure 3.3). Minor inhibition (15%) of erythro-4'-OH-hydrobupropion formation was detected upon incubation of erythrohydrobupropion with sulfaphenazole, suggesting potentially minor involvement of CYP2C19 in erythro-4'OH-hydrobupropion formation. However, due to the 96% inhibition of metabolite formation by N-benzylnirvanol and lack of metabolite formation in CYP2C9 supersomes, CYP2C19 is likely the only enzyme involved in erythro-4'-OH-hydrobupropion formation.

3.4.2 Characterization of the formation kinetics of bupropion metabolites in human liver S9 fractions.

In order to assess the relative importance of the metabolic pathways of bupropion in human liver, OH-bupropion, threohydrobupropion, erythrohydrobupropion and 4'-OH-bupropion formation was measured in human liver S9 fractions. Overall, marked stereoselectivity was observed in the formation of bupropion metabolites. The CL_{int} for S,S-OH-bupropion formation was twice that of R,R-OH-bupropion. The CL_{int} for threohydrobupropion and erythrohydrobupropion was 8 and 2 fold higher upon incubation with S-bupropion than R-bupropion, respectively. No difference was observed between the intrinsic formation clearance of 4'-OH-bupropion following incubation with R- and S-bupropion. Metabolite formation versus concentration plots are shown in Figure 3.5 and a summary of the in vitro CL_{int} are shown in Table 3.2. The sum of the metabolic clearances from S-bupropion was 5-fold higher than that for R-bupropion. The formation of S,S-threohydrobupropion accounted for 83% of the metabolic clearance of S-bupropion in the S9 fractions, while the formation of the additional metabolites contributed to 12 % (S,S-OH-bupropion), 4% (R,S-erythrohydrobupropion) and 2% (4'-OH-bupropion) of the total predicted metabolic intrinsic clearance (Table 3.2). Similarly, threohydrobupropion formation was the major clearance pathway for R-bupropion, accounting for 50% of the total metabolic intrinsic clearance. The formation of R,R-OH-bupropion accounted for 34% of

the CL_{int}, while the remaining 8 and 7% of the clearance was attributed to S,R-erythrohydrobupropion and 4'-OH-bupropion formation, respectively. Taking into account the total racemic bupropion $CL_{int, H}$, threohydrobupropion is expected to contribute to 66% of overall bupropion clearance while the remaining clearance is attributed to OH-bupropion formation (23%), erythrohydrobupropion (6%) and 4'-OH-bupropion (5%). Taking into account the fractional contribution of CYP2B6 to OH-bupropion formation, the predicted $f_{mCYP2B6}$ was 0.3, 0.10 and 0.21 for R-bupropion, S-bupropion and racemin bupropion, respectively. Accounting for the contribution of CYP2C19 in the formation of OH-bupropion, as well as the fraction of bupropion metabolized to 4'-OH-bupropion, the $f_{mCYP2C19}$ was estimated to be 0.09, 0.03 and 0.06 for R-bupropion, S-bupropion and racemic bupropion, respectively.

3.4.3 Inhibitory Effects of Ticlopidine on the Formation of Bupropion Metabolites.

Ticlopidine is a known mechanism based inhibitor of CYP2C19 and CYP2B6 (Ha-Duong et al., 2001; Nishiya et al., 2009a, 2009b; Richter et al., 2004) and causes a 61% increase in bupropion AUC in vivo (Turpeinen et al., 2005). As expected, ticlopidine was found to inhibit the formation of OH-bupropion (CYP2B6) and 4'-OH-bupropion (CYP2C19), with IC_{50}'s of 0.53 and 0.9 μM, respectively (Table 3.3, Figure 3.6). To assess the potential for ticlopidine to inhibit 11β-HSD-1, threo- and erythrohydrobupropion formation was measured in the presence and absence of ticlopidine. Interestingly, ticlopidine inhibited the formation of threohydrobupropion (IC_{50} 10 μM) and erythrohydrobupropion (IC_{50} 12 μM) in HLM when preincubated for 30 minutes in the absence of NADPH. Furthermore, 7.6- (OH-bupropion), 6.4- (4'-OH-bupropion), 2.1-(threohydrobupropion) and 2.7-fold (erythrohydrobupropion) shifts in the IC_{50} values were observed following a 30 minute preincubation in the presence of NADPH, suggesting the potential for time dependent inhibition.

3.4.4 The Contribution of Bupropion Isomerization to the Stereoselective Disposition in vivo.

R- and S-bupropion have been reported to exhibit stereoselective disposition in vivo, with a reported R:S AUC ratio of 2.93. In order to determine whether a steady state R:S ratio of 2.93 could be predicted from our data, a Simbiology model as built to account for isomerization clearance. The fraction unbound for R- and S- bupropion in human plasma were 0.5 and 0.6, respectively. The blood to plasma concentration ratio of bupropion was 0.42. Based on these data and the in vitro metabolic clearances, the calculated hepatic clearance values for R- and S- bupropion were 43.5 and 12.2 L/hr, respectively. $CL_{H,R}$ and $CL_{H,S}$ were used as input in the Simbiology model as shown in Figure 3.7, as "$CL_{e,R}$" and "$CL_{e,S}$" in order to simulate the concentration ratio of R- and S- bupropion at steady state. When the isomerization rate was set to 0 L/h, the predicted ratio of R:S bupropion was 3.56, in comparison to the observed ratio of 2.93 ± 1.4 (Kharasch et al., 2008). When the isomerization rates were varied between 0.2 and 10 L/hr, the steady state R:S ratio decreased with increasing isomerization rates. The relationship between isomerization rate and the steady state R:S bupropion ratio is shown in Figure 3.8. At an isomerization rate of 2 L/hr the exact observed R:S ratio was achieved. To determine if this value was in agreement with actual plasma isomerization clearance, the isomerization rates of R- and S-bupropion were determined in human plasma. Upon incubation of R- or S-bupropion in human plasma, the rate of interconversion was determined to be 0.54 hr^{-1}. Scaling this value to blood volume (5 L) resulted in an estimated in vivo isomerization CL of 2.7 L/hr. This isomerization clearance is expected to yield a steady state R to S ratio of 2.8, which is in good agreement with the observed ratio of 2.93 ± 1.4. The fraction metabolized to each metabolite was determined following incorporation of a 2.7 L/hr isomerization rate into the model. In the presence of isomerization, the fraction of bupropion metabolized to each metabolite was not substantially altered. The predicted f_m values were 0.21 (OH-bupropion), 0.68 (threohydrobupropion), 0.06 (erythrohydrobupropion), 0.04 (4'-OH-bupropion) .

Based on this data, the in vivo fm values for CYP2B6 and CYP2C19 are estimated to be 0.19 and 0.05, respectively.

3.5 DISCUSSION

Bupropion's fm_{CYP2B6} has been proposed to be 26-40% based on changes in exposure following clopidogrel or ticlopidine administration (Turpeinen et al., 2005). Furthermore, CYP2C19 has been proposed to be a quantitatively important elimination pathway for bupropion based on in vivo pharmacokinetic data and in vitro incubations (Chen et al., 2010; Zhu et al., 2014). Here, we demonstrate, using in vitro intrinsic clearance data, that CYP2B6 and CYP2C19 are minor elimination pathways of bupropion and that time dependent inhibition of 11B-HSD-1 by ticlopidine likely explains why the fm_{CYP2B6} is overestimated based on the DDI data.

Based on the predicted $CL_{int,H}$ values reported in this study, CYP2B6 mediated hydroxylation is a relatively minor pathway, accounting for only 19% of the total $CL_{int, H}$. This is consistent with mass balance data showing that OH-bupropion and its conjugates only account for 13% of the drug related material recovered in urine over a steady state dosing interval. Our finding is also in agreement with the observation that CYP2B6*6 and *18 variants, which result in reduced activity, significantly reducehydroxybupropion formation without causing any changes in the circulating concentrations of bupropion (Benowitz et al., 2013). However, this minor contribution of CYP2B6 to bupropion elimination contradicts the proposed fm_{CYP2B6} value of 0.4 based on ticlopidine inhibition in vivo. One potential explanation for why ticlopidine and clopidogrel DDI studies overpredict the true fm_{CYP2B6} is that these inhibitors inhibit additional bupropion elimination pathways. It is well established that ticlopidine and clopidogrel are time dependent inhibitors of CYP2B6 and CYP2C19 (Ha-Duong et al., 2001; Nishiya et al., 2009a, 2009b; Richter et al., 2004). However, the CYP2C19-mediated formation of 4'-OH-bupropion is only predicted to contribute to 5% of bupropion clearance, and 4'-OH-bupropion also is a minor component of the drug related material recovered in urine (Sager et al., 2016). Thus

CYP2C19 is not likely to explain the magnitude of the in vivo DDIs. However, bupropion reduction via microsomal 11β-HSD-1 is a major elimination pathway (Connarn et al., 2015; Meyer et al., 2013; Sager et al., 2016), yet the effects of ticlopidine on the formation of threo- and erythrohydrobupropion have not been previously assessed. This study demonstrates that ticlopidine inhibits threo- and erythrohydrobupropion formation. Reversible inhibition alone is unlikely to cause any in vivo inhibition of threo- and erythrohydrobupropion formation though, given the $IC_{50,u}$'s of 1.3-1.5 μM and the unbound ticlopidine C_{ss} of 0.05 μM ($I_u/IC_{50,u}$ <0.1). However, IC_{50} shifts were observed upon a 30 minute preincubation in the presence of NADPH, suggesting that ticlopidine is a time dependent inhibitor of 11β-HSD-1, and possibly a clinically relevant inhibitor of bupropion reduction pathways. Given that 19% of bupropion elimination is attributed to CYP2B6 and another 5% to CYP2C19, only 22% inhibition of threo- and erythrohydrobupropion formation would be needed to yield the observed 40% inhibition of bupropion clearance observed in vivo. As a result, the fm_{CYP2B6} values used for bupropion should be reevaluated in order to prevent errors in IVIVE or misinterpretation of clinical study results.

Recent studies have suggested that CYP2C19 is a quantitatively important bupropion elimination pathway. Zhu et al reported significantly higher exposures to bupropion (13%), threohydrobupropion (40%) and erythrohydrobupropion (30%) in CYP2C19 intermediate metabolizers (IMs) when compared to extensive metabolizers (EMs) (Zhu et al., 2014). However, in the same study no difference was observed between EMs and subjects carrying at least one copy of CYP2C19*17, which confers increased activity (Zhu et al., 2014). The results of this study suggest that the contribution of CYP2C19 to bupropion clearance is minor, with only about 4% of overall bupropion clearance estimated to be due to CYP2C19. Thus, further investigations into the effects of CYP2C19 genetic polymorphisms on bupropion pharmacokinetics may be needed to clarify the contribution of CYP2C19 to bupropion metabolism in vivo. Despite suggesting the minor involvement of CYP2C19 in bupropion clearance, our findings show that CYP2C19 catalyzes the formation of threo- and erythro-4'-

OH-hydrobupropion from threo- and erythrohydrobupropion, respectively. Mass balance data suggests that 4' hydroxylation accounts for 20% of threohydrobupropion clearance and 70% of erythrohydrobupropion clearance. This is consistent with the observation that threo- and erythrohydrobupropion exposure is increased in individuals carrying at least one copy of CYP2C19*2 (Zhu et al., 2014).

Aside from erythrohydrobupropion, the rank order of the formation clearances of the other bupropion metabolites is consistent with mass balance data (Sager et al., 2016). Threohydrobupropion formation accounts for 68% of the total predicted metabolite formation clearance and 4'-OH-formation accounts for approximately 4% of the total. This is in agreement with the percent of the drug related material recovered in urine as threohydrobupropion and its metabolites (67%) and 4'-OH-bupropion and its conjugates (2%). However, while erythrohydrobupropion and its sequential metabolites account for 15% of the drug related material recovered in urine over a steady state dosing interval (Sager et al., 2016) the predicted f_m for erythrohydrobupropion is only 6% of total bupropion clearance. This discrepancy may be due to extrahepatic metabolism that is not accounted for in the in vitro system and further characterization of extrahepatic bupropion metabolism is warranted.

Marked stereoselectivity was observed in bupropion metabolism. Overall predicted hepatic intrinsic clearance of S-bupropion was 5 fold higher than that of R-bupropion. This disagrees with the observed AUC ratio of 2.97 ± 1.4 for R- and S-bupropion in vivo (Kharasch et al., 2008). Bupropion is known to isomerize readily (Kharasch et al., 2008; Sager et al., 2016), and this study demonstrates that incorporating isomerization clearance into a Simbiology model accounting for R and S- bupropion metabolic clearance as well as isomerization clearance predicted a steady state R:S ratio of 2.8, which was in close agreement with the observed ratio of 2.97. This suggests that bupropion isomerization may contribute to the in vivo stereoselective disposition of bupropion and could potentially account for the discrepancies between in vitro and in vivo data.

Bupropion is used as both an in vitro and in vivo CYP2B6 probe. In vitro, OH-bupropion formation is used as a measure of CYP2B6 activity, based on the assumption that OH-bupropion formation is selective for CYP2B6. However, no previous studies have systematically characterized the enzymes involved in the formation of OH-bupropion at clinically relevant concentrations. Here, we report that CYP2B6 contributes to over90% of both R,R- and S,S-OH-bupropion formation while the contribution of CYP2C19 and CYP3A4 is minor. These results suggest that the use of OH-bupropion in vitro formation clearance is selective for CYP2B6. However, since OH-bupropion is subsequently conjugated, in scenarios where OH-bupropion clearance is altered alone, or in combinations with changes in CYP2B6 activity, the OH-bupropion/bupropion AUC or C_{ss} ratio may not be reflective of changes in CYP2B6. Thus, in vivo OH-bupropion formation clearance may be a more appropriate marker of CYP2B6 activity than the metabolite to parent AUC ratio.

In conclusion, this study demonstrates that R,R-OH-bupropion and S,S-OH-bupropion are primarily formed by CYP2B6, while the contribution of CYP2B6 to overall bupropion metabolism is relatively minor. Past overestimations of bupropion's fm_{CYP2B6} based on ticlopidine inhibition may be due inhibition of bupropion's reduction pathways. Furthermore, CYP2C19 contributes to bupropion, threohydrobupropion and erythrohydrobupropion elimination, but its relative contribution to bupropion clearance is low. Finally, this study demonstrates that hepatic intrinsic clearance of S-bupropion is 5 fold greater than that of R-bupropion in vitro, but that isomerization may also play a role in bupropion's stereoselective disposition.

Table 3.1. In vitro intrinsic clearance values for R-bupropion, S-bupropion, threohydrobupropion and erythrohydrobupropion in recombinant enzymes. Metabolite formation was assessed in recombinant enzymes that formed the metabolites in a screen of a panel of P450 supersomes. In vitro intrinsic clearance values (CL_{int}) as well as scaled hepatic intrinsic clearance values ($CL_{int, H}$) are shown.

Substrate	**Product**	**Enzyme**	**CL_{int}** (μL/min/nmol P450)	**$CL_{int, H}$**[a] (L/hr)
R-bupropion	R,R-OH-bupropion	CYP2B6	69	3.6
		CYP2C19	0.9	0.1
		CYP3A4	0.5	0.3
	4'-OH-bupropion	CYP2C19	19	1.1
S-bupropion	S,S-OH-bupropion	CYP2B6	130	6.6
		CYP2C19	12	0.7
		CYP3A4	0.1	0.1
	4'-OH-bupropion	CYP2C19	18	1.1
Erythrohydrobupropion	Erythro-4'-OH-hydrobupropion	CYP2C19	10	0.6
Threohydrobupropion	Threo-4'-OH-hydrobupropion	CYP2C19	42	2.6

Intrinsic clearance values in recombinant enzyme systems were scaled to hepatic intrinsic clearance ($CL_{int, H}$) assuming 137 pmol/mg protein for CYP3A4 (Stringer et al., 2009), 17 pmol/mg protein for CYP2C19 (Stringer et al., 2009), 14.2 pmol/mg protein for CYP2B6 (Totah et al., 2008) and 40 mg microsomal protein/ gram liver (Brown et al., 2007). The fractional contribution of CYP2B6, CYP2C19 and CYP3A4 to the formation of R,R- and S,S-OH-bupropion ($fm_{R,R\text{-}OH, rCYPX}$ or $fm_{S,S\text{-}OH, rCYPX}$) was calculated by dividing the hepatic intrinsic clearance for each enzyme by the total hepatic intrinsic formation clearance for the given metabolite.

Table 3.2. Intrinsic clearance of R- and S-bupropion in human liver S9 fractions.

Substrate	Product	CL_{int} (μL/min/mg S9 protein)	$CL_{int,H}$[a] (L/hr)	$f_{m,\ enantiomer}$[b]	f_m[c]
R-bupropion	R,R-hydroxybupropion	0.47	4.1	0.34	0.17
	R,R-threohydrobupropion	0.69	6.0	0.5	0.25
	S,R-erythrohydrobupropion	0.11	0.9	0.08	0.04
	4'-OH-bupropion	0.11	0.9	0.07	0.37
	Total R-BUP CL_{int}		11.9		
S-Bupropion	S,S-hydroxybupropion	0.81	7.0	0.12	0.06
	S,S-threohydrobupropion	5.6	49	0.82	0.41
	R,S-erythrohydrobupropion	0.25	2.1	0.04	0.02
	4'-OH hydroxybupropion	0.13	1.1	0.02	0.01
	Total S-BUP CL_{int}		59.2		

[a] S9 fraction intrinsic clearance values were scaled to hepatic intrinsic clearance ($CL_{int,H}$) using the scaling factor of 96.1 mg protein/g liver (Watanabe et al., 2009). 1500g was used as the liver weight and 21.4g liver/kg body weight (Ito and Houston, 2005). Protein binding in the incubations was negligible so $CL_{int,\ H}$ values are equivalent to unbound $CL_{int,H}$. [b] The fraction of the metabolism of a given bupropion enantiomer was calculated ($f_{m,\ enantiomer}$) was calculated from the ratio of the $CL_{int,H}$ of a given metabolite scaled from S9 fractions to the sum of all of the scaled S9 formation clearances for the respective substrate. [c] The fraction of total bupropion metabolism (fm) attributed to each elimination pathway was calculated from the ratio of the $CL_{int,H}$ of a given metabolite(s) in S9 fractions to the sum of all of the S9 formation clearances.

Table 3.3. IC_{50} values of ticlopidine for CYP2B6, CYP2C19 and 11β-HSD-1 in the presence and absence of a 30 minute preincubation in NADPH in HLM. Values are expressed as mean (95% CI).

Metabolite	Primary Enzyme	IC_{50} (μM) -NADPH	IC_{50} (μM) + NADPH	Fold Shift
OH-bupropion	CYP2B6	0.53 (0.4-0.8)	0.07 (0.1-0.2)	7.6
4'-OH-bupropion	CYP2C19	0.9 (0.3-3)	0.14 (0.4-1)	6.4
Threohydrobupropion	11β-HSD-1	10.2 (6-24)	4.9 (2.4-10)	2.1
Erythrohydrobupropion	11β-HSD-1	12 (4-24)	4.4 (2.1-9.3)	2.7

OH-bupropion and 4'-OH-bupropion formation were used as a measure of CYP2B6 and CYP2C19 activity, respectively. Based on previous reports, the formation of threohydrobupropion and erythrohydrobupropion in HLM were attributed to 11β-HSD-1 (Meyer et al., 2013; Skarydova et al., 2013). Ticlopidine IC_{50} values were based on measured ticlopidine concentrations prior to the 7 min bupropion incubation. Ticlopidine f_u in 0.5mg/mL HLM was 0.13, so the unbound IC_{50} values were 0.069 (OH-bupropion), 0.12 (4'-OH-bupropion), 1.3 (threohydrobupropion) and 1.5 (erythrohydrobupropion) μM.

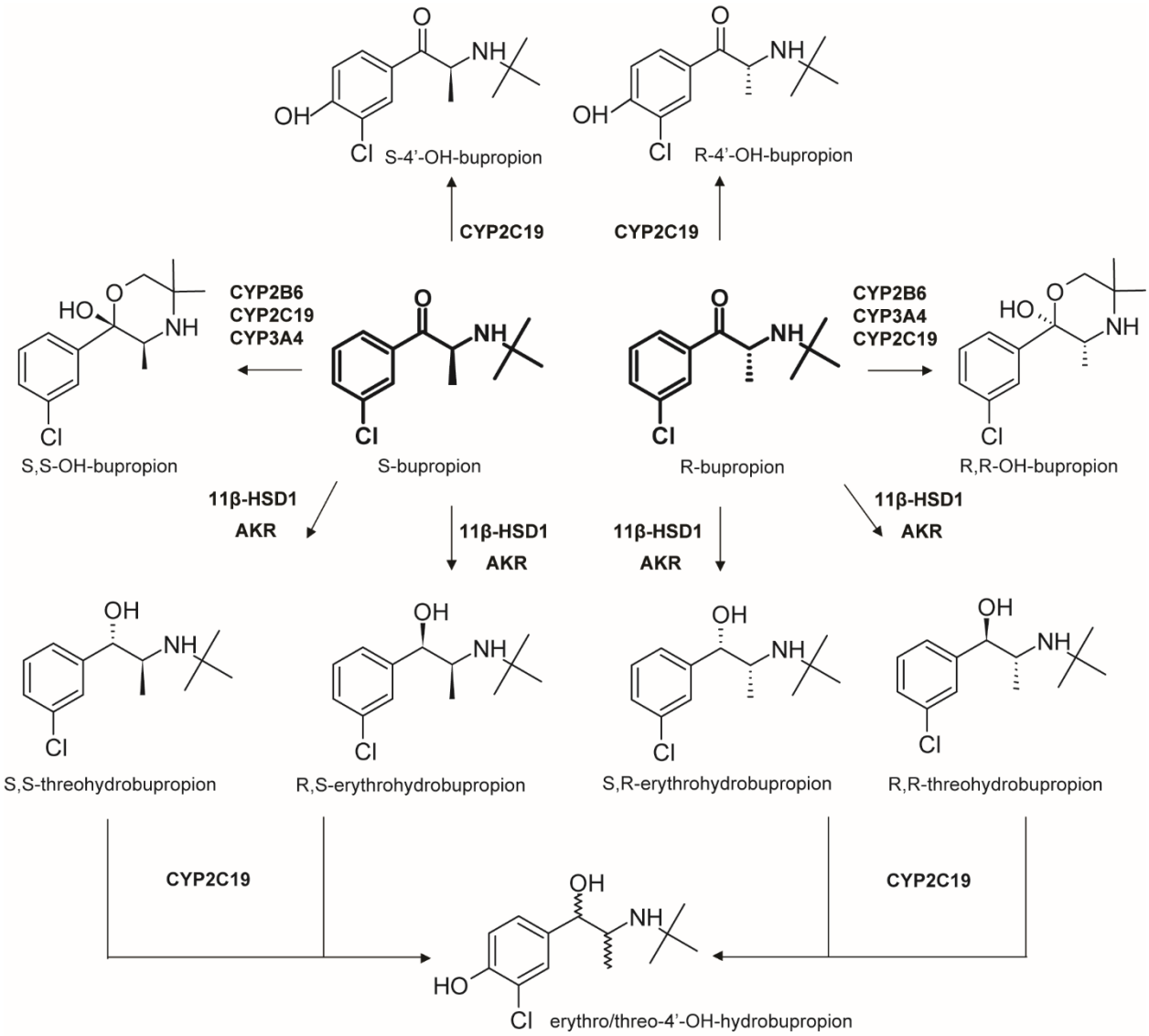

Figure 3.1. Proposed Bupropion Metabolic Scheme. Bupropion is administered as a racemate and undergoes stereoselective metabolism in vitro. Metabolites include R,R-OH-bupropion, S,S-OH-bupropion, S,S-threohydrobupropion, R,R-threohydrobupropion, S,R-erythrohydrobupropion and R,S-erythrohydrobupropion (Bondarev et al., 2003). Formation of OH-bupropion is attributed primarily to CYP2B6 but the minor involvement of CYP2C19 and CYP3A4 has also been reported (Chen et al., 2010; Coles and Kharasch, 2008; Faucette et al., 2000). Formation of threo- and erythrohydrobupropion is catalyzed primarily by 11β-HSD1 (Connarn et al., 2015; Skarydova et al., 2013). Additionally, bupropion is metabolized to 4'-OH-bupropion via CYP2C19 (Sager et al., 2016). Formation of erythro-4'-OH-hydrobupropion from erythrohydrobupropion and threo-4'-OH-hydrobupropion from threohydrobupropion is catalyzed exclusively by CYP2C19 (Sager et al., 2016).

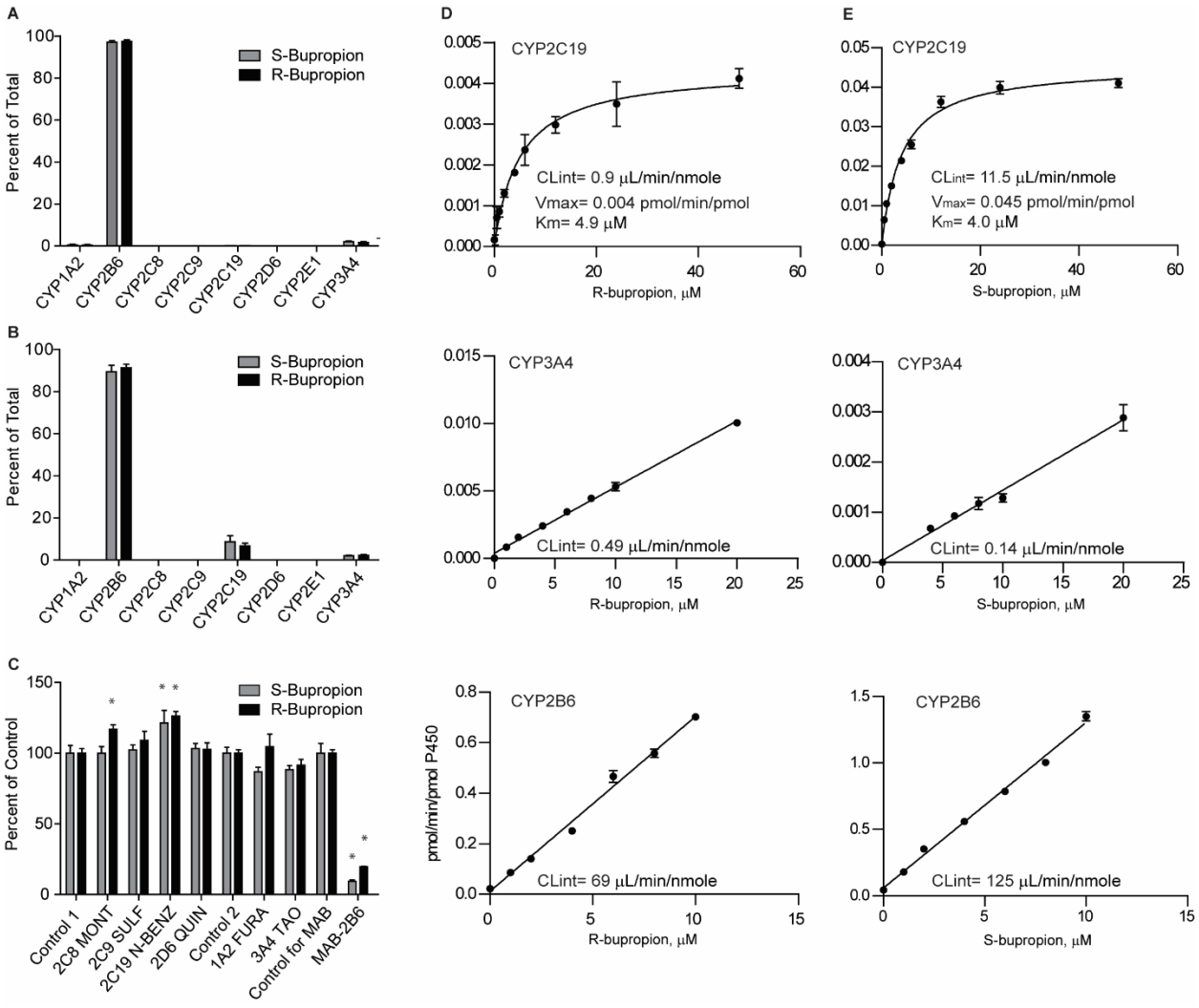

Figure 3.2. The contribution of individual P450s to S,S and R,R-OH-bupropion formation and formation kinetics in recombinant enzymes. OH-bupropion formation following R- or S- bupropion incubation in a P450 supersome panel using 100µM (A) or 1µM (B) substrate. (C) The percent of control OH-bupropion formation upon incubation of 1 µM R- or S-bupropion in the presence of specific P450 inhibitors and a CYP2B6 inhibitory antibody (MAB-2B6). Control 1 is the control for the reversible inhibitors montelukast (2C8 MONT) sulfaphenazole (2C9 SULF), (+)-N-3-benzylnirvanol (2C19 N-BENZ) and Quinidine (2D6 QUIN). Control 2 is the control for time dependent inhibitors troleandomycin (3A4 TAO) and furaphylline (1A2 FURA). * $p<0.05$, one- way ANOVA. (D) Formation kinetics of R,R-OH-bupropion in CYP2C19, CYP3A4 and CYP2B6 supersomes upon incubation with R-bupropion. (E) Formation kinetics of S,S-OH-bupropion in CYP2C19, CYP3A4 and CYP2B6 supersomes upon incubation with S-bupropion.

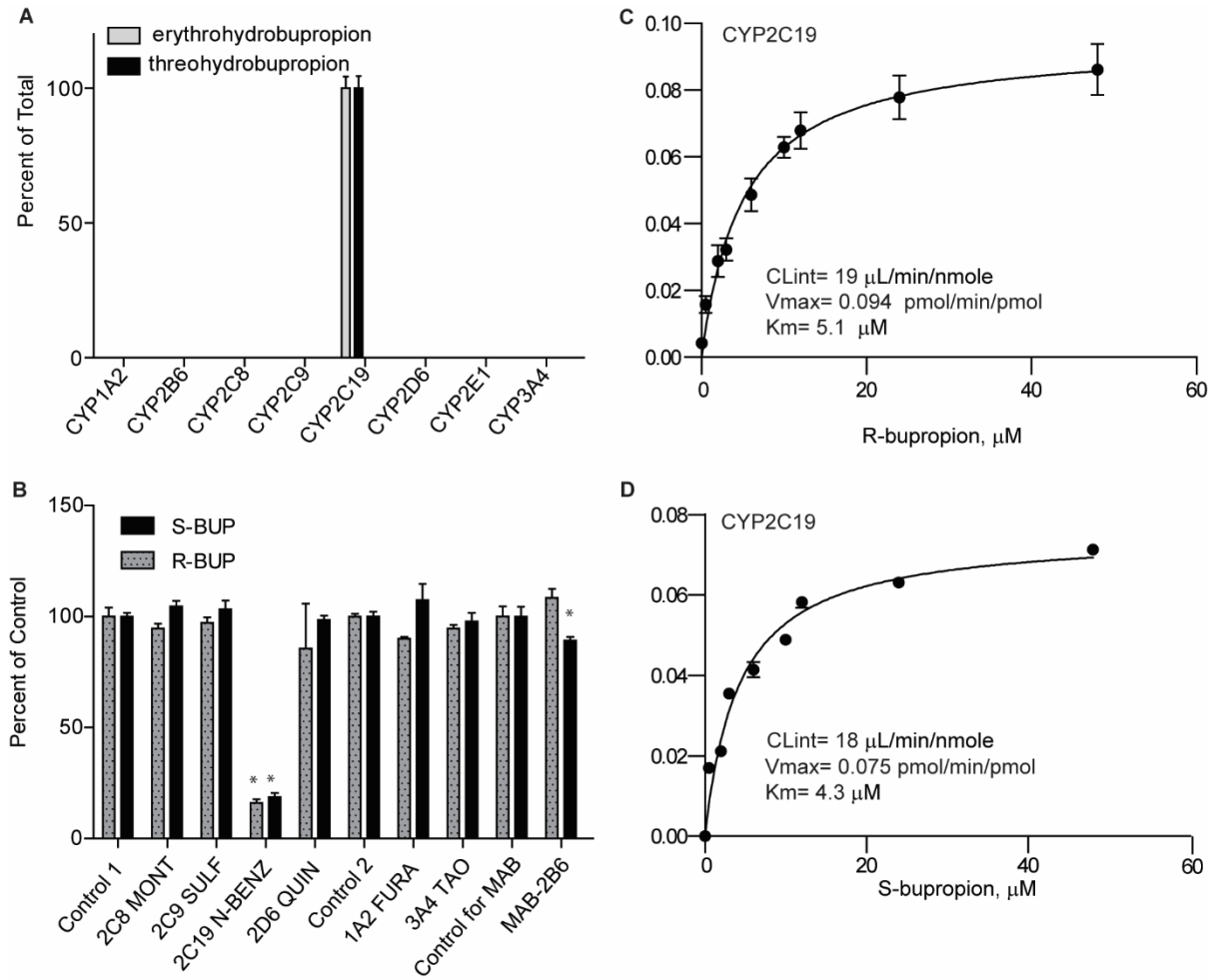

Figure 3.3. The contribution of individual P450s involved in 4'-OH-bupropion formation recombinant enzyme formation kinetics. (A) 4'-OH-bupropion following bupropion (1 µM) incubation in a panel of P450 supersomes. (B) 4'-OH-bupropion formation, as a percent of control following incubation of R- or S- bupropion in HLM in the presence of selective P450 inhibitors or a CY2B6 inhibitory antibody (MAB-2B6). Saturation plot of 4'-OH-bupropion formation from R-bupropion in CYP2C19 supersomes. (D) Saturation plot of 4'-OH-bupropion formation upon incubation of S-bupropion in CYP2C19 supersomes. (C) *$p<0.05$ one-way ANOVA.

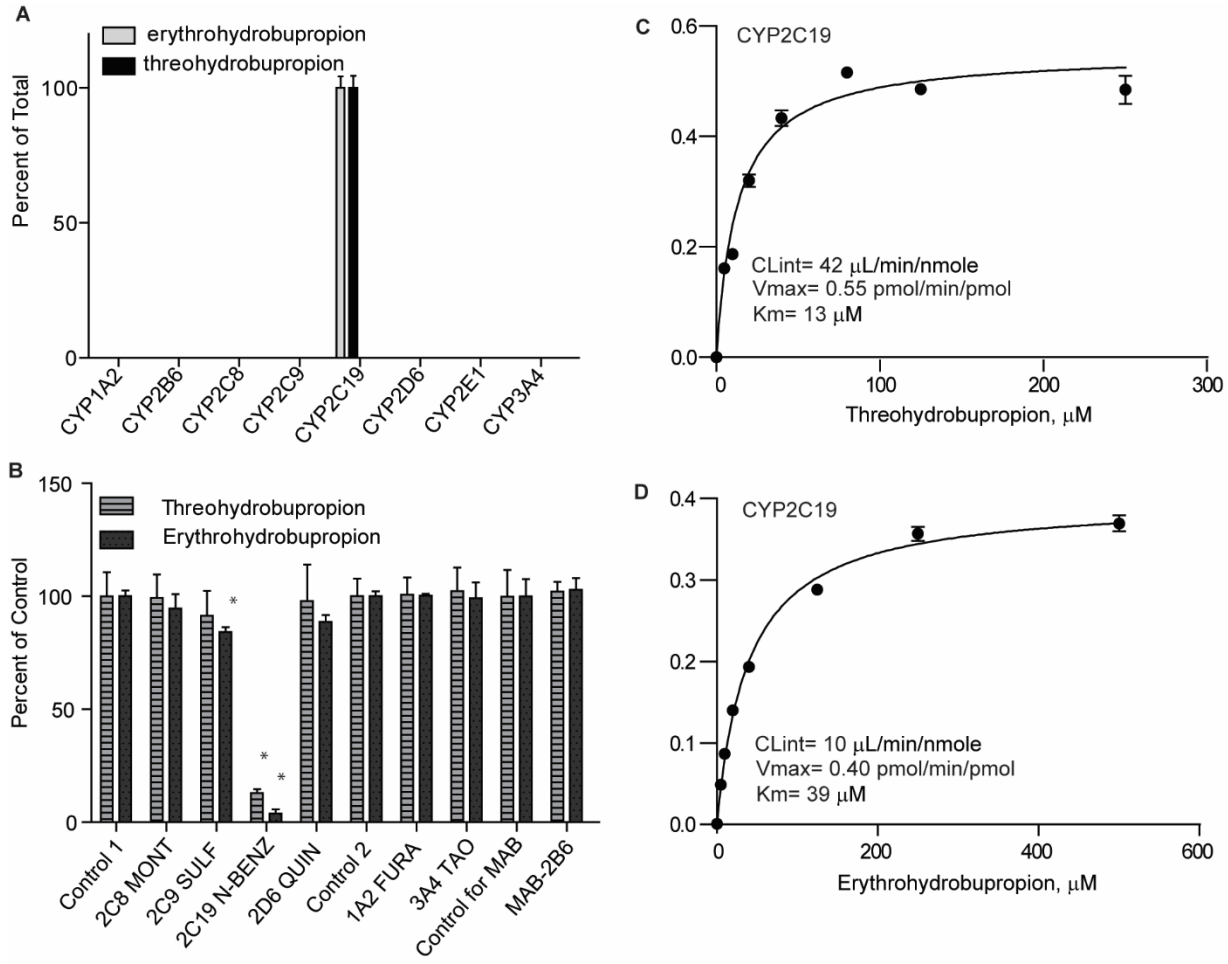

Figure 3.4. Relative contribution of individual P450 isoforms to the formation of threo-4'-OH-hydrobupropion and erythro-4'-OH-hydrobupropion. (A) Erythro- and threo-4'-OH-hydrobupropion formation following incubation of erythro- and threohydrobupropion, respectively, in a panel of P450 supersomes. (B) Formation of threo-4'-OH-bupropion and erythro-4'-OH-bupropion as a percent of control following incubation of threo- or erythrohydrobupropion (1 μM) in the presence of selective P450 inhibitors or MAB-2B6. (C and D) Formation of threo-4'-OH-hydrobupropion (C) and erythro-4'-OH-hydrobupropion (D) in CYP2C19 supersomes following incubation of threo- and erthrohydrobupropion, respectively. *$p<0.05$ one-way ANOVA.

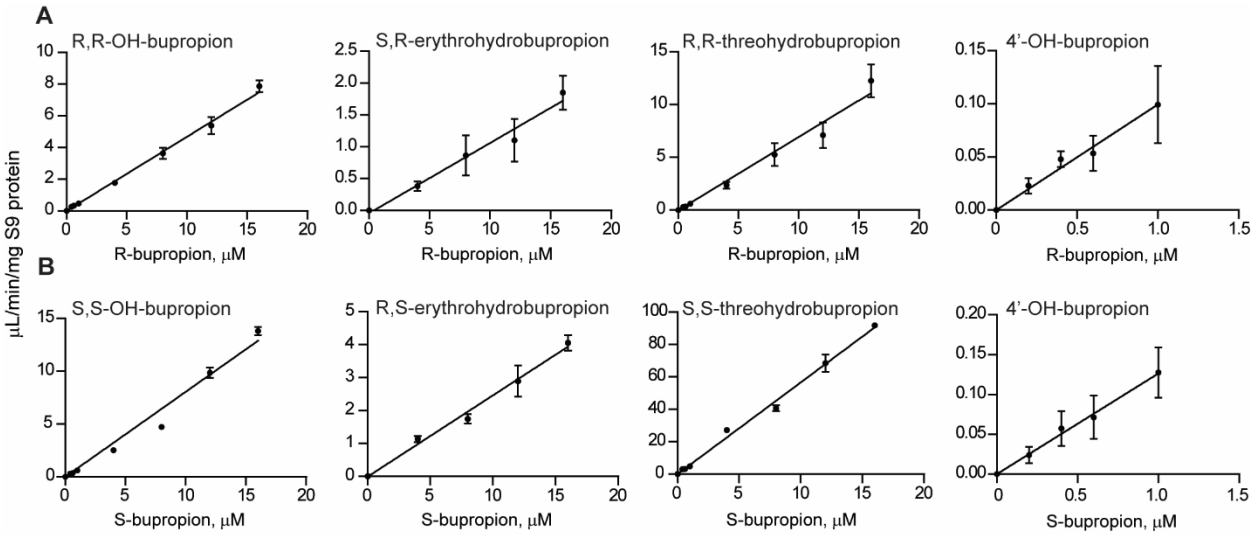

Figure 3.5. Kinetic Characterization of Bupropion Metabolite Formation in Human Liver S9 Fractions. (A) Formation of R,R-OH-bupropion, S,R-erythrohydrobupropion, R,R-threohydrobupropion and 4'-OH-bupropion from R-bupropion in S9 fractions. (B) Formation of S,S-OH-bupropion, R,S-erythrohydrobupropion, S,S-threohydrobupropion and 4'-OH-bupropion following incubation of S-bupropion in S9 fractions.

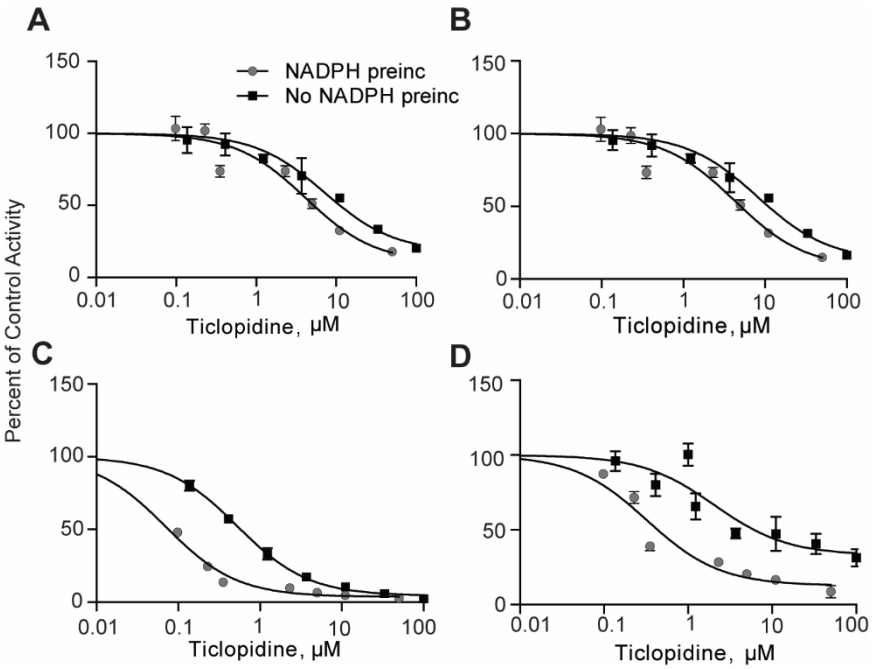

Figure 3.6. NADPH-dependent IC_{50} shifts for ticlopidine following a 30 minute preincubation in the presence or absence of NADPH. IC_{50} shifts for ticlopidine for 11β-HSD-1 catalyzed (A) erythrohydrobupropion formation and (B) threohydrobupropion formation in HLM. IC_{50} shifts for ticlopidine for (C) CYP2B6 catalyzed OH-bupropion formation and (D) CYP2C19 catalyzed 4'-OH-formation.

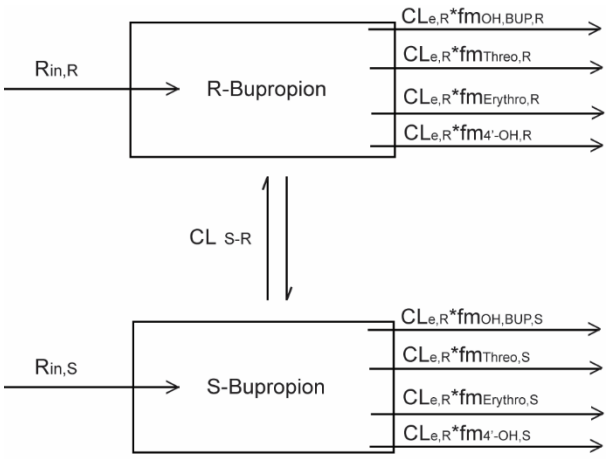

Figure 3.7. Illustration of the Simbiology Model of R- and S-bupropion. $R_{in,\,R}$ and $R_{in,\,S}$ are the steady state constant rate inputs of R and S bupropion, respectively (75 mg/hr). $CL_{e,\,R}$ (12.4 L/hr) and $CL_{e,\,S}$ (43.5 L/hr) are the hepatic clearances of R- and S-bupropion, respectively. The $fm_{OH\text{-}BUP,R}$ (0.34) and $fm_{OH\text{-}BUP,S}$ (0.12) are the fractions of R- or S-bupropion, respectively, metabolized to OH-bupropion based on ($fm_{enantiomer}$ from Table 2). The $fm_{Threo,R}$ (0.50) and $fm_{Threo,S}$ (0.82) are the fractions of R- or S-bupropion, respectively, metabolized to threohydrobupropion ($fm_{enantiomer}$ from Table 2). The fraction of R- or S-bupropion metabolized to erythrohydrobupropion is described by $fm_{Erythro,R}$ (0.08) and $fm_{Erythro,S}$ (0.04), respectively while the fraction of R- and S-bupropion metabolized to 4'-OH-bupropion is represented by $fm_{4'\text{-}OH,R}$ (0.07) and $fm_{4'\text{-}OH,S}$ (0.02) ($fm_{enantiomer}$ from Table 2). Simulations were performed in the absence of isomerization or in the presence of a reversible isomerization clearance, $CL_{S\text{-}R}$ (18 values ranging from 0.2-10 L/hr).

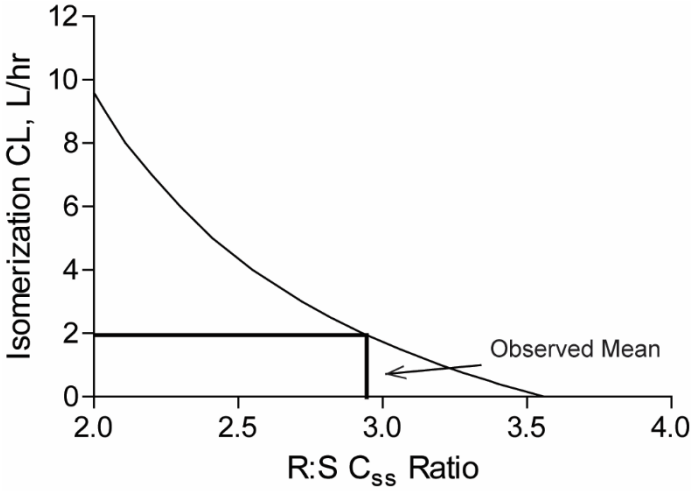

Figure 3.8. The relationship between isomerization clearance and the predicted ratio of the steady state concentrations of R and S- bupropion. The black vertical line indicates the observed mean ratio, and the black horizontal line denotes the isomerization clearance value (2L/hr) at which the observed R to S ratio is achieved.

Chapter 4.

SIMULTANEOUS REVERSIBLE INHIBITION AND DOWN REGULATION OF CYP2D6 BY BUPROPION AND ITS METABOLITES EXPLAINS THE STRONG CYP2D6 INHIBITION IN VIVO

This chapter was submitted, in part, to *Biochemical Pharmacology*

4.1 ABSTRACT

Bupropion is a widely used antidepressant and smoking cessation aid and a strong inhibitor of CYP2D6 in vivo. However, bupropion and its metabolites are weak inhibitors of CYP2D6 in vitro, and the magnitude of the in vivo drug-drug interactions (DDI) cannot be explained by the in vitro data. The aim of this study was to quantitatively explain the in vivo CYP2D6 DDI magnitude caused by bupropion. Bupropion and its metabolites were found to inhibit CYP2D6 stereoselectively with up to 10-fold difference in inhibition potency between enantiomers. However, the reversible inhibition or active uptake to hepatocytes did not explain the in vivo DDIs. The in vivo DDI was quantitatively predicted by significant downregulation of CYP2D6 mRNA and activity in human hepatocytes by bupropion and its metabolites. This study is the first example of a DDI resulting from P450 downregulation and first demonstration of a CYP2D6 interaction resulting from transcriptional regulation.

4.1 INTRODUCTION

Reliable identification of drug-drug interaction (DDI) risk and accurate prediction of the magnitude of clinical DDIs from in vitro data is critical in drug development. The decision to conduct dedicated DDI studies and the design of the DDI studies during new drug development depend on accurate identification of DDI risk (European Medicines Agency Committee for Medicinal Products for Human Use, 2012; Jones et al., 2015; Shardlow et al., 2013; U.S. Food and Drug Administration Center for Drug Evaluation and Research (CDER), 2012; Zhang et al., 2009). The cornerstone of DDI predictions is in vitro to in vivo extrapolation (IVIVE) of DDIs arising from reversible P450 inhibition, and in vivo DDI risk is generally identified once all inhibitory species, including metabolites, are accounted for (Fahmi et al., 2009; Templeton et al., 2010; Vieira et al., 2014; Yeung et al., 2011). Similarly, DDI risk is usually identified for time dependent inhibitors, transporter mediated DDIs and for DDIs involving P450 induction (Baneyx et al., 2014; Chen et al., 2015; Einolf et al., 2014; Fahmi et

al., 2008; Rajoli et al., 2014; Rekic et al., 2011; Varma et al., 2012, 2013, 2015b; Zhao and Hu, 2014) but quantitative predictions in these areas are still challenging (Jones et al., 2015; Varma et al., 2015a). Nevertheless, trust in DDI risk identification is still overshadowed by clinically observed DDIs that cannot be predicted from in vitro data despite considerable in vitro research efforts. An example of such DDI is the strong inhibition of CYP2D6 by bupropion in vivo, which cannot be predicted using current in vitro data.

Bupropion is a commonly used norepinephrine and dopamine reuptake inhibitor approved for use as an antidepressant (Wellbutrin) (U.S. Food and Drug Administration Center for Drug Evaluation, 2013a), a smoking cessation aid (Zyban) (U.S. Food and Drug Administration Center for Drug Evaluation, 1997) and a weight loss therapy in combination with naltrexone (Contrave) (U.S. Food and Drug Administration, Center for Drug Evaluation and Research, 2014). Bupropion is a strong in vivo CYP2D6 inhibitor increasing desipramine AUC by 5.2-fold (Reese et al., 2008; U.S. Food and Drug Administration Center for Drug Evaluation, 2001). Bupropion also increases methamphetamine (Newton et al., 2005) and venlafaxine (Kennedy et al., 2002) exposures 1.5- and 3-fold, respectively, and dextromethorphan/dextrorphan urinary ratio significantly (Kotlyar et al., 2005). Considering the fractional contribution (f_m) of CYP2D6 in the clearance of desipramine (0.9) (Brøsen et al., 1993; Ito et al., 2005) and venlafaxine (0.8) (Nichols et al., 2011; Preskorn et al., 2009) these DDIs can be explained by approximately 90% decrease in CYP2D6 activity.

It has been widely accepted that inhibition of CYP2D6 by the major circulating metabolites of bupropion, hydroxybupropion (OH-bupropion), threohydrobupropion and erythrohydrobupropion, can partially explain the in vivo CYP2D6 inhibition (Lutz and Isoherranen, 2012a; Sager et al., 2014; Shirasaka et al., 2013; Templeton et al., 2010; Yeung et al., 2011; Yu and Tweedie, 2013). While CYP2D6 DDI risk is missed when only bupropion is considered for DDI risk assessment, the DDI risk is captured when bupropion and its circulating metabolites are included in DDI risk assessment (Reese et al., 2008; Yeung et al., 2011). However, only a 1.4-fold increase in desipramine AUC is predicted

(Reese et al., 2008), in comparison to the observed 5.2-fold increase demonstrating a concerning 5-fold underprediction of the in vivo DDI. Liver partitioning of bupropion and its metabolites, based on whole body autoradiography studies in rats has been proposed to explain the underprediction, but even after accounting for 5-9-fold higher liver than plasma concentrations of bupropion and its metabolites only a 2.9 to 3.8-fold increase in desipramine AUC is predicted. As such, existing IVIVE methods for DDI predictions have failed to appropriately identify the clinical DDI risk of bupropion.

We hypothesized that the reason for the failure to predict CYP2D6 inhibition by bupropion is due to incomplete understanding of the stereoselective disposition and CYP2D6 inhibition by bupropion and its metabolites and lack of information of the effects of bupropion on CYP2D6 expression. The aim of this study was to quantitatively explain the in vivo CYP2D6 inhibition by bupropion through characterization of the stereoselective disposition of bupropion and the effects of bupropion and its metabolites on CYP2D6 transcription. The data shows that downregulation of CYP2D6 by bupropion and its metabolites together with reversible inhibition quantitatively explain the in vivo CYP2D6 inhibition and resolves the long standing concern over the lack of predictability of this strong DDI.

4.2 MATERIALS AND METHODS

4.2.1 Chemicals and Reagents

Bupropion and its metabolites were purchased from Toronto Research Chemicals (Ontario, Canada), α-OH-midazolam-d_4 from Cerilliant (Round Rock, TX) and dextromethorphan, dextrorphan, and Krebs-Henseleit buffer from Sigma-Aldrich (St. Louis, MO). Cryopreserved human suspension hepatocytes (Hu4010, Male age 53) and all other reagents, solvents and buffers were purchased from Thermo Fisher Scientific (Waltham, MA). Human liver microsomes (HLM) from 4 CYP2C19 and CYP2D6 extensive metabolizer donors based on genotypes were obtained from the University of Washington Human Liver Bank

(Seattle, WA). Cyroplateable human hepatocytes (HC2-34, HC2-31 and HC3-38) and hepatocyte isolation kits K2000 were obtained from Xenotech (Kansas City, KS).

4.2.2 Clinical Study

The clinical study was approved by the University of Washington institutional review board. 5 female subjects (3 white and 2 unknown) participated in this study after providing written informed consent. The average body weight was 108±23 kg, the average age was 35±6 years and the average height was 153±5cm). Subjects taking CYP2B6 inhibitors or inducers were excluded from the study. All subjects were taking bupropion XL chronically (150-450 mg/day) for therapeutic reasons and had a single blood sample drawn midway through a steady state dosing interval. Plasma was isolated from blood by centrifugation for 10 min at 1000g and stored at -80 until analysis.

4.2.3 Determination of unbound fractions

Protein binding in plasma or HLM (0.1mg/mL) was determined using ultracentrifugation as described (Shirasaka et al., 2013). Due to the isomerization of bupropion (Coles and Kharasch, 2008), racemic bupropion was added to plasma or HLM and the individual enantiomers were measured. Concentrations of analytes in HLM and plasma approximated their IC_{50} values and $C_{ss,avg}$ values, respectively; 20µM and 0.5µM (bupropion), 6µM and 3µM (R,R-OH-bupropion), 15µM and 0.2 µM (S,S-OH-bupropion, 12.5µM and 2µM (threohydrobupropion), 5µM and 0.5µM (erythrohydrobupropion). Samples were quenched with an equal volume of acetonitrile (HLM incubations) or 2x volume 1:3 methanol:acetonitrile (plasma) containing 100nM OH-bupropion-d_6, bupropion-d_9 and threohydrobupropion-d_9 as internal standards.

4.2.4 Suspension Hepatocyte Partitioning and IC_{50} Determination.

Cells were thawed and isolated using hepatocyte isolation kit (K2000, Xenotech) according to the manufacturer's protocol. Cell count and viability were determined using Trypan Blue staining. Hepatocytes were resuspended in protein free Krebs-Henseleit Buffer. For cell partitioning measures, bupropion, OH-bupropion, threohydrobupropion or erythrohydrobupropion (1µM) were incubated with hepatocytes ($1x10^5$ cells) in a final volume of 100µL. After 30min, cells were pelleted by centrifugation at 100g for 5 min. The media was removed and quenched with 100µL of acetonitrile containing 100nM OH-bupropion-d_6, bupropion-d_9 and threohydrobupropion-d_9. The cell pellet was washed with fresh media, centrifuged and the cell pellet was extracted with 100µL acetonitrile. The concentration of analyte in the media and cells was determined by dividing the amount of the analyte by the volume of media (93uL) or cells (3.9uL per $1x10^6$ cells) (Reinoso et al., 2001), respectively. For IC_{50} determination, incubations were performed at 37°C in protein-free Krebs-Henseleit Buffer containing $1x10^5$ cells, 1µM dextromethorphan as the substrate and bupropion, OH-bupropion, threohydrobupropion, or erythrohydrobupropion (0.13- 500µM) in a final volume of 100µL. Reactions were initiated with the addition of hepatocytes to a pre-warmed mixture of inhibitor and substrate and terminated after 30 min by the addition of 100µL of acetonitrile containing 100 nM OH-bupriopion-d_6. Linear formation of dextromethorphan and absence of substrate depletion within the incubation time was confirmed.

4.2.5 IC_{50} Determination in HLM

To determine IC_{50}-values towards CYP2D6, bupropion and its metabolites (0.5–1000 µM) were incubated with HLM (0.1 mg/ml) in 100 mM potassium phosphate buffer (KPi; pH 7.4) with dextromethorphan (1 µM) in 100 µl., The mixtures were preincubated for 5 minutes at

37°C before initiating reactions with NADPH (1mM, final). Reactions were terminated after 5 minutes by adding an equal volume of acetonitrile containing 100 nM α-OH-midazolam-d_4 internal standard. Interconversion of S- and R-bupropion was <5% in the incubations.

4.2.6 HepG2 Cell Culture

HepG2 cells were cultured in 6-well plates (Corning Life Sciences, Corning, NY) as described (Tripathy et al., 2016). Cells were treated with vehicle (0.1% ethanol), bupropion (0.5µM, 2.5µM, 5 µM), R,R-OH-bupropion (5µM, 25µM, 50µM), S,S-OH-bupropion (0.5µM, 2.5µM, 5µM), erythrohydrobupropion (0.5µM, 2.5µM, 5µM) or threohydrobupropion (2µM, 10µM, 20µM) for 72 hours. The concentrations were approximately 1X, 5X and 10X the C_{ss} following 300mg/day bupropion dosing. Every 24 hours, media was aspirated and replaced with new media containing the test compound(s). At 72 hours, media was quenched with 1:3 methanol: acetonitrile containing 1µM bupropion-d_9, threohydrobupropion-d_9 and OH-bupropion-d_9 as internal standards and cells were harvested for mRNA analysis.

4.2.7 Human Hepatocyte Culture

Cryopreserved human hepatocytes from three donors (3 females, 52, 45 and 9 years of age) were obtained from Xenotech (Lenexa, KS) and cultured as described (Tripathy et al., 2016). Donors were chosen based on cell viability (>85%) and extensive CYP2D6 metabolism. Cells were treated in triplicate with vehicle (0.01% ethanol) or bupropion and its metabolites at concentrations approximately 5x $C_{ss,avg}$; 2.5 µM for bupropion, erythrohydrobupropion and S,S-OH-bupropion, 10 µM for threohydrobupropion and 25 µM for R-R-OH-bupropion. Media was changed daily and after 3 days of treatment media was collected for LC/MS analysis and cells harvested for analysis of CYP2D6 mRNA expression. CYP2D6 activity and inhibition were

measured in a one hour incubation with 1µM dextromethorphan and vehicle or test compounds. Following the 1 hour incubation, the incubation media was added to an equal volume of 1:3 methanol:acetonitrile containing 1µM bupropion-d_9, threohydrobupropion-d_9 and OH-bupropion-d_9 as internal standards. Dextrorphan formation and media concentrations of bupropion and its metabolites were measured by LC/MS. The inhibition experiment was repeated after 71 hours of treatment as described for the initial assay.

4.2.8 mRNA Analysis

CYP2D6 and SHP mRNA were quantified using q-RT-PCR (StepOnePlus™, Applied Biosystems, Carlsbad, CA) as previously described using GAPDH as a housekeeping control (Tripathy et al., 2016). Cells were harvested using Tri-reagent (Invitrogen, Grand Island, NY) and mRNA extracted according to the manufacturer's recommendations. All samples were analyzed in triplicate.

4.2.9 Analysis of Bupropion and its Metabolites in Human Plasma and Urine.

Plasma samples (40 µL for chiral assay and 10 µL for non-chiral analysis) were protein precipitated with 3:1 acetonitrile:methanol (160µL and 190 µL respectively) containing 100nM OH-bupropion-d_6, bupropion-d_9, and threohydrobupropion-d_9 and centrifuged for 40 minutes at 3000g.

4.2.10 LC/MS/MS Quantification Methods.

The concentrations of analytes were determined using an LC/MS/MS system consisting of an AB-Sciex API 4500 triple quadrupole mass spectrometer (AB Sciex, Foster City, CA) coupled with an LC-20AD ultra-fast liquid chromatography system (Shimadzu Co., Kyoto, Japan). The turbo ion spray interface was operated in positive ion mode and an Agilent

ZORBAX XDB-C18 column (50 x2.1mm, 5µm) was used for analyte separations in incubations and protein binding assays using a previously described gradient method (Shirasaka et al., 2013). Dextromethorphan, dextrorphan, and α-OH-midazolam-d4 were analyzed as described (Lutz and Isoherranen, 2012a). Bupropion and OH-bupropion enantiomer concentrations in plasma were determined using an α-acid glycoprotein column (100 x 2 mm, 5 µm) with a guard cartridge (10 x 2 mm, 5µm) (ChromTech, Apple Valley, MO) . The mobile phase consisted of 20 mM ammonium formate, pH 5.7 (A) and methanol (B). A gradient elution at 0.22 mL/min starting at 10% B, increasing to 21.2% B by 25 min and 23.5% B by 34 minutes was used with re-equilibration to initial conditions by 45 min. Concentrations of bupropion, OH-bupropion, threohydrobupropion, erythrohydrobupropion in cell media were measured using an Agilent ZORBAX XDB-C18 column (150 x 4.6 mm, 5 µm) as previously described (Connarn et al., 2015). Bupropion and its metabolites were detected with the following MRM mass transitions (*m*/*z*): 240→184 (bupropion), 249→189 (bupropion-d_9), 256→238 (OH-bupropion), 262→244 (OH-bupropion-d_6), 242→168 (threo- and erythrohydrobupropion), 251→168 (threohydrobupropion-d_9).

4.2.11 Drug-drug Interaction Predictions

DDI risk due to reversible inhibition was determined using $[I]_u/Ki,_u$ ratios where $[I]_u$ is the unbound inhibitor concentration at steady state. The unbound IC_{50} values are assumed to approximate the $K_{i,u}$ values since the concentration of dextromethorphan used was well below the reported K_m value for CYP2D6 (Lutz and Isoherranen, 2012b). Due to variable dosing regimens between clinical subjects, bupropion and metabolite concentrations were normalized to 300mg dose, based on dose-linear kinetics (U.S. Food and Drug Administration Center for Drug

Evaluation and Research, 2003). The percent inhibition of CYP2D6 due to reversible inhibition was predicted using equation 4.1.

$$percent\,CYP2D6\,inhibition = \left(1 - \frac{1}{1 + \frac{[I]_u}{K_i}}\right) * 100 \qquad \text{Equation 4.1}$$

In order to account for CYP2D6 downregulation in static predictions a previously published equation to predict simultaneous reversible inhibition and induction (Fahmi et al., 2008) was modified to account for fold downregulation as opposed to fold induction (equation 4.2).

$$percent\,CYP2D6\,inhibition = \left(1 - \left(\frac{1}{1 + \frac{[I]_u}{K_i}} * (\,fold\ downregulation)\right)\right) * 100 \qquad \text{Equation 4.2}$$

4.2.12 Data Analysis

All experiments were performed in triplicate and data is presented as the mean and standard deviation unless otherwise specified. IC_{50} values were estimated by fitting Equation 4.3 to the data where v_I and v_o are the formation velocity in absence and presence of an inhibitor at a given inhibitor concentration (I). In vitro constants were calculated using nonlinear least-squares analysis in GraphPad Prism (San Diego, CA).

$$v_{I=} v_{0\left(1-\frac{I}{IC_{50}+I}\right)} \qquad \text{Equation 4.3}$$

One-way ANOVA with posthoc Tukey test was used to test for significance of changes in CYP2D6 mRNA and activity.

4.3 RESULTS

Steady-state plasma concentrations of the stereoisomers of bupropion and its metabolites were measured in five subjects taking 150-450 mg/day bupropion (Wellbutrin XL) chronically for therapeutic reasons. The observed plasma concentrations, mean dose-normalized concentrations and plasma unbound fractions are shown in Table 4.1. Consistent with reported concentrations following a single dose (Kharasch et al., 2008), the steady state average concentration ($C_{ss,avg}$) of R-bupropion was approximately 3-fold higher ($p<0.05$) than that of S-bupropion, and the R,R-OH-bupropion $C_{ss,avg}$ was 13-fold higher ($p<0.05$) than that of S,S-OH-bupropion. In addition, all metabolites had circulating concentrations equal to or higher than that of bupropion (Table 4.1) suggesting a need for characterization of the inhibition potential of each metabolite.

Bupropion, and OH-bupropion enantiomers and threo- and erythrohydrobupropion inhibited CYP2D6 in HLMs with IC_{50} values between 3 and 40 μM (Table 4.2). There was a marked difference in the inhibition potency between the enantiomers of bupropion and OH-bupropion. R-bupropion had a 14-fold higher IC_{50} value than S-bupropion while S,S-OH-bupropion had a 3-fold higher IC_{50} value than R,R-OH-bupropion. Similarly, erythrohydrobupropion was nearly 10-fold more potent than threohydrobupropion. Using the unbound stereoselective IC_{50} values and the circulating concentrations calculated for 300 mg/day dosing of bupropion, the CYP2D6 DDI risk was identified assuming reversible inhibition of CYP2D6 by all compounds (Table 4.2). Each compound alone was predicted to result in only 0.3-34% inhibition of CYP2D6 with all circulating compounds together resulting in a predicted 43% (31-57%) decrease ($\sum I_u/IC_{50,u}$ 0.76) in CYP2D6 activity in vivo (Table 4.2) suggesting only weak CYP2D6 inhibition in vivo.

To determine whether the underprediction was due to the accumulation of free compounds within hepatocytes, CYP2D6 inhibition and cell partitioning were assessed in human suspension hepatocytes. The cell to media ratios showed 20-fold partitioning for bupropion, 11-fold partitioning for OH-bupropion and threohydrobupropion and 9-fold partitioning for erythrohydrobupropion into hepatocytes but the high partitioning did not decrease media concentrations of the inhibitors due to the small overall volume of the cells. Despite the partitioning, the IC_{50} values were not different between suspension hepatocytes and HLM suggesting that the partitioning is a result of intracellular binding or trapping of bupropion and its metabolites within intracellular organelles, rather than active uptake of the free drug. The IC_{50} values in suspension hepatocytes were 18 µM (90% C.I.:14-22µM) for bupropion, 14µM (90% C.I.:12-17µM) for OH-bupropion, 12µM (90% C.I.:8.6-16.6µM) for threohydrobupropion and 2.3µM (90% C.I.: 1.9-2.8µM) for erythrohydrobupropion. The IC_{50} values are based on the initial inhibitor concentrations in media.

It is possible that in suspension hepatocytes some uptake transporters are not localized correctly and hence, CYP2D6 inhibition was further assessed in plated human hepatocytes from three donors using concentrations of bupropion and its metabolites 5 times that of their mean C_{ss} values. In addition, changes in the inhibition potency over treatment time were evaluated in human hepatocytes with 72-hour treatment with bupropion or its metabolites. The mean percent CYP2D6 inhibition observed over the first hour of treatment in the presence of S,S-OH-bupropion, threohydrobupropion and erythrohydrobupropion was 2-4-fold greater than predicted from measured media concentrations and HLM $IC_{50,u}$ values (Table 4.3), suggesting that active uptake of these compounds may occur. However, the observed percent inhibition for bupropion, R,R-OH-bupropion and the mixture of all compounds was not different from predicted. Despite the

higher inhibition observed for some compounds, potential active uptake and/or hepatocyte partitioning were not sufficient to explain the in vivo DDI (Table 4.3). Interestingly, when hepatocytes were treated with bupropion for 72 hours, up to 3-fold increase in the magnitude of CYP2D6 inhibition was observed without any changes in inhibitor concentrations (Table 4.3) suggesting time-dependent changes in CYP2D6 activity possibly via downregulation of CYP2D6.

When tested in HepG2 cells, bupropion and all of its metabolites decreased CYP2D6 mRNA expression significantly in a dose-dependent manner (Figure 4.1). This downregulation was observed at concentrations exceeding circulating plasma concentrations, but likely due to nonspecific binding and inhibitor depletion, no significant downregulation was observed following treatment at initial concentrations approximating steady-state plasma concentrations. To test whether the downregulation of CYP2D6 by bupropion is due to similar mechanisms as has been described with all-trans retinoic acid (Koh et al., 2014), the induction of the small heterodimer partner (SHP) was assessed. However, bupropion and its metabolites had no effect on SHP mRNA (data not shown). Based on the results in HepG2 cells, downregulation of CYP2D6 was further assessed in plated human hepatocytes from three donors after 72 hours of treatment with bupropion and its metabolites alone or in a mixture at concentrations equivalent to 5 times the steady state concentrations. This was predicted to yield media concentrations comparable to the observed C_{ss} in plasma. Bupropion and its metabolites significantly ($P<0.05$) decreased CYP2D6 mRNA and activity in the plated hepatocytes (Figure 4.2a). The mean CYP2D6 mRNA levels following 72 hours of treatment were 20% (erythrohydrobupropion), 18% (threohydrobupropion), 28% (R,R-OH-bupropion), 26% (S,S-OH-bupropion), 15% (bupropion) and 7% (Mix) of the mRNA levels in vehicle treated cells (Figure 4.2). In the same treatments no significant differences were observed between the initial media concentrations added and the media concentrations at the end

of the treatment except for bupropion (93% reduction) and R,R-OH-bupropion (33% reduction) (Figure 4.2b). In bupropion-treated cells formation of bupropion metabolites was also detected in accordance with the significant depletion of bupropion (Table 4.4), but the concentrations of erythrohydrobupropion (0.08 µM), threohydrobupropion (1.4 µM), and OH-bupropion (0.12 µM) remained lower than those observed in circulation.

To assess whether simultaneous CYP2D6 inhibition and downregulation would allow for accurate DDI predictions, static prediction method (Fahmi et al., 2008) was modified to incorporate both reversible inhibition and fold CYP2D6 downregulation. Using the fold downregulation observed following treatment with the mixture of bupropion and its metabolites, a 96% decrease in CYP2D6 activity is predicted in vivo. For each of the individual compounds, 85% (bupropion), 80% (erythrohydrobupropion), 84% (threohydrobupropion), 82% (R,R-OH-bupropion) and 73% (S,S-hydroxybupropion) decreases in CYP2D6 activity are predicted. This magnitude of change in CYP2D6 activity is in agreement with the approximately 90% inhibition observed using desipramine and venlafaxine as CYP2D6 probes/substrates.

4.4 DISCUSSION

The DDI liability of bupropion has been attributed to its circulating metabolites as the inhibitory potency of bupropion towards CYP2D6 does not identify the in vivo DDI risk of bupropion (Callegari et al., 2013; Isoherranen et al., 2009; Yeung et al., 2011; Yu and Tweedie, 2013; Yu et al., 2015). However, no prior study has evaluated the stereoselective CYP2D6 inhibition by bupropion and its metabolites, and whether incorporating stereoselective disposition and CYP2D6 inhibition would improve DDI predictions or alter the identification of the main inhibitory species. Consistent with previous data demonstrating stereoselective disposition of bupropion and OH-

bupropion following a single oral dose (Kharasch et al., 2008), this study found that stereoselective disposition is also observed at steady state. Furthermore, CYP2D6 inhibition by bupropion and OH-bupropion was found to be stereoselective. S-bupropion, despite its 3-fold lower circulating concentration had a 5-fold higher I/K_i than R-bupropion due to the 14-fold more potent inhibition of CYP2D6 by S-bupropion than R-bupropion. In contrast, R,R-OH-bupropion was 3-fold more potent inhibitor of CYP2D6 than S,S-OH-bupropion. Due to the 13-fold higher steady state concentration of R,R-OH-bupropion in comparison to S,S-OH-bupropion it had a 36-fold higher I/K_i. In fact, R,R-OH-bupropion had the highest I/K_i value of all the compounds, 0.5, and approximately a third (34%) of the CYP2D6 inhibition was predicted to be caused by R,R-OH-bupropion. In previous studies, threohydrobupropion has been considered to be responsible for the majority of the CYP2D6 inhibition (Reese et al., 2008). However, the stereoselective data shows that in fact threohydrobupropion accounts only for approximately 14% and erythrohydrobupropion another 6% of the CYP2D6 inhibition in vivo. Of note, only threohydrobupropion and R,R-OH-bupropion I/K_i values were higher than the 0.1 cutoff for DDI risk assessment. Consistent with previous work, even after accounting for all the metabolite contributions, only weak in vivo CYP2D6 inhibition would be expected resulting in a significant underprediction of the DDI potential of bupropion.

Hepatic partitioning of the inhibitory species has been proposed as an explanation for the underprediction of the bupropion DDIs (Reese et al., 2008). In agreement with previous work that demonstrated hepatic partitioning of radioactivity following administration of labeled bupropion and OH-bupropion in rats, significant partitioning of bupropion and its metabolites into human hepatocytes was observed. Yet, the IC_{50} values in suspension hepatocytes were not different from human liver microsomes suggesting that high nonspecific binding to the hepatocyte protein or

sequestration to intracellular organelles rather than active uptake of bupropion into hepatocytes is responsible for the high liver partitioning. Interestingly, in plated hepatocytes the observed inhibition by bupropion, S,S-OH-bupropion, threohydrobupropion and erythrohydrobupropion was more than 2-fold higher than predicted, indicating potential active uptake. However, when CYP2D6 activity was evaluated following treatment with a combination of bupropion and its metabolites at 5x circulating concentrations, the observed and predicted percent inhibition were similar. This suggests that while the 2-fold increase in the inhibitory potency of bupropion and its metabolites in hepatocytes may be due to active uptake, the observed inhibition is not sufficient to explain the magnitude of the in vivo CYP2D6 interaction.

Evaluation of CYP2D6 inhibition by bupropion and its metabolites in plated hepatocytes also allowed for the determination of possible time-dependent changes in CYP2D6 inhibition during treatment. While bupropion and its metabolite concentrations in hepatocyte media were not significantly different between the 0 hour and 72-hour inhibition assays, the observed CYP2D6 inhibition was significantly greater after 72-hours than after 0 hours of treatment, suggesting that bupropion may alter CYP2D6 expression. Indeed, this study shows that bupropion and its metabolites downregulate CYP2D6 mRNA expression both in HepG2 cells and in human hepatocytes. However, the magnitude of change in mRNA levels (93% reduction) far exceeded the changes in CYP2D6 activity (60%). The discrepancy between the magnitude of change in CYP2D6 mRNA levels and CYP2D6 activity is likely due to differences in mRNA versus protein half-lives. A 93% reduction in CYP2D6 mRNA levels was observed over 72 hours, suggesting that the mRNA half-life is approximately 19 hours. In contrast, CYP2D6 activity was decreased by about 60% in the presence of bupropion and its metabolites. The CYP2D6 protein half-life has been reported to be 51 hours (Venkatakrishnan, 2005) and therefore the treatment for 72 hours

only spans 1.4 protein half-lives and only 60% of the expected steady-state protein levels can be reached. Based on these calculations, nearly a 100% loss of CYP2D6 activity is expected at protein steady state. Interestingly, despite 93% depletion of bupropion, and subclinical concentrations of the formed metabolites, CYP2D6 mRNA and protein expression were decreased to a greater extent in bupropion-treated cells than following treatment with any of its metabolites at concentrations exceeding steady state concentrations. In fact, the extent of downregulation of CYP2D6 by bupropion itself can explain the in vivo DDIs without considering metabolite contribution, challenging the dogma that in vivo CYP2D6 inhibition is caused only by bupropion's metabolites. While it is likely that in vivo DDIs are caused by downregulation of CYP2D6 and reversible inhibition by bupropion and its metabolites, it is not possible to determine the relative contributions of each of the compounds to in vivo DDIs.

To the best of our knowledge, this is the first example of a xenobiotic causing a drug-drug interaction via CYP2D6 downregulation and there are no examples of clinical DDIs resulting from downregulation of any P450 enzyme. Current FDA and EMA guidance recommend induction studies with CYP1A2, CYP3A4 and CYP2B6 (European Medicines Agency Committee for Medicinal Products for Human Use, 2012; U.S. Food and Drug Administration Center for Drug Evaluation and Research (CDER), 2012), and CYP2C in some cases. The EMA also acknowledges that concentration- dependent downregulation of P450s could be monitored in the same system. However, downregulation is not systematically assessed in current drug development workflows. Critically, evaluation of CYP2D6 induction is not recommended as CYP2D6 is not considered to be inducible by xenobiotics. Yet, transcriptional regulation of CYP2D6 has recently been shown with retinoic acid (Koh et al., 2014; Mamoon et al., 2014) and GW4064 in vitro and in mice (Pan et al., 2015), and CYP2D6 activity is increased during

pregnancy (Isoherranen and Thummel, 2013). Retinoic acid and GW4064 appear to act via inducing SHP (Koh et al., 2014; Mamoon et al., 2014; Pan et al., 2015), a transcriptional repressor of CYP2D6 expression. However, bupropion and its metabolites had no effect on SHP expression, suggesting that these compounds regulate CYP2D6 expression via a novel mechanism. In addition to SHP, CYP2D6 is reported to be induced by corticosteroids (Farooq et al., 2016), and thus investigation into the impact of bupropion and its metabolites on the glucocorticoid receptor may be warranted. Nitric oxide has also been shown to alter the regulation of CYP2D6 (Hara and Adachi, 2002), and thus it may be appropriate to determine whether bupropion and or its metabolites induce inflammation.

Whether bupropion is a unique example of a xenobiotic that can cause CYP2D6 downregulation or there are other xenobiotics that downregulate CYP2D6 expression is not known. The data shown here suggest that detailed studies in this area are needed. If such downregulation is a more common phenomenon, this could have substantial clinical consequences. Taken together this study shows that downregulation of P450s including CYP2D6 can result in potent in vivo DDIs with major clinical consequences.

Table 4.1. Steady-state concentrations of bupropion and its metabolites

	$C_{ss,}$ µM						Percent of Parent	$f_{u,p}$ (S.D. n=3)
Subject	1	2	3	4	5	Mean adjusted for 300 mg/day dose[a] (Range, n=5)		
Dose, mg/day	300	450	150	150	300			
R-Bupropion	0.29	0.42	0.03	0.17	0.11	0.22 (0.05-0.34)		0.5±0.1
S-Bupropion	0.11	0.14	0.01	0.05	0.05	0.08* (0.02-0.11)		0.6±0.1
R,R-OH-bupropion	3.5	14	2.2	2.4	3.0	5.0 (3.0-9.4)	2500 ± 2200	0.5±0.1
S,S-OH-bupropion	0.26	1.0	0.18	0.20	0.29	0.39* (0.26-0.67)	200 ± 170	0.5±0.1
Threohydrobupropion	3.5	4.37	0.57	0.88	1.34	2.1 (1.1-3.5)	900 ± 440	1.0±0.1
Erythrohydrobupropion	0.40	0.62	0.09	0.11	0.24	0.29 (0.19-0.41)	130 ± 80	0.7±0.1

[a] Mean and range of steady-state concentrations, adjusted to a 300mg/day dose. *Significantly different from the other enantiomer, P<0.05, Student's *t*-test.

Table 4.2. In vitro CYP2D6 inhibition parameters and predictions of the magnitude of CYP2D6 inhibition.

	$IC_{50,u}$,µM[a] Mean (95% C.I.)	Mean[b] $[I]_u/IC_{50,u}$	Low[c] $[I]_u/IC_{50,u}$	High[d] $[I]_u/IC_{50,u}$	Percent Inhibition[e] Mean (Range)
R-Bupropion	41 (32-53)	0.003	0.001	0.004	0.3 (0.07-0.36)
S-Bupropion	3 (2-4)	0.015	0.004	0.022	1.5 (0.35-2.1)
R,R-OH-bupropion	5 (3-8)	0.504	0.299	0.941	34 (23-48)
S,S-OH-bupropion	14 (9-21)	0.014	0.009	0.024	1.4 (0.9-2.3)
Threohydrobupropion	13 (8-21)	0.160	0.084	0.256	13.5 (2.7-20)
Erythrohydrobupropion	3 (3-4)	0.07	0.043	0.096	6.2 (4.1-8.8)
Total		0.76	0.44	1.34	43 (31-57)

[a] No binding was observed for any of the compounds in 0.1 mg/mL HLM, so the total IC_{50} values are equivalent to the unbound IC_{50} values. [b] $[I]_u/IC_{50,u}$ based on mean plasma concentrations. [c] $[I]_u/IC_{50,u}$ based on the lowest observed plasma concentrations for each compound. [d] $[I]_u/IC_{50,u}$ based on the highest observed plasma concentrations for each compound. [e] The mean predicted percent inhibition is based on the mean $[I]_u/IC_{50,u}$ values, and low and upper ends of the range were based on the low and high $[I]_u/IC_{50,u}$ values.

Table 4.3. Inhibition of CYP2D6 by bupropion and its metabolites in plated human hepatocytes. The initial treatment concentrations were 2.5 µM for bupropion, erythrohydrobupropion and S,S-OH-bupropion, 10 µM for threohydrobupropion and 25 µM for R-R-OH-bupropion at time 0 and at time 71 hours. The table shows the measured concentrations at the end of the 1-hour activity assay. The cells were treated with bupropion for 71 hours and the media was changed for the inhibition experiment. Predicted and observed CYP2D6 activity in hepatocytes in the presence of bupropion and its metabolites at the two time points, 1 hour and 72 hours.

	Media Concentration, µM Mean ± S.D.	Predicted Percent Inhibition	Observed Percent Inhibition	Fold Change in Percent Inhibition
1-hour treatment				
Bupropion	1.5 ± 0.5	6.5 ± 2.1	37 ± 16	
R,R-OH-bupropion	16 ± 1	76 ± 1	63 ± 8	
S,S-OH-bupropion	1.3 ± 0.1	8.5 ± 0.3	22 ± 16	
Threohydrobupropion	7.1 ± 0.6	35 ± 2	80 ± 2	
Erythrohydrobupropion	1.6 ± 0.1	35 ± 0.5	81 ± 2	
Mix[a]		83 ± 2	83 ± 2	
72-hour treatment				
Bupropion	1.7 ± 0.5	7.0 ± 1.8	81 ± 5	2.2
R,R-OH-bupropion	19 ± 3	78 ± 2	83 ± 3	1.3
S,S-OH-bupropion	1.5 ± 0.2	9.8 ± 1.1	60 ± 11	2.7
Threohydrobupropion	8.2 ± 1.4	38 ± 4	92 ± 2	1.2
Erythrohydrobupropion	2.1 ± 0.3	40 ± 4	93 ± 1	1.1
Mix		86 ± 1	93 ± 1	1.1

[a] The mix was composed of bupropion, R,R-OH-bupropion, S,S-OH-bupropion, threohydrobupropion and erythrohydrobupropion. Measured concentrations in the mixture were 1.6 µM ± 0.5 (Bupropion), 16.5 µM ± 1.3 (R,R-OH-bupropion), 1.4 µM ± 0.1 (S,S-OH-bupropion), 7 µM ± 0.2 (threohydrobupropion), 2.1 µM ± 0.1 (erythrohydrobupropion).

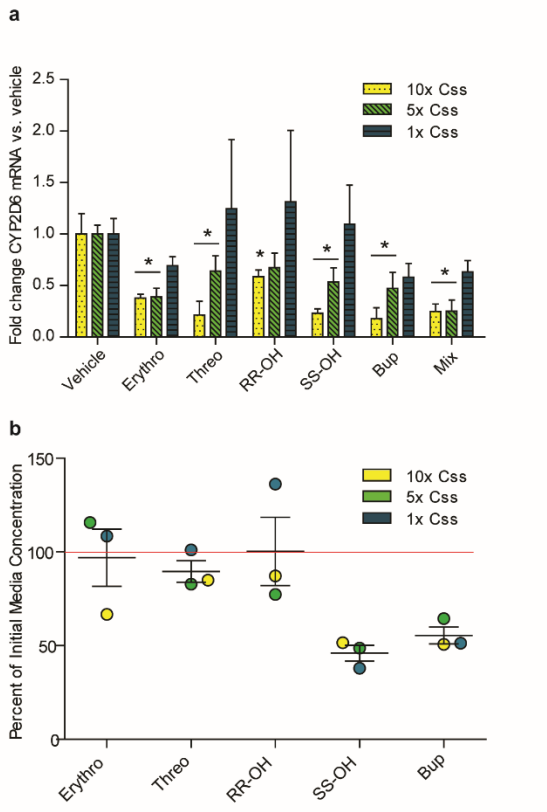

Figure 4.1. Impact of bupropion and its metabolites on CYP2D6 expression and activity in HEPG2 cells. (a) Fold change in CYP2D6 mRNA levels following treatment of HepG2 cells with vehicle, erythrohyrobupropion (Erythro), threohydrobupropion (Threo), bupropion (Bup), R,R-OH-bupropion (R,R-OH), S,S-OH-bupropion (S,S-OH) or a mixture (Mix) at concentrations 1x, 5x and 10x observed steady state concentrations. **(b)** The percent of the original media concentrations at 72 hours following daily treatment with bupropion or its metabolites. *P<0.05, compared to vehicle control cells based on one-way ANOVA with the posthoc Tukey test.

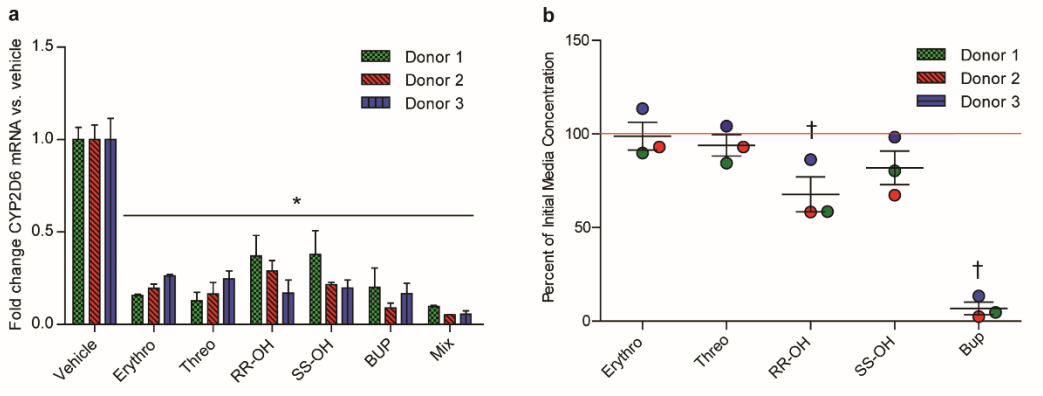

Figure 4.2. Impact of bupropion and its metabolites on CYP2D6 expression and activity in human hepatocytes. (a) Fold change in CYP2D6 mRNA levels as percent of 0 hour activity following dosing with vehicle, erythrohyrobupropion (Erythro), threohydrobupropion (Threo), bupropion (Bup), R,R-OH-bupropion (R,R-OH), S,S-OH-bupropion (S,S-OH) or a mixture (Mix) at concentrations 5x the observed steady state concentrations. **(b)** The percent of the original media concentrations at 71 hours following daily treatment with bupropion or its metabolites. *P<0.05, compared to vehicle control cells, $^{\#}$P<0.05 compared to 0 hour activity, † P<0.05 compared to initial media concentrations based on one-way ANOVA with posthoc Tukey test.

Chapter 5.

THE EFFECTS OF PREGANCY ON BUPROPION PHARMACOKINETICS: INSIGHT INTO CHANGES IN CYP2B6 EXPRESSION

5.1 ABSTRACT

The aim of this study was to determine the effects of pregnancy on the pharmacokinetics of bupropion. Dosing interval urine was collected, along with steady state plasma samples from women taking bupropion (Wellbutrin XL, 150-450 mg/day) during second trimester (n=3), third trimester (n=4) and 6 weeks postpartum (n=5). No significant changes in circulating steady state concentrations of bupropion or its metabolites were observed, suggesting that there may not be a need for a dose adjustment during pregnancy. However, a significant two-fold change in OH-bupropion formation clearance was observed in the third trimester, when compared to postpartum. This induction in formation clearance occurred in the absence of a change in the OH-bupropion/bupropion C_{ss} ratio, suggesting that OH-bupropion clearance may also be induced. Furthermore, a reduction in the threohydrobupropion:bupropion and erythrohydrobupropion:bupropion ratios was observed, potentially due to induced metabolism of threo- and erythrohydrobupropion. The results of this study indicate that CYP2B6 is induced during pregnancy and that dose adjustments may be warranted for CYP2B6 substrates to avoid loss of therapeutic efficacy.

5.2 INTRODUCTION

Bupropion is classified as a pregnancy category C drug, indicating that it is not recommended for use in pregnant women unless the potential benefits outweigh the risks. Yet, major depression and smoking cessation treatment are common among pregnant women (Marcus et al., 2003; Tong et al., 2013). Approximately 12% of women quit smoking during pregnancy while another 12% continue to smoke throughout pregnancy (Tong et al., 2013). Furthermore, 20% of women report experiencing elevated depressive symptoms during pregnancy (Marcus et al., 2003). As a result, approximately 0.5% of women are exposed to bupropion during pregnancy (Alwan et al., 2010). Yet, nothing is known about bupropion disposition or pharmacodynamics in pregnant women. In baboons, bupropion and OH-bupropion C_{max} and exposure levels trended lower during pregnancy when compared to nonpregnant animals (Rytting et al., 2014). However, marked species differences in bupropion pharmacokinetics have been reported (Welch et al., 1987), and therefore the results in baboons are not necessarily reflective of expected changes in bupropion disposition during human pregnancy.

Understanding the effects of pregnancy on the pharmacokinetics of bupropion and its metabolites is clinically relevant. A strong dose-response relationship has been reported for bupropion smoking cessation treatment (U.S. Food and Drug Administration Center for Drug Evaluation, 1997) and trough concentrations of bupropion have been reported to be an important determinant of antidepressant response (Goodnick, 1992; Preskorn, 1983). Thus changes during pregnancy that could result in altered steady state bupropion concentrations may lead to a loss of therapeutic efficacy. Bupropion also has three active metabolites; hydroxybupropion (OH-bupropion), threo- and erythrohydrobupropion which have been implicated in pharmacological response and adverse events. OH-bupropion, particularly the S,S- enantiomer, is thought to be

the main contributor to smoking cessation and antidepressant activity (Bondarev et al., 2003; Carroll et al., 2011; Damaj et al., 2004; Jefferson et al., 2005; Martin et al., 1990; Musso et al., 1993; Welch et al., 1987; Zhu et al., 2012a). Threo-and erythrohydrobupropion are reported to have approximately 20% of the antidepressant activity of bupropion (Jefferson et al., 2005). In pediatric subjects, responders to antidepressant treatment had higher levels of bupropion and all three metabolites than non-responders and OH-bupropion concentrations were most strongly associated with clinical outcomes (Daviss et al., 2006). Conversely, in adults, metabolite levels in responders have been reported to be significantly lower than in non-responders (Golden, 1988), and high levels of metabolites are correlated with poor clinical outcomes (Golden, 1988) and increased adverse effects such as dry mouth and insomnia (U.S. Food and Drug Administration Center for Drug Evaluation, 1997). This is consistent with toxicity studies in mouse models in which all three metabolites produced dose dependent increases in convulsion risk (Silverstone et al., 2008). Additionally, OH-bupropion has been reported to have the lowest LD_{50} value in mice (Welch et al., 1987). Because clinical outcomes and tolerability are dependent on the circulating concentrations of bupropion and its metabolites, understanding whether pregnancy alters bupropion pharmacokinetics is critical to making informed decisions regarding safe and efficacious doses for pregnant women.

Based on our knowledge of the changes in the expression of drug metabolizing enzymes in pregnancy, bupropopion pharmacokinetics are expected to be altered during human pregnancy. CYP2B6, which catalyzes the formation of OH-bupropion (Coles and Kharasch, 2008, 2008; European Medicines Agency Committee for Medicinal Products for Human Use, 2012; Faucette et al., 2000; U.S. Food and Drug Administration Center for Drug Evaluation and Research (CDER), 2012), is induced by estradiol in vitro (Choi et al., 2013; Dickmann and

Isoherranen, 2013; Koh et al., 2012). Based on the circulating free concentrations of estradiol during pregnancy (Abduljalil et al., 2012; O'Leary et al., 1991; Soldin et al., 2005), CYP2B6 expression is expected to increase by 1.1, 1.4 and 1.9 fold in the first, second and third trimesters (Dickmann and Isoherranen, 2013). Several studies have evaluated the effects of pregnancy on the PK of CYP2B6 substrates, including methadone, sertraline, nevirapine and efavirenz (Table 5.1), yet the effects of pregnancy on CYP2B6 remain unclear (Capparelli et al., 2008a; Freeman et al., 2008; Pond et al., 1985). Methadone clearance was dramatically increased and the exposure was decreased during pregnancy in two independent studies (Pond et al., 1985; Wolff et al., 2005). A lack of change in renal clearance was reported in one of the studies (Pond et al., 1985), suggesting induction of CYP2B6, CYP3A4 or CY2D6, or a combination during pregnancy. However, exposure to efavirenz, a sensitive CYP2B6 substrate, was unchanged in pregnancy (Cressey et al., 2012). Additionally, no change in nevirapine exposure or clearance was observed in pregnancy in CYP2B6 extensive metabolizers (Olagunju et al., 2016). In the same study, significant increases in clearance and decreases in AUC were observed in CYP2B6 intermediate metabolizers or the mixed population, which is inconsistent with the lack of change reported in two independent studies that assessed the effects of pregnancy on nevirapine in non-genotyped populations (Capparelli et al., 2008b; Nellen et al., 2008). The apparent lack of agreement between these results and those of the methadone studies could be due to the fact that efavirenz and nelfinavir are both inducers (Lamson et al., 1999; Robertson et al., 2008) of CYP2B6 and efavirenz is also a CYP2B6 inactivator (Bumpus et al., 2006). No change in sertraline has also been reported in pregnancy (Freeman et al., 2008), but interpretation of the in vivo data is complicated by the fact that sertraline has many different eliminated pathways aside from CYP2B6 that may mask the true effects of pregnancy on CYP2B6 activity (Obach et al.,

2005). Because of the inconsistencies in the published in vivo data, evaluating the effects of pregnancy on OH-bupropion formation clearance may clarify the impact of pregnancy on CYP2B6 expression and activity.

CYP2C19, which is exclusively involved in the formation of 4'- OH-bupropion (Sager et al., 2016) is also expected to be altered in pregnancy. Oral contraceptives have been shown to significantly reduce CYP2C19 activity, as evidenced by a 2-fold increase in the omeprazole/hydroxyomeprazole ratio as well as the S/R mephenytoin ratio in humans (Laine, 2000). This has been attributed in part to reversible inhibition of CYP2C19 by estradiol and progesterone (Chang et al., 2009; Choi et al., 2013; Foti and Wahlstrom, 2008; Rodrigues and Lu, 2004) but as estrogen concentrations are generally much lower than the Ki values, this decrease in activity is most likely due to estradiol downregulation of CYP2C19 through estrogen receptor α (Mwinyi et al., 2010). However, changes in CYP2C19 during pregnancy remain unclear since no studies have been conducted with selective CYP2C19 probes. A study assessing proguanil pharmacokinetics during pregnancy reported a 40% decrease in both proguanil oral clearance and the cycloguanil/proguanil single point concentration ratio in pregnant women (McGready et al., 2003a, 2003b). However, renal clearance contributes substantially to proguanil clearance (Funck-Brentano et al., 1997) and it is unknown whether pregnancy changes cycloguanil elimination. Thus, these changes may not be solely reflective of changes in CYP2C19 activity.

Reduction of bupropion to threo- and erythrohydrobupropion is catalyzed primarily by 11β-hydroxysteroid dehydrogenase type 1 (11β-HSD1), with minor involvement of aldoketoreductases (Connarn et al., 2015; Meyer et al., 2013). Progesterone has been reported to inhibit 11β-HSD1 in vitro, with an IC_{50} of 1.7 μM (Diederich et al., 2000). However, based on

the maximum third trimester concentration of 0.6μM (Abduljalil et al., 2012) and an unbound fraction of 0.10 (Yannone et al., 1969), less than a 5% change in 11β-HSD1 is predicted during pregnancy due to competitive inhibition of the enzymes reducing bupropion.

The purpose of this study was to determine the effects of pregnancy on the pharamcokinetics of bupropion and its metabolites. We hypothesize that CYP2B6 mediated clearance to OH-bupropion will increase while the CYP2C19 mediated clearance to 4'-OH-bupropion will decrease during pregnancy. To test this hypothesis we collected plasma and urine from women during and after pregnancy to assess changes in bupropion pharmacokinetics.

5.3 Materials and Methods

5.3.1 Chemicals and Reagents.

Bupropion, R-bupropion, S-bupropion, OH-bupropion, R,R-hydroxybupropion, S,S-hydroxybupropion, threohydrobupropion, erythrohydrobupropion, bupropion-d9, OH-bupropion-d6, and threohydrobupropion-d9 were purchased from Toronto Research Chemicals (Ontario, Canada). Optima grade formic acid and ammonium formate was purchased from Sigma-Aldrich (St. Louis, MO). Optima grade Acetonitrile (ACN), Methanol (MeOH), and Water (H2O) were purchased from Fisher Scientific (Waltham, MA).

5.3.2 Clinical Study.

The study was approved by the University of Washington Institutional Review Board. 5 female subjects were enrolled in the study after providing written informed consent. All subjects were taking bupropion for therapeutic reasons at the time of enrollment and maintained their normal dosing schedule throughout the duration of the study. During each trimester of

enrollment, and again 6 weeks postpartum, a single steady state blood sample was collected from each subject, and urine was collected over one dosing interval. Subjects were genotyped for CYP2C19*2, CYP2C19*3 and CYP2C19*17 as described previously (Sager et al., 2014; Zhu et al., 2014).

5.3.3 Patient Demographics and Genotyping Information

5 female subjects (3 white and 2 unknown) participated in this study after providing written informed consent. All subjects were determined to be CYP2C19*1/*1 genotype. At the time of enrollment, the average body weight was 108±23 kg, the average age was 35±6 years and the average height was 153±5cm. All subjects were taking bupropion XL chronically (150-450 mg/day) for therapeutic reasons. Subjects taking CYP2B6 inhibitors or inducers were excluded from the study. Co-medications included metformin (n=2), omeprazole (n=1), albuterol (n=1), risperidone (n=1), escitalopram (n=1), insulin (n=1) and oxycodone (n=1). Second trimester samples were collected from 3 subjects and third trimester samples were collected from 4 subjects (Table 5.2).

5.3.4 Analysis of Bupropion and its Metabolites in Human Plasma and Urine.

Plasma and urine samples (40 µL for chiral assay and 10 µL for non-chiral analysis) were protein precipitated with 3:1 acetonitrile:methanol (160 µL and 190 µL respectively) containing 100 nM OH-bupropion-d_6, bupropion-d_9, and threohydrobupropion-d_9 and centrifuged for 40

minutes at 3000 g. Deconjugation was performed using an acidification method described previously (Chapter 2).

5.3.5 LC/MS/MS Quantification Methods.

The concentrations of analytes were determined using an LC/MS/MS system consisting of an AB-Sciex API 4500 triple quadrupole mass spectrometer (AB Sciex, Foster City, CA) coupled with an LC-20AD ultra-fast liquid chromatography system (Shimadzu Co., Kyoto, Japan). The turbo ion spray interface was operated in positive ion mode for all analytes. To determine the concentrations of bupropion, OH-bupropion, threohydrobupropion, erythrohydrobupropion, threo-4'-OH-bupropion, erythro-4'-OH-bupropion, and 4'OH-bupropion in human plasma and urine, an Agilent ZORBAX XDB-C18 column (150 x 4.6mm, 5µm) was used with a 0.8 mL/min isocratic flow consisting of 35% MeOH and 0.04% formic acid (Connarn et al., 2015). Concentrations of bupropion and OH-bupropion enantiomers in plasma and urine were measured using a chiral α-acid glycoprotein (AGP) column (100 x 2 mm, 5µm) with a chiral AGP guard cartridge (10 x 2 mm, 5 µm) (ChromTech, Apple Valley, MO) as described previously (DDI paper) The mobile phase consisted of 20 mM ammonium formate buffer, pH 5.7 (A) and MeOH (B). Data analysis was performed using Analyst software version 1.6.2 (AB Sciex).

5.3.6 Pharmacokinetic Analysis.

For all calculations, linear kinetics were assumed and thus exposure following a single dose $AUC_{0-\infty}$ was assumed to be equal to the exposure over a single dosing interval at steady

state $AUC_{0\text{-}T,ss}$. Clearance was calculated from the average steady state concentrations using equation 1, where T represents the dosing interval.

$$\frac{CL}{F} = \frac{D}{C_{ss,avg} * \mathrm{T}} \qquad \text{Equation 5.1}$$

Renal clearance (CL_R) was calculated using equation 2, where ($A_{e0\text{-}T}$) is the amount of unchanged drug excreted in the urine over the dosing interval.

$$CL_f = \frac{Ae_{total,0-T}}{C_{ss,p} * \mathrm{T}} \qquad \text{Equation 5.2}$$

The total amount of each compound excreted over a dosing interval was determined by multiplying the concentrations by the total volume of urine collected over the dosing interval. In vivo CL_f was calculated using equation 3 where $Ae_{total\ 0\text{-}T}$ for OH-bupropion is the total amount measured following acid deconjugation. For threo- and erythrohydrobupropion, $Ae_{total\ 0\text{-}T}$ is the sum of the amount of free drug measured following acid deconjugation and the amount measured as the subsequent hydroxylation products.

$$CL_f = \frac{Ae_{total,0-T}}{C_{ss,p} * \mathrm{T}} \qquad \text{Equation 5.3}$$

5.3.7 Statistical Analysis.

Two-sided paired t-tests were used to evaluate the significance of changes in pharmacokinetic parameters in T2 compared to the PP values in the same subjects or T3 when

compared to the PP values in the same subjects. Statistical analyses were performed in GraphPad Prism (Graphpad Software, San Diego, CA).

5.4 RESULTS

5.4.1 Effect of Pregnancy on Bupropion Pharmacokinetics

Steady state concentrations of bupropion and its metabolites in T2, T3 and PP were measured (Table 5.3). No significant changes were observed in the dose-normalized T2 or T3 steady state plasma concentrations of bupropion or its metabolites (Table 5.3) or in the concentrations as percent postpartum (Table 5.3, Figure 5.1) when compared to the PP values in the same subjects. Consistent with a lack of change in circulating concentrations, oral clearance (CL/F) and renal clearance (CL_R) of bupropion, R-bupropion and S-bupropion were unaltered in T2 and T3, when compared to matched postpartum values (Table 5.4). Due to high variability in bupropion clearance between subjects, the effect of pregnancy on clearance was also assessed by normalizing clearance values to postpartum levels. No significant changes were detected in the second or third trimesters, when compared to postpartum (Table 5.4, Figure 5.2).

The formation clearances (CL_f) of OH-bupropion, R,R-OH-bupropion, S,S-OH-bupropion, 4'-OH-bupropion, threo- and erythrohydrobupropion were evaluated in order to assess pregnancy related changes in CYP2B6, CYP2C19 and 11B-HSD1 activity, respectively. The T2 and T3 formation clearances were not significantly different than the PP values in the same subjects (Table 5.5). However, when the formation clearance was assessed as a percent of postpartum levels, a significant 2-fold increase in OH-bupropion (200% postpartum) and R,R-OH-bupropion (210% postpartum) was detected in T3 (Table 5.5, Figure 5.3). Similarly, the formation clearance for S,S,-OH-bupropion was 203% higher than the postpartum levels, but the difference was not statistically significant. The formation clearance of erythrohydrobupropion in

T2 was significantly reduced (25% reduction) when compared to the postpartum values in the same subjects but no change in threohydrobupropion formation clearance was detected.

Changes in metabolite to parent steady state concentration ratios were assessed in order to provide information about potential changes in metabolite clearance. No significant changes were observed in the metabolite to parent ratios during either T2 or T3 when compared to matched postpartum values (Table 5.6). However, when the ratios were expressed as a percentage of postpartum values, the threohydrobupropion:bupropion and erythrohydrobupropion:bupropion ratios were lower (38 and 47%, respectively) in the second trimester of pregnancy (Table 5.6, Figure 5.4).

5.5 DISCUSSION

This study aimed to determine whether bupropion pharmacokinetics are altered in pregnancy. Of foremost concern was whether any pharmacokinetic changes would occur that would impact maternal safety and efficacy. Because bupropion and its metabolites contribute to the therapeutic efficacy and safety, the circulating concentrations of bupropion and its metabolites were monitored during second and third trimester of pregnancy, and compared to the postpartum control values in the same subjects. The steady state concentrations of bupropion and its pharmacologically active metabolites were not altered during pregnancy. Furthermore, the circulating concentrations of the individual enantiomers of bupropion and OH-bupropion were unchanged in pregnant women. As a result, dose adjustments may not be necessary in pregnant women in order to maintain therapeutically efficacious maternal concentrations. However, an investigation in a larger, sufficiently powered study may be necessary to rule out the need for dose adjustments.

As expected, CYP2B6 appeared to be induced during the third trimester of pregnancy, resulting in 2-fold higher formation clearance of OH-bupropion when compared to postpartum. This magnitude of induction is in agreement with the 1.9-fold induction previously predicted from in vitro induction data (Dickmann and Isoherranen, 2013; Ke et al., 2014). Second trimester formation clearances were 140% (OH-bupropion), 130% (R,R-OH-bupropion) and 150% (S,S-OH-bupropion) higher than postpartum levels. The magnitude of change during T2 is in close agreement with the 1.4-fold predicted induction (Dickmann and Isoherranen, 2013), however the change was not statistically significant, likely due to the small sample size (n=3). This magnitude of induction, however, did not alter bupropion C_{ss}, likely due to the fact that CYP2B6 is a quantitatively minor elimination pathway for bupropion (Chapter 2, Chapter 3). This is the first study that has used a CYP2B6 probe under conditions that allow mechanistic interpretation of the study results. Efavirenz pharmacokinetics have been evaluated in pregnancy (Cressey et al., 2012), but due to the multiple dose study design, simultaneous inactivation and induction likely masked any pregnancy-induced changes in CYP2B6 activity. This finding suggests that dose adjustments may need to be considered when administering drugs that have CYP2B6-mediated elimination pathways, particularly when alteration of CYP2B6 expression could result in adverse events or therapeutic failure.

Unexpectedly, no change in CYP2C19 activity was detected in this study. Pregnancy and the use of oral contraceptives have been suggested to result in reduced CYP2C19 activity, based on a 40% reduction in the cycloguanil/proguanil AUC ratio (McGready et al., 2003b). The lack of agreement between the current study and previously published work (McGready et al., 2003b) could simply be a result of the small size of the current study. However, it is also possible that in the previous study, the clearance of cycloguanil was increased. This would lead to a reduction of

the metabolite to parent AUC ratio in absence of any changes in CYP2C19 mediated formation clearance. Very little is known about the clearance pathways of cycloguanil but its renal clearance exceeds unbound GFR, suggesting that active renal excretion is involved in its elimination (U.S. Food and Drug Administration Center for Drug Evaluation, 2000) and may contribute to increased clearance during pregnancy.

Threo- and erythrohydrobupropion formation is catalyzed primarily by 11β-HSD-1 in the liver (Connarn et al., 2015), however, a 25% decrease in erythrohydrobupropion formation clearance was observed while no trend towards a decrease in threohydrobupropion formation clearance was detected. This finding suggests that the observed change may not be due to inhibition of 11β-HSD-1. Based on mass balance data (Chapter 2) and the in vivo formation clearances presented in this study, the fraction of bupropion metabolized to erythrohydrobupropion is approximately equivalent to that of OH-bupropion. However, in vitro data from human liver S9 fractions suggests that erythrohydrobupropion formation plays a much smaller role in bupropion elimination (Chapter 3). This suggests that extrahepatic metabolism may be responsible for a portion of erythrohydrobupropion formation. A previous investigation into intestinal metabolism of bupropion failed to detect any erythrohydrobupropion formation in intestinal S9 fractions, so investigation into other potential sites of metabolism is warranted.

Despite the induced formation clearance of OH-bupropion and R,R-OH-bupropion, the circulating concentrations of OH-bupropion and its enantiomers were unchanged. This, considered with the fact that the metabolite to parent C_{ss} ratios for OH-bupropion and bupropion enantiomers were unaltered in pregnancy, suggests that the elimination of OH-bupropion is also induced during pregnancy. Little is known about the specific enzymes involved in the elimination of OH-bupropropion. UGT2B7 has been implicated as the major enzyme involved

in O-glucuronidation of R,R- and S,S-OH-bupropion (Gufford et al., 2016). However, because glucuronidation has been reported to introduce a new chiral center and the resulting conjugates exhibit high resistance to β-glucuronidase, OH-bupropion is thought to primarily undergo N-glucuronidation. UGT1A4 and UGT2B10 are considered to be important enzymes involved in N-glucuronidation (Kaivosaari et al., 2011). While no data is currently available regarding changes in UGT2B10 during pregnancy, UGT1A4 is thought to be induced during pregnancy due to an observed 2.5-fold change in the lamotrigine-2-N-glucuronide to lamotrigine ratio in the third trimester of pregnancy. Potential involvement of UGT1A4 in OH-bupropion elimination could explain the observed induction of OH- bupropion clearance.

While the erythrohydrobupropion: bupropion C_{ss} ratio is expected to be lower in the second trimester as opposed to postpartum due to reduced formation clearance of erythrohydrobupropion, a reduction in the threohydrobupropion:bupropion C_{ss} ratio was also observed. As with OH-bupropion, this observation is likely due to induction of metabolite clearance. Conjugation accounts for 30% of threo- and erythrohydrobupropion elimination (Chapter 2). N-glucuronidation has been proposed to be the main conjugation pathway (Petsalo et al., 2007). Thus, UGT1A4 induction could also be a potential explanation for the reduction in the threohydrobupropion:bupropion C_{ss} ratios in the second trimester and further contribute to the reduction of the erythrohydrobupropion:bupropion C_{ss} ratio.

In conclusion, this study shows that CYP2B6 is induced in pregnancy, resulting in 2-fold greater activity in the third trimester of pregnancy when compared to postpartum. However, this magnitude of induction would not have been observed had the OH-bupropion:bupropion C_{ss} ratio been used. This is likely due to simultaneous induction of formation and elimination clearances. This finding highlights the importance of exercising caution when using metabolite to parent C_{ss}

or AUC ratios to assess changes in enzyme activity in special populations. In such cases, in vivo formation clearances may be the most appropriate indicator of changes in enzyme activity.

Table 5.1. Summary of Pharmacokinetic Changes Observed for CYP2B6 Substrates During Pregnancy

CYP2B6 Substrate		T1	T2	T3	Pregnancy	Postpartum	Reference
Nevirapine							
	CYP2B6 EM						(Olagunju et al., 2016)
	CL/F (L/hr)				5.7 (n=6)	5.5 (n=8)	
	AUC_{0-24} (µg*hr/mL)				36.5 (n=6)	36.3 (n=8)	
	CYP2B6 IM [a]						
	CL/F (L/hr)				4.5* (n=19)	3.2 (n=10)	
	AUC_{0-24} (µg*hr/mL)				44.6*(n=19)	63.3 (n=10)	
	Pooled						
	CL/F (L/hr)				4.5* (n=31)	3.7 (n=28)	
	AUC_{0-24} (µg*hr/mL)				44.2* (n=31)	54.7 (n=28)	
	Not Genotyped AUC_{0-T} (µg*hr/mL)				56 (n=26)	61 (n=26)	(Capparelli et al., 2008a)
	Not Genotyped C_{ss}(mg/L)				4.8 (n=45)	5.8 (n=152)	(Nellen et al., 2008)
Sertraline	AUC_{0-T} (ng*hr/mL)		836 (n=8)	911 (n=6)		951[b] (n=3)	(Freeman et al., 2008)
Methadone	CL/F (L/hr)	9.5 (n=4)	7.6 (n=4)	7.2 (n=8)		2.0 (n=3)	(Wolff et al., 2005)
	AUC (mg.h/L)	4.5 (n=4)	3.8 (n=4)	2.2 (n=8)		6.2 (n=3)	
	CL/F (mL/min)		311[c*] (n=8)	256[d*] (n=9)		161 (n=8)	(Pond et al., 1985)
Efavirenz	AUC_{0-24} (µg*hr/mL)			55 (n=25)		58 (n=25)	(Cressey et al., 2012)

[a] Values taken from the CYP2B6 516GT or 983TC group
[b] estimated based on the reported 4.4% increase from T3 to postpartum
[c] Samples from week 20-34 of pregnancy or [d] 35 to 40 weeks.
*reported p<0.5

Table 5.2. Subject Demographics

Subject	Visits	Dose (mg/day)	Age (yr)	Weight (kg)	Height (cm)	Comedications
1	T3, PP	300	28	129	169	Omeprazole Albuterol metformin
2	T2, T3, PP	450	42	124	170	Risperdal
3	T2, T3, PP	150	35	72	178	Insulin Escitalopram Oxycodone
4	T2, PP	150	35	110	165	Metformin
5	T3, PP	300	28	81	172	-

Table 5.3. Dose-Normalized Steady State Concentrations of Bupropion and Its Metabolites in Pregnancy and Postpartum.

	T2 vs Matched Postpartum (n=3)		T3 vs Matched Postpartum (n=4)	
	T2	**Postpartum**	**T3**	**Postpartum**
Bupropion				
$C_{ss,\,avg}$ (µM/g)	1.1±0.6	1.0±0.7	0.8±0.6	0.8±0.5
$C_{ss,\,avg}$ percent PP	131±48		88±26	
S-bupropion				
$C_{ss,\,avg}$ (µM/g)	0.3±0.1	0.2±0.2	0.2±0.2	0.2±0.1
$C_{ss,\,avg}$ percent PP	133±53		84±33	
R-bupropion				
$C_{ss,\,avg}$ (µM/g)	0.8±0.4	0.8±0.5	0.6±0.4	0.6±0.4
$C_{ss,\,avg}$ percent PP	130±46		90±23	
OH-bupropion				
$C_{ss,\,avg}$ (µM/g)	17.6±0.6	22.5±9.8	15.5±0.82	18.4±10.5
$C_{ss,\,avg}$ percent PP	86±29		97±61	
S,S-OH-bupropion		1.8±0.6		
$C_{ss,\,avg}$ (µM/g)	1.5±0.1		1.2±0.5	1.5±0.7
$C_{ss,\,avg}$ percent PP	90±32		95±49	
R,R-OH-bupropion		20.8±9.2		
$C_{ss,\,avg}$ (µM/g)	16.1±0.8		14.3±7.7	17.0±9.8
$C_{ss,\,avg}$ percent PP	86±29		98±62	
Erythrohydrobupropion				
$C_{ss,\,avg}$ (µM/g)	0.6±0.2	0.9±0.4	0.6±0.6	1.0±0.4
$C_{ss,\,avg}$ percent PP	90±35		70±21	
Threohydrobupropion				
$C_{ss,\,avg}$ (µM/g)	5.0±0.7	6.4±3.0	5.7±2.4	7.4±3.9
$C_{ss,\,avg}$ percent PP	89±35		90±25	

Table 5.4. Bupropion CL/F and CL_R in pregnancy and postpartum

	T2 vs Matched Postpartum (n=3)		T3 vs Matched Postpartum (n=4)	
	T2	Postpartum	T3	Postpartum
Bupropion				
CL/F	214±159	327±348	401±310	329±281
CL/F percent PP	83±28		124±52	
CL_R	0.9±0.2	1.2±1.3	1.0±0.63	2.8±4.1
CL_R percent PP	146±94		120±145	
S-Bupropion				
CL/F	423±300	661±700	822±652	620±577
CL/F percent PP	83± 33		143 ±91	
CL_R	1.0±0.38	1.3±1.2	1.28±0.85	2.66±3.39
CL_R percent PP	112±53		113±130	
R-Bupropion				
CL/F	143±108	217±231	531±407	225±186
CL/F percent PP	83±26		124±52	
CL_R	0.85±0.12	1.1±1.3	0.93±0.56	2.5±4.6
CL_R percent PP	259±265		165±114	

Table 5.5. Formation Clearance of Bupropion Metabolites in Pregnancy and Postpartum

	T2 vs Matched Postpartum (n=3)		T3 vs Matched Postpartum (n=4)	
	T2	Postpartum	T3	Postpartum
OH-bupropion				
CL_f	17±15	18±20	24±23	15±18
CL_f percent PP	140±93		202±64*	
S,S-OH-bupropion				
CL_f	25±22	29±32	36±35	23±29
CL_f percent PP	130±66		203±70	
R,R-OH-bupropion				
CL_f	14±12	14±16	20±19	12±14
CL_f percent PP	151±110		207±67*	
Erythrohydrobupropion				
CL_f	13±18	18±23	34±40	18±19
CL_f percent PP	75±6 *		116±52	
Threohydrobupropion				
CL_f	58±49	52±40	89±85	61±40
CL_f percent PP	108±20		130±51	
4'-OH-bupropion				
CL_f	5.2±8.8	2.5±2.3	1.5±1.7	1.5±2.2
CL_f percent PP	179±201		103±61	

*$p<0.05$

Table 5.6. Ratio of Metabolite to Parent Steady State Concentrations; The Effects of Pregnancy

	T2 vs Matched Postpartum (n=3)		**T3 vs Matched Postpartum (n=4)**	
	T2	Postpartum	T3	Postpartum
OH-bupropion/bupropion	22±16	35±29	36±43	31±25
Percent PP	70±31		110±52	
S,S-OH- bupropion/bupropion	7.2±5.1	11±10	12±13	9.7±8.6
Percent PP	75±43		120±45	
R,R-OH- bupropion/bupropion	27±20	43±35	45±53	39±31
Percent PP	70±29		110±56	
Erythro/ bupropion	0.8±0.7	1.4±1.1	1.4±1.0	1.5±0.7
Percent PP	53±9*		85±47	
Threo/ bupropion	5.8±4.6	9.2±6.2	11±6.2	10.2±3.9
Percent PP	62±10*		110±72	

*$p<0.05$

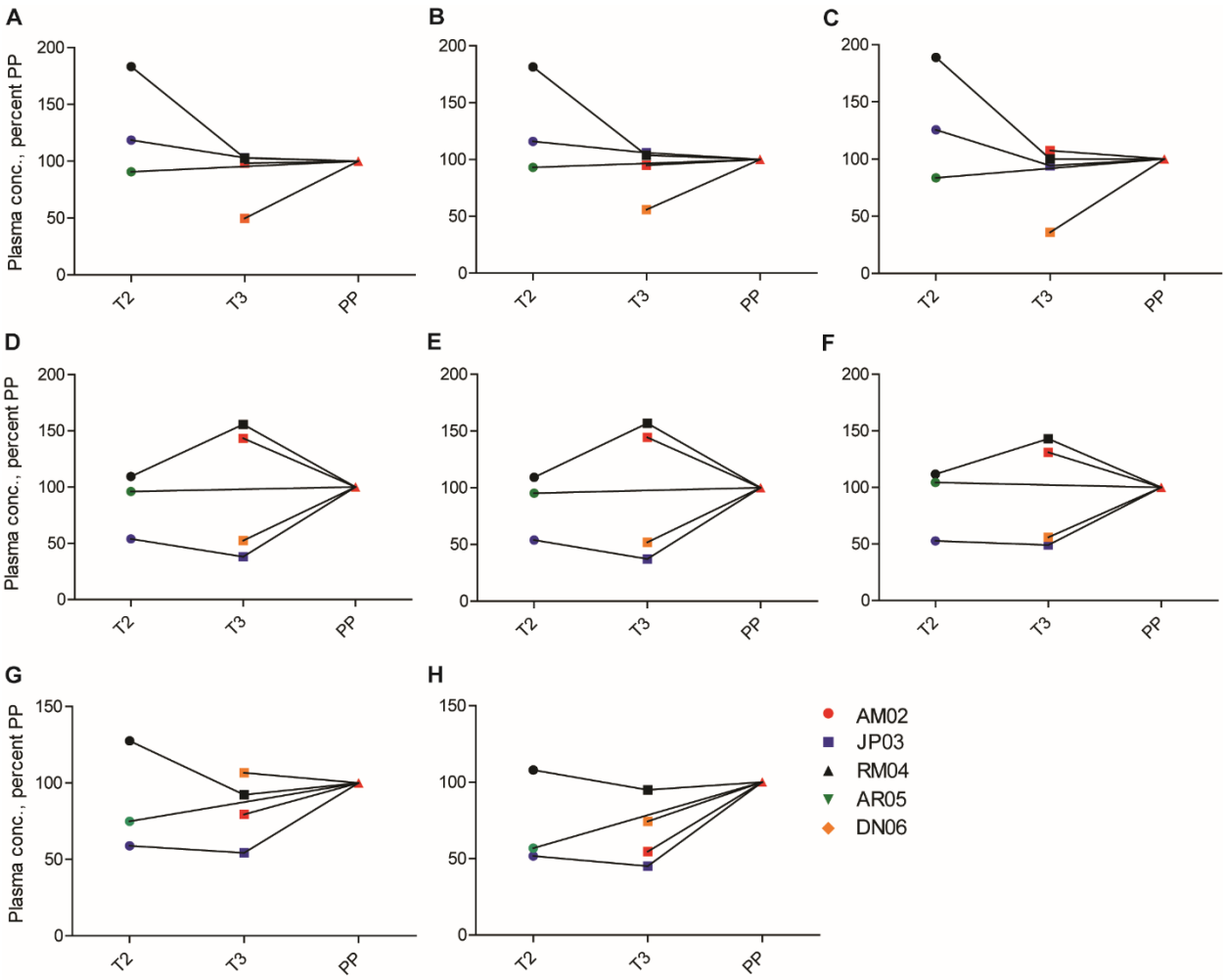

Figure 5.1. Plasma steady state concentrations of bupropion and its metabolites in each subject as percent of matched postpartum levels. Second trimester (T2) and third trimester (T3) C_{ss} values are shown as percent of the postpartum (PP) values in the same subjects. (A) bupropion, (B) R-bupropion, (C) S-bupropion, (D) OH-bupropion, (E) R,R-OH-bupropion, (F) S,S-OH-bupropion, (G) threohydrobupropion, and (H) erythrohydrobupropion.

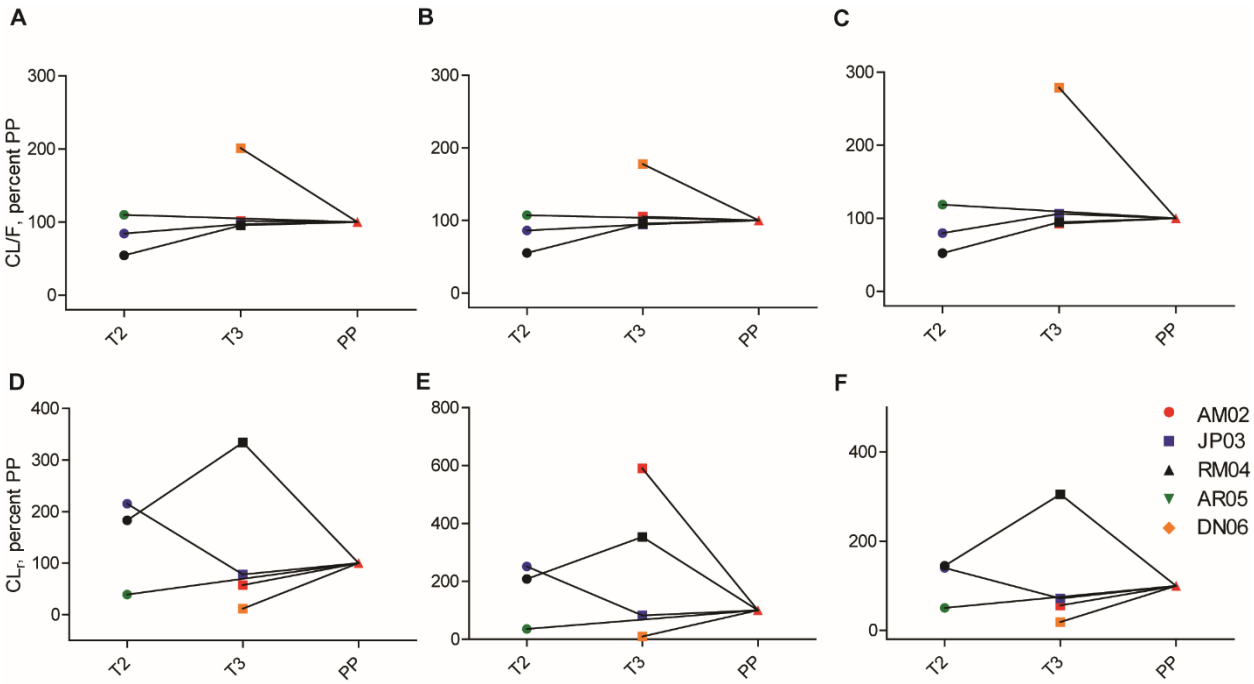

Figure 5.2. Bupropion clearance and renal clearance as percent of postpartum. The CL/F and CL_R of bupropion (A, D), R-bupropion (B, E), S-bupropion (C, E), in the second (T2) and third (T3) trimester as expressed as percent of the postpartum (PP) value in the same subject.

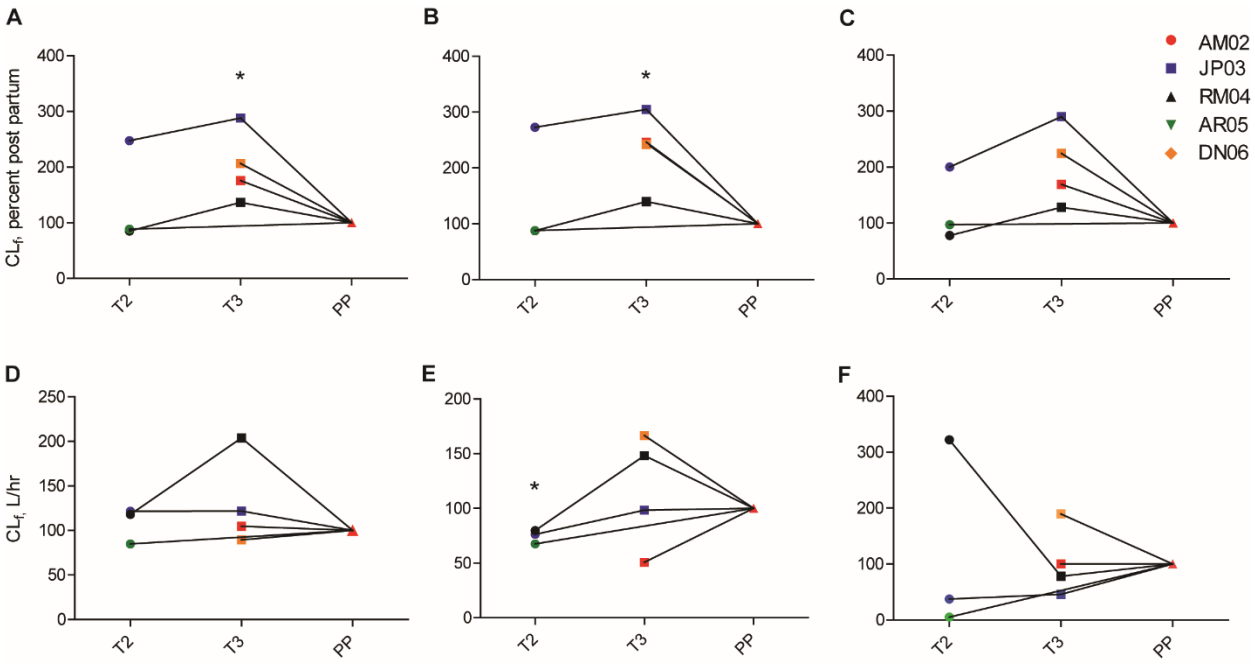

Figure 5.3. Bupropion metabolite formation clearance as percent of postpartum levels. The formation clearances of bupropion metabolites in each subject in second trimester (T2) and third trimester (T3) as percent of the matched postpartum (PP) value. (A) OH-bupropion, (B) R,R-OH-bupropion, (C) S,S-OH-bupropion, (D) threohydrobupropion, (E) erythrohydrobupropion and (F) 4'-OH-bupropion. * $p<0.05$

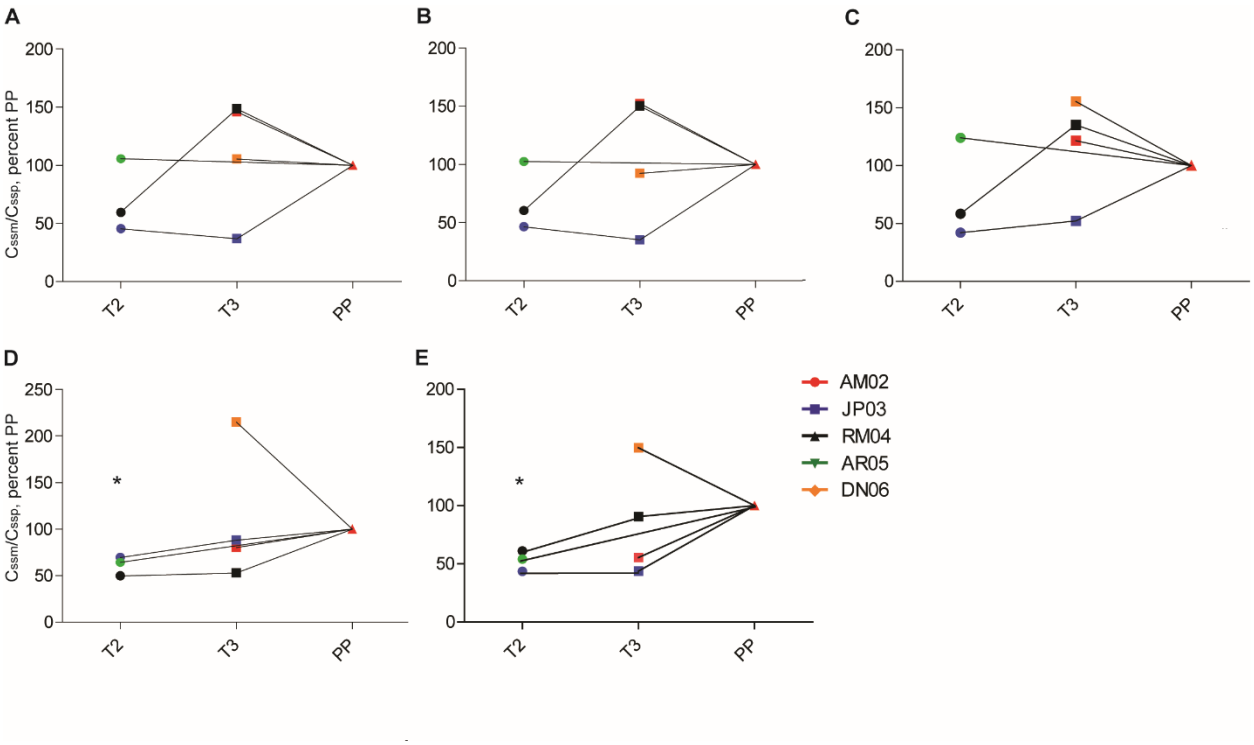

Figure 5.4. Metabolite to parent steady state concentration ratios as percent of postpartum levels. (A) OH-bupropion/bupropion, (B) R,R-OH-bupropion/R-bupropion, (C) S,S-OH-bupropion/S-bupropion, (D) threohydrobupropion/bupropion and (E) erythrohydrobupropion/bupropion. * $p<0.05$

Chapter 6.

GENERAL CONCLUSIONS

The projects included in this thesis demonstrate that through thorough characterization of bupropion's stereoselective metabolism and in vivo pharmacokinetics, the relative contribution of the bupropion elimination pathways and the magnitude of the bupropion-CYP2D6 interaction can be elucidated.

In order to completely characterize the elimination pathways and fractional contribution of each pathway to bupropion elimination, a study was first conducted to identify additional metabolites of bupropion in human urine and determine their quantitative importance to bupropion elimination. Three metabolites were isolated from the urine of a clinical study subject. The metabolites were identified as 4'-OH-bupropion, erythro-4'-OH-hydrobupropion and threo-4'-OH-hydrobupropion on the basis of MS/MS, NMR, UV and accurate mass. On average, 4'-OH-bupropion, threo-4'-OH-hydrobupropion and erythro-4'-OH-hydrobupropion and their conjugates account for 1.9 %, 14 % and 11 % of the total oral bupropion dose excreted in urine, respectively. While contributing to a relatively small percent of the total bupropion related drug material excreted, 4'-hydroxylation accounts for approximately 20 and 70% of threo- and erythrohydrobupropion elimination, respectively, suggesting that changes in the formation of these metabolites may significantly alter concentrations of the two active metabolites.

Next, the fractional contribution of each of bupropion's elimination pathways were assessed using in vitro intrinsic clearance values from recombinant enzymes and human liver S9 fractions. Based on our data, CYP2B6 and CYP2C19 were determined to be minor elimination pathways of bupropion, contributing to only 21 and 6% of bupropion elimination, respectively. Based on the magnitude of change in bupropion AUC following ticlopidine administration, the fm has previously been estimated to be 0.4. Here, we show that the estimated fm based on

ticlopidine data is likely an overestimate of the true $fm_{CYP2B6 + CYP2C19}$ since ticlopidine is a time dependent inhibitor of 11B-HSD-1, which is involved in threo- and erythrohydrobupropion formation.

To elucidate the cause of the bupropion-CYP2D6 interaction, the inhibition potential the individual stereoisomers of bupropion and OH-bupropion was investigated. Bupropion and its metabolites were found to inhibit CYP2D6 stereoselectively, yet based on static predictions, reversible inhibition did not explain the in vivo DDIs. The potential for active uptake was then further assessed in human suspension hepatocytes, but no uptake was observed. Finally the effects of bupropion and its metabolites on CYP2D6 regulation were monitored. Bupropion and all of its metabolites were found to significantly downregulate CYP2D6 on the basis of activity and mRNA levels. Using static predictions, the in vivo DDI was quantitatively predicted by significant downregulation of CYP2D6 mRNA and activity in human hepatocytes by bupropion and its metabolites. This study is the first example of a DDI resulting from P450 downregulation and first demonstration of a CYP2D6 interaction resulting from transcriptional regulation.

In order to assess the effects of pregnancy on bupropion pharmacokinetics, 5 female subjects, taking bupropion, were enrolled in a clinical study in which steady state urine and plasma samples were collected. Plasma concentrations and urine amounts of bupropion and its metabolites were measured both during pregnancy and post partum. No significant changes in steady state plasma concentrations of bupropion or its metabolites were observed, which suggests that there may not be a need for a dose adjustment during pregnancy. However, a significant two-fold change in OH-bupropion formation clearance was observed in the third trimester, when compared to postpartum. This induction of OH-bupropion formation clearance

occurred in the absence of a change in the OH-bupropion/bupropion C_{ss} ratio, which suggests that OH-bupropion clearance is also likely induced.

Taken together, these results encompass novel findings that greatly enhance our current understanding of bupropion elimination and its drug interaction potential.

REFERENCES

Abduljalil, D.K., Furness, P., Johnson, T.N., Rostami-Hodjegan, A., and Soltani, H. (2012). Anatomical, Physiological and Metabolic Changes with Gestational Age during Normal Pregnancy. Clin. Pharmacokinet. *51*, 365–396.

Alwan, S., Reefhuis, J., Botto, L.D., Rasmussen, S.A., Correa, A., and Friedman, J.M. (2010). Maternal use of bupropion and risk for congenital heart defects. Am. J. Obstet. Gynecol. *203*, 52.e1-52.e6.

Apovian, C.M. (2015). Naltrexone/bupropion for the treatment of obesity and obesity with Type 2 diabetes. Future Cardiol. *12*, 129–138.

Ascher, J.A., Cole, J.O., Colin, J.N., Feighner, J.P., Ferris, R.M., Fibiger, H.C., Golden, R.N., Martin, P., Potter, W.Z., and Richelson, E. (1995a). Bupropion: a review of its mechanism of antidepressant activity. *56*, 395–401.

Ascher, J.A., Cole, J.O., Colin, J.-N., Feighner, J.P., Ferris, R.M., Fibiger, H.C., Golden, R.N., Martin, P., Potter, W.Z., and Richelson, E. (1995b). Bupropion: a review of its mechanism of antidepressant activity. J. Clin. Psychiatry.

Baneyx, G., Parrott, N., Meille, C., Iliadis, A., and Lavé, T. (2014). Physiologically based pharmacokinetic modeling of CYP3A4 induction by rifampicin in human: Influence of time between substrate and inducer administration. Eur. J. Pharm. Sci. *56*, 1–15.

Benowitz, N.L., Zhu, A.Z.X., Tyndale, R.F., Dempsey, D., and Jacob, P., 3rd (2013). Influence of CYP2B6 genetic variants on plasma and urine concentrations of bupropion and metabolites at steady state. Pharmacogenet. Genomics *23*, 135–141.

Bondarev, M.L., Bondareva, T.S., Young, R., and Glennon, R.A. (2003). Behavioral and biochemical investigations of bupropion metabolites. Eur. J. Pharmacol. *474*, 85–93.

Brøsen, K., Hansen, J.G., Nielsen, K.K., Sindrup, S.H., and Gram, L.F. (1993). Inhibition by paroxetine of desipramine metabolism in extensive but not in poor metabolizers of sparteine. Eur. J. Clin. Pharmacol. *44*, 349–355.

Brown, H.S., Griffin, M., and Houston, J.B. (2007). Evaluation of Cryopreserved Human Hepatocytes as an Alternative in Vitro System to Microsomes for the Prediction of Metabolic Clearance. Drug Metab. Dispos. *35*, 293–301.

Bumpus, N.N., Kent, U.M., and Hollenberg, P.F. (2006). Metabolism of Efavirenz and 8-Hydroxyefavirenz by P450 2B6 Leads to Inactivation by Two Distinct Mechanisms. J. Pharmacol. Exp. Ther. *318*, 345–351.

Butz, R.F., Schroeder, D.H., Welch, R.M., Mehta, N.B., Phillips, A.P., and Findlay, J.W. (1981). Radioimmunoassay and pharmacokinetic profile of bupropion in the dog. J. Pharmacol. Exp. Ther. *217*, 602–610.

Callegari, E., Kalgutkar, A.S., Leung, L., Obach, R.S., Plowchalk, D.R., and Tse, S. (2013). Drug Metabolites as Cytochrome P450 Inhibitors: A Retrospective Analysis and Proposed Algorithm for Evaluation of the Pharmacokinetic Interaction Potential of Metabolites in Drug Discovery and Development. Drug Metab. Dispos. *41*, 2047–2055.

Capparelli, E., Aweeka, F., Hitti, J., Stek, A., Hu, C., Burchett, S., Best, B., Smith, E., Read, J., Watts, H., et al. (2008a). Chronic administration of nevirapine during pregnancy: impact of pregnancy on pharmacokinetics. HIV Med. *9*, 214–220.

Capparelli, E.V., Aweeka, F., Hitti, J., Stek, A., Hu, C., Burchett, S.K., Best, B., Smith, E., Read, J.S., Watts, H., et al. (2008b). Chronic administration of nevirapine during pregnancy: impact of pregnancy on pharmacokinetics. HIV Med. *9*, 214–220.

Carroll, F.I., Muresan, A.Z., Blough, B.E., Navarro, H.A., Mascarella, S.W., Eaton, J.B., Huang, X., Damaj, M.I., and Lukas, R.J. (2011). Synthesis of 2-(Substituted phenyl)-3,5,5-trimethylmorpholine Analogues and Their Effects on Monoamine Uptake, Nicotinic Acetylcholine Receptor Function, and Behavioral Effects of Nicotine. J. Med. Chem. *54*, 1441–1448.

Chang, S.-Y., Chen, C., Yang, Z., and Rodrigues, A.D. (2009). Further Assessment of 17α-Ethinyl Estradiol as an Inhibitor of Different Human Cytochrome P450 Forms in Vitro. Drug Metab. Dispos. *37*, 1667–1675.

Chen, Y., Liu, H., Liu, L., Nguyen, K., Jones, E.B., and Fretland, A.J. (2010). The *in vitro* metabolism of bupropion revisited: concentration dependent involvement of cytochrome P450 2C19. Xenobiotica *40*, 536–546.

Chen, Y., Mao, J., and Hop, C.E.C.A. (2015). Physiologically Based Pharmacokinetic Modeling to Predict Drug-Drug Interactions Involving Inhibitory Metabolite: A Case Study of Amiodarone. Drug Metab. Dispos. *43*, 182–189.

Choi, S.-Y., Koh, K.H., and Jeong, H. (2013). Isoform-Specific Regulation of Cytochromes P450 Expression by Estradiol and Progesterone. Drug Metab. Dispos. *41*, 263–269.

Chouinard, G. (1983). Bupropion and amitriptyline in the treatment of depressed patients. J. Clin. Psychiatry *44*, 121–129.

Cole, J.A., Modell, J.G., Haight, B.R., Cosmatos, I.S., Stoler, J.M., and Walker, A.M. (2007). Bupropion in pregnancy and the prevalence of congenital malformations. Pharmacoepidemiol. Drug Saf. *16*, 474–484.

Coleman, T. (2007). Recommendations for the Use of Pharmacological Smoking Cessation Strategies in Pregnant Women. CNS Drugs 2007 *21*, 983–993.

Coles, R., and Kharasch, E.D. (2008). Stereoselective Metabolism of Bupropion by Cytochrome P4502B6 (CYP2B6) and Human Liver Microsomes. Pharm. Res. *25*, 1405–1411.

Connarn, J.N., Zhang, X., Babiskin, A., and Sun, D. (2015). Metabolism of bupropion by carbonyl reductases in liver and intestine. Drug Metab. Dispos. Biol. Fate Chem. *43*, 1019–1027.

Covey, L.S., Glassman, A.H., and Stetner, F. (1990). Depression and depressive symptoms in smoking cessation. Compr. Psychiatry *31*, 350–354.

Cressey, T.R., Stek, A., Capparelli, E., Bowonwatanuwong, C., Prommas, S., Sirivatanapa, P., Yuthavisuthi, P., Neungton, C., Huo, Y., Smith, E., et al. (2012). Efavirenz pharmacokinetics during the third trimester of pregnancy and postpartum. J. Acquir. Immune Defic. Syndr. 1999 *59*, 245–252.

Damaj, M.I., Carroll, F.I., Eaton, J.B., Navarro, H.A., Blough, B.E., Mirza, S., Lukas, R.J., and Martin, B.R. (2004). Enantioselective Effects of Hydroxy Metabolites of Bupropion on Behavior and on Function of Monoamine Transporters and Nicotinic Receptors. Mol. Pharmacol. *66*, 675–682.

Damaj, M.I., Grabus, S.D., Navarro, H.A., Vann, R.E., Warner, J.A., King, L.S., Wiley, J.L., Blough, B.E., Lukas, R.J., and Carroll, F.I. (2010). Effects of Hydroxymetabolites of Bupropion on Nicotine Dependence Behavior in Mice. J. Pharmacol. Exp. Ther. *334*, 1087–1095.

Daviss, W.B., Perel, J.M., Brent, D.A., Axelson, D.A., Rudolph, G.R., Gilchrist, R., Nuss, S., and Birmaher, B. (2006). Acute antidepressant response and plasma levels of bupropion and metabolites in a pediatric-aged sample: an exploratory study. Ther. Drug Monit. *28*, 190–198.

Dickmann, L.J., and Isoherranen, N. (2013). Quantitative Prediction of CYP2B6 Induction by Estradiol During Pregnancy: Potential Explanation for Increased Methadone Clearance During Pregnancy. Drug Metab. Dispos. *41*, 270–274.

Diederich, S., Grossmann, C., Hanke, B., Quinkler, M., Herrmann, M., Bahr, V., and Oelkers, W. (2000). In the search for specific inhibitors of human 11beta-hydroxysteroid-dehydrogenases (11beta-HSDs): chenodeoxycholic acid selectively inhibits 11beta-HSD-I. Eur. J. Endocrinol. *142*, 200–207.

Dunner, D.L., Zisook, S., Billow, A.A., Batey, S.R., and Ascher, J.A. (1998). A Prospective Safety Surveillance Study for Bupropion Sustained-Release in the Treatment of Depression. J. Clin. Psychiatry *59*, 366–373.

Einolf, H.J., Chen, L., Fahmi, O.A., Gibson, C.R., Obach, R.S., Shebley, M., Silva, J., Sinz, M.W., Unadkat, J.D., Zhang, L., et al. (2014). Evaluation of Various Static and Dynamic Modeling Methods to Predict Clinical CYP3A Induction Using In Vitro CYP3A4 mRNA Induction Data. Clin. Pharmacol. Ther. *95*, 179–188.

Erickson, D.A., Mather, G., Trager, W.F., Levy, R.H., and Keirns, J.J. (1999). Characterization of the In Vitro Biotransformation of the HIV-1 Reverse Transcriptase Inhibitor Nevirapine by Human Hepatic Cytochromes P-450. Drug Metab. Dispos. *27*, 1488–1495.

European Medicines Agency Committee for Medicinal Products for Human Use (2012). Guideline on the Investigation of Drug-Drug Interactions.

Fahmi, O.A., Maurer, T.S., Kish, M., Cardenas, E., Boldt, S., and Nettleton, D. (2008). A Combined Model for Predicting CYP3A4 Clinical Net Drug-Drug Interaction Based on CYP3A4 Inhibition, Inactivation, and Induction Determined in Vitro. Drug Metab. Dispos. *36*, 1698–1708.

Fahmi, O.A., Hurst, S., Plowchalk, D., Cook, J., Guo, F., Youdim, K., Dickins, M., Phipps, A., Darekar, A., Hyland, R., et al. (2009). Comparison of Different Algorithms for Predicting Clinical Drug-Drug Interactions, Based on the Use of CYP3A4 in Vitro Data: Predictions of Compounds as Precipitants of Interaction. Drug Metab. Dispos. *37*, 1658–1666.

Farooq, M., Kelly, E.J., and Unadkat, J.D. (2016). CYP2D6 Is Inducible by Endogenous and Exogenous Corticosteroids. Drug Metab. Dispos. *44*, 750–757.

Fatemi, S.H., Emamian, E.S., and Kist, D.A. (1999). Venlafaxine and bupropion combination therapy in a case of treatment-resistant depression. Ann. Pharmacother. *33*, 701–703.

Faucette, S.R., Hawke, R.L., Lecluyse, E.L., Shord, S.S., Yan, B., Laethem, R.M., and Lindley, C.M. (2000). Validation of Bupropion Hydroxylation as a Selective Marker of Human Cytochrome P450 2B6 Catalytic Activity. Drug Metab. Dispos. *28*, 1222–1230.

Fava, M., Rush, A.J., Thase, M.E., Clayton, A., Stahl, S.M., Pradko, J.F., and Johnston, J.A. (2005). 15 Years of Clinical Experience With Bupropion HCl: From Bupropion to Bupropion SR to Bupropion XL. Prim. Care Companion J. Clin. Psychiatry *7*, 106–113.

Feighner, J., Hendrickson, G., Miller, L.P., and Stern, W.P. (1986). Double-Blind Comparison of Doxepin Versus Bupropion in Outpatients with a Major Depressive Disorder. J. Clin. Psychopharmacol. *6*, 27–31.

Feighner, J.P., Gardner, E.A., Johnston, J.A., Batey, S.R., Khayrallah, M.A., Ascher, J.A., and Lineberry, C.G. (1991). Double-blind comparison of bupropion and fluoxetine in depressed outpatients. J. Clin. Psychiatry *52*, 329–335.

Ferry, L., and Burchette, R. (1994). Efficacy of bupropion for smoking cessation in non-depressed smokers. J Addict Dis *13*, 249.

Findlay, J.W., Van Wyck Fleet, J., Smith, P.G., Butz, R.F., Hinton, M.L., Blum, M.R., and Schroeder, D.H. (1981). Pharmacokinetics of bupropion, a novel antidepressant agent, following oral administration to healthy subjects. Eur. J. Clin. Pharmacol. *21*, 127–135.

Foti, R.S., and Wahlstrom, J.L. (2008). CYP2C19 Inhibition: The Impact of Substrate Probe Selection on in Vitro Inhibition Profiles. Drug Metab. Dispos. *36*, 523–528.

Freeman, M.P., Nolan, P.E., Davis, M.F., Anthony, M., Fried, K., Fankhauser, M., Woosley, R.L., and Moreno, F. (2008). Pharmacokinetics of Sertraline Across Pregnancy and Postpartum: J. Clin. Psychopharmacol. *28*, 646–653.

Funck-Brentano, C., Becquemont, L., Leneveu, A., Roux, A., Jaillon, P., and Beaune, P. (1997). Inhibition by Omeprazole of Proguanil Metabolism: Mechanism of the Interaction In Vitro and Prediction of In Vivo Results from the In VitroExperiments. J. Pharmacol. Exp. Ther. *280*, 730–738.

Garcia-Pares, G. (2011). Role of bupropion in the treatment of resistant depression. Management of bupropion in combination therapy. Actas EspPsiquiatr *39*, 8–13.

Glassman, A.H., Helzer, J.E., Covey, L.S., Cottler, L.B., Stetner, F., Tipp, J.E., and Johnson, J. (1990). Smoking, smoking cessation, and major depression. JAMA *264*, 1546–1549.

Golden, R.N. (1988). Bupropion in Depression. II The role of metabolites in clinical outcome. Arch. Gen. Psychiatry *45*, 145–149.

Goodnick, P.J. (1992). Blood levels and acute response to bupropion. Am. J. Psychiatry *149*, 399–400.

Grabus, S.D., Carroll, F.I., and Damaj, M.I. (2012). Bupropion and its Main Metabolite Reverse Nicotine Chronic Tolerance in the Mouse. Nicotine Tob. Res. *14*, 1356–1361.

Greenway, F.L., Dunayevich, E., Tollefson, G., Erickson, J., Guttadauria, M., Fujioka, K., and Cowley, M.A. (2009). Comparison of Combined Bupropion and Naltrexone Therapy for Obesity with Monotherapy and Placebo. J. Clin. Endocrinol. Metab. *94*, 4898–4906.

Gufford, B.T., Lu, J.B.L., Metzger, I.F., Jones, D.R., and Desta, Z. (2016). Stereoselective Glucuronidation of Bupropion Metabolites In Vitro and In Vivo. Drug Metab. Dispos. *44*, 544–553.

Ha-Duong, N.T., Dijols, S., Macherey, A.C., Goldstein, J.A., Dansette, P.M., and Mansuy, D. (2001). Ticlopidine as a selective mechanism-based inhibitor of human cytochrome P450 2C19. Biochemistry (Mosc.) *40*, 12112–12122.

Hall, S.M., Munoz, R., and Reus, V. (1990). Smoking cessation, depression and dysphoria. NIDA Res. Monogr. *105*, 312–313.

Hall, S.M., Muñoz, R.F., and Reus, V.I. (1994). Cognitive-behavioral intervention increases abstinence rates for depressive-history smokers. J. Consult. Clin. Psychol. *62*, 141–146.

Hara, H., and Adachi, T. (2002). Contribution of hepatocyte nuclear factor-4 to down-regulation of CYP2D6 gene expression by nitric oxide. Mol. Pharmacol. *61*, 194–200.

Hesse, L.M., Venkatakrishnan, K., von Moltke, L.L., Duan, S.X., Shader, R.I., Greenblatt, D.J., and others (2000). CYP2B6 mediates the in vitro hydroxylation of bupropion: potential drug interactions with other antidepressants. Drug Metab. Dispos. *28*, 1176–1183.

Hill, S., Sikand, H., and Lee, J. (2007). A Case Report of Seizure Induced by Bupropion Nasal Insufflation. Prim. Care Companion J. Clin. Psychiatry *9*, 67.

Horst, W.D., and Preskorn, S.H. (1998). Mechanisms of action and clinical characteristics of three atypical antidepressants: venlafaxine, nefazodone, bupropion. J. Affect. Disord. *51*, 237–254.

Hurt, R.D., Sachs, D.P.L., Glover, E.D., Offord, K.P., Johnston, J.A., Dale, L.C., Khayrallah, M.A., Schroeder, D.R., Glover, P.N., Sullivan, C.R., et al. (1997). A Comparison of Sustained-Release Bupropion and Placebo for Smoking Cessation. N. Engl. J. Med. *337*, 1195–1202.

Isoherranen, N., and Thummel, K.E. (2013). Drug Metabolism and Transport During Pregnancy: How Does Drug Disposition Change during Pregnancy and What Are the Mechanisms that Cause Such Changes? Drug Metab. Dispos. *41*, 256–262.

Isoherranen, N., Hachad, H., Yeung, C.K., and Levy, R.H. (2009). Qualitative Analysis of the Role of Metabolites in Inhibitory Drug−Drug Interactions: Literature Evaluation Based on the Metabolism and Transport Drug Interaction Database. Chem. Res. Toxicol. *22*, 294–298.

Ito, K., and Houston, J.B. (2005). Prediction of Human Drug Clearance from in Vitro and Preclinical Data Using Physiologically Based and Empirical Approaches. Pharm. Res. *22*, 103–112.

Ito, K., Hallifax, D., Obach, R.S., and Houston, J.B. (2005). Impact of Parallel Pathways of Drug Elimination and Multiple Cytochrome P450 Involvement on Drug-Drug Interactions: Cyp2d6 Paradigm. Drug Metab. Dispos. *33*, 837–844.

Jefferson, J.W., Pradko, J.F., and Muir, K.T. (2005). Bupropion for major depressive disorder: Pharmacokinetic and formulation considerations. Clin. Ther. *27*, 1685–1695.

Johnston, J.A., Fiedler-Kelly, J., Glover, E.D., Sachs, D.P., Grasela, T.H., and DeVeaugh-Geiss, J. (2001). Relationship between drug exposure and the efficacy and safety of bupropion sustained release for smoking cessation. Nicotine Tob. Res. Off. J. Soc. Res. Nicotine Tob. *3*, 131–140.

Jones, H., Chen, Y., Gibson, C., Heimbach, T., Parrott, N., Peters, S., Snoeys, J., Upreti, V., Zheng, M., and Hall, S. (2015). Physiologically based pharmacokinetic modeling in drug discovery and development: A pharmaceutical industry perspective. Clin. Pharmacol. Ther. *97*, 247–262.

Jorenby, D. (1999). A Controlled Trial of Sustained Release Bupropion, A Nicotine Patch or Both For Smoking Cessation. N. Engl. J. Med. *340*, 685–691.

Kaivosaari, S., Finel, M., and Koskinen, M. (2011). N-glucuronidation of drugs and other xenobiotics by human and animal UDP-glucuronosyltransferases. Xenobiotica *41*, 652–669.

Ke, A.B., Nallani, S.C., Zhao, P., Rostami-Hodjegan, A., and Unadkat, J.D. (2014). Expansion of a PBPK Model to Predict Disposition in Pregnant Women of Drugs Cleared via Multiple CYP Enzymes, Including CYP2B6, CYP2C9 and CYP2C19. Br. J. Clin. Pharmacol. *77*, 554–570.

Kennedy, S.H., McCann, S.M., Masellis, M., McIntyre, R.S., Raskin, J., McKay, G., and Baker, G.B. (2002). Combining bupropion SR with venlafaxine, paroxetine, or fluoxetine: a preliminary report on pharmacokinetic, therapeutic, and sexual dysfunction effects. J. Clin. Psychiatry *63*, 181–186.

Kharasch, E.D., Mitchell, D., and Coles, R. (2008). Stereoselective Bupropion Hydroxylation as an In Vivo Phenotypic Probe for Cytochrome P4502B6 (CYP2B6) Activity. J. Clin. Pharmacol. *48*, 464–474.

Kharasch, E.D., Campbell, S., Stubbert, K., Crafford, A., London, A., Kim, T., Whittington, D., Ensign, D., Hoffer, C., and Bedynek, P.S. (2012). Mechanism of efavirenz influence on methadone pharmacokinetics and pharmacodynamics II: Hepatic and intestinal CYP2B6, CYP3A and transporter activities. Clin. Pharmacol. Ther. *91*, 673–684.

Koh, K.H., Jurkovic, S., Yang, K., Choi, S.-Y., Jung, J.W., Kim, K.P., Zhang, W., and Jeong, H. (2012). Estradiol induces cytochrome P450 2B6 expression at high concentrations: Implication in estrogen-mediated gene regulation in pregnancy. Biochem. Pharmacol. *84*, 93–103.

Koh, K.H., Pan, X., Shen, H.-W., Arnold, S.L.M., Yu, A.-M., Gonzalez, F.J., Isoherranen, N., and Jeong, H. (2014). Altered Expression of Small Heterodimer Partner Governs Cytochrome P450 (CYP) 2D6 Induction during Pregnancy in CYP2D6-humanized Mice. J. Biol. Chem. *289*, 3105–3113.

Kotlyar, M.P., Brauer, L.H., Tracy, T.S., Hatsukami, D.K., Harris, J.B., Bronars, C.A., and Adson, D.E. (2005). Inhibition of CYP2D6 Activity by Bupropion. J. Clin. Psychopharmacol. June 2005 *25*, 226–229.

Lai, A.A., and Schroeder, D.H. (1983). Clinical pharmacokinetics of bupropion: a review. J. Clin. Psychiatry *44*, 82–84.

Laine, K. (2000). No sex-related differences but significant inhibition by oral contraceptives of CYP2C19 activity as measured by the probe drugs mephenytoin and omeprazole in healthy Swedish white subjects. Clin. Pharmacol. Ther. *68*, 151–159.

Laizure, S.C., and DeVane, C.L. (1985). Stability of bupropion and its major metabolites in human plasma. Ther. Drug Monit. *7*, 447–450.

Lamson, M., MacGregor, T., Riska, P., Erickson, D., Maxfield, P., Rowland, L., Gigliotti, M., Robinson, P., Azzam, S., and Keirns, J. (1999). Nevirapine induces both CYP3A4 and CYP2B6 metabolic pathways. Clin. Pharmacol. 38 Ther. *65*, 137–137.

Learned-Coughlin, S.M., Bergström, M., Savitcheva, I., Ascher, J., Schmith, V.D., and Långstrom, B. (2003). In vivo activity of bupropion at the human dopamine transporter as measured by positron emission tomography. Biol. Psychiatry *54*, 800–805.

Luche, J.L. (1978). Lanthanides in organic chemistry. 1. Selective 1,2 reductions of conjugated ketones. J. Am. Chem. Soc. *100*, 2226–2227.

Lutz, J.D., and Isoherranen, N. (2012a). Prediction of Relative In Vivo Metabolite Exposure from In Vitro Data Using Two Model Drugs: Dextromethorphan and Omeprazole. Drug Metab. Dispos. *40*, 159–168.

Lutz, J.D., and Isoherranen, N. (2012b). In vitro-to-in vivo predictions of drug–drug interactions involving multiple reversible inhibitors. Expert Opin. Drug Metab. Toxicol. *8*, 449–466.

M. Árgyelán, Z.S. (2006). P.2.b.009 The activity of dopamine transporter (DAT) in depression and the effect of sertraline - preliminary results by β-CIT SPECT. Eur. Neuropsychopharmacol. - EUR NEUROPSYCHOPHARMACOL *16*.

Mamoon, A., Subauste, A., Subauste, M.C., and Subauste, J. (2014). Retinoic acid regulates several genes in bile acid and lipid metabolism via upregulation of small heterodimer partner in hepatocytes. Gene *550*, 165–170.

Marcus, S.M., Flynn, H.A., Blow, F.C., and Barry, K.L. (2003). Depressive symptoms among pregnant women screened in obstetrics settings. J. Womens Health 2002 *12*, 373–380.

Marshall, R.D., Johannet, C.M., Collins, P.Y., Smith, H., Kahn, D.A., and Douglas, C.J. (1995). Bupropion and sertraline combination treatment in refractory depression. J. Psychopharmacol. Oxf. Engl. *9*, 284–286.

Martin, P., Massol, J., Colin, J., Lacomblez, L., and Puech, A. (1990). Antidepressant Profile of Bupropion and three Metabolites in Mice. Pharmacopsychiatry *23*, 187–194.

Maxwell, R.A. (1985). The Pharmacological Rationale for Bupropion. In Psychiatry the State of the Art, P. Pichot, P. Berner, R. Wolf, and K. Thau, eds. (Springer US), pp. 135–140.

McAffee, T. (1998). Sustained-Release Bupropion for Smoking Cessation. N. Engl. J. Med. *338*, 619–620.

McGready, R., Stepniewska, K., Edstein, M.D., Cho, T., Gilveray, G., Looareesuwan, S., White, N.J., and Nosten, F. (2003a). The pharmacokinetics of atovaquone and proguanil in pregnant women with acute falciparum malaria. Eur. J. Clin. Pharmacol. *59*, 545–552.

McGready, R., Stepniewska, K., Seaton, E., Cho, T., Cho, D., Ginsberg, A., Edstein, M.D., Ashley, E., Looareesuwan, S., White, N.J., et al. (2003b). Pregnancy and use of oral contraceptives reduces the biotransformation of proguanil to cycloguanil. Eur. J. Clin. Pharmacol. *59*, 553–557.

Mendels, J., Amin, M.M., Chouinard, G., Cooper, A.J., Miles, J.E., Remick, R.A., Saxena, B., Secunda, S.K., and Singh, A.N. (1983). A comparative study of bupropion and amitriptyline in depressed outpatients. J. Clin. Psychiatry *44*, 118–120.

Meyer, A., Vuorinen, A., Zielinska, A.E., Strajhar, P., Lavery, G.G., Schuster, D., and Odermatt, A. (2013). Formation of Threohydrobupropion from Bupropion Is Dependent on 11β-Hydroxysteroid Dehydrogenase 1. Drug Metab. Dispos. *41*, 1671–1678.

Musso, D.L., Mehta, N.B., Soroko, F.E., Ferris, R.M., Hollingsworth, E.B., and Kenney, B.T. (1993). Synthesis and evaluation of the antidepressant activity of the enantiomers of bupropion. Chirality *5*, 495–500.

Mwinyi, J., Cavaco, I., Pedersen, R.S., Persson, A., Burkhardt, S., Mkrtchian, S., and Ingelman-Sundberg, M. (2010). Regulation of CYP2C19 Expression by Estrogen Receptor α: Implications for Estrogen-Dependent Inhibition of Drug Metabolism. Mol. Pharmacol. *78*, 886–894.

Nellen, J., Damming, M., Godfried, M., Boer, K., Van Der Ende, M., Burger, D., De Wolf, F., Wit, F., and Prins, J. (2008). Steady-state nevirapine plasma concentrations are influenced by pregnancy. HIV Med. *9*, 234–238.

Nemoto, N., and Sakurai, J. (1995). Glucocorticoid and Sex Hormones as Activating or Modulating Factors for Expression of Cyp2b-9 and Cyp2b-L0 in the Mouse Liver and Hepatocytes. Arch. Biochem. Biophys. *319*, 286–292.

Newton, T.F., Roache, J.D., Ii, R.D.L.G., Fong, T., Wallace, C.L., Li, S.-H., Elkashef, A., Chiang, N., and Kahn, R. (2005). Safety of intravenous methamphetamine administration during treatment with bupropion. Psychopharmacology (Berl.) *182*, 426–435.

Nichols, A.I., Focht, K., Jiang, Q., Preskorn, S.H., and Kane, C.P. (2011). Pharmacokinetics of venlafaxine extended release 75 mg and desvenlafaxine 50 mg in healthy CYP2D6 extensive and poor metabolizers: a randomized, open-label, two-period, parallel-group, crossover study. Clin. Drug Investig. *31*, 155–167.

Nishiya, Y., Hagihara, K., Kurihara, A., Okudaira, N., Farid, N.A., Okazaki, O., and Ikeda, T. (2009a). Comparison of mechanism-based inhibition of human cytochrome P450 2C19 by ticlopidine, clopidogrel, and prasugrel. Xenobiotica Fate Foreign Compd. Biol. Syst. *39*, 836–843.

Nishiya, Y., Hagihara, K., Ito, T., Tajima, M., Miura, S., Kurihara, A., Farid, N.A., and Ikeda, T. (2009b). Mechanism-Based Inhibition of Human Cytochrome P450 2B6 by Ticlopidine, Clopidogrel, and the Thiolactone Metabolite of Prasugrel. Drug Metab. Dispos. *37*, 589–593.

Nomikos, G.G., Damsma, G., Wenkstern, D., and Fibiger, H.C. (1989). Acute effects of bupropion on extracellular dopamine concentrations in rat striatum and nucleus accumbens studied by in vivo microdialysis. Neuropsychopharmacol. Off. Publ. Am. Coll. Neuropsychopharmacol. *2*, 273–279.

Nomikos, G.G., Damsma, G., Wenkstern, D., and Fibiger, H.C. (1992). Effects of chronic bupropion on interstitial concentrations of dopamine in rat nucleus accumbens and striatum. Neuropsychopharmacol. Off. Publ. Am. Coll. Neuropsychopharmacol. *7*, 7–14.

Obach, R.S., Cox, L.M., and Tremaine, L.M. (2005). Sertraline Is Metabolized by Multiple Cytochrome P450 Enzymes, Monoamine Oxidases, and Glucuronyl Transferases in Human: An in Vitro Study. Drug Metab. Dispos. *33*, 262–270.

Olagunju, A., Bolaji, O., Neary, M., Back, D., Khoo, S., and Owen, A. (2016). Pregnancy affects nevirapine pharmacokinetics: evidence from a CYP2B6 genotype-guided observational study. Pharmacogenet. Genomics.

O'Leary, P., Boyne, P., Flett, P., Beilby, J., and James, I. (1991). Longitudinal assessment of changes in reproductive hormones during normal pregnancy. Clin. Chem. *37*, 667–672.

Pan, X., Lee, Y.-K., and Jeong, H. (2015). Farnesoid X Receptor Agonist Represses Cytochrome P450 2D6 Expression by Upregulating Small Heterodimer Partner. Drug Metab. Dispos. *43*, 1002–1007.

Peng, C.-C., Templeton, I., Thummel, K.E., Davis, C., Kunze, K.L., and Isoherranen, N. (2011). Evaluation of 6β-hydroxycortisol, 6β-hydroxycortisone and their combination as endogenous probes for inhibition of CYP3A4 in vivo. Clin. Pharmacol. Ther. *89*, 888–895.

Perrine, D.M., Ross, J.T., Nervi, S.J., and Zimmerman, R.H. (2000). A Short, One-Pot Synthesis of Bupropion (Zyban, Wellbutrin). J. Chem. Educ. *77*, 1479.

Petsalo, A., Turpeinen, M., and Tolonen, A. (2007). Identification of bupropion urinary metabolites by liquid chromatography/mass spectrometry. Rapid Commun. Mass Spectrom. *21*, 2547–2554.

Pond, S.M., Kreek, M.J., Tong, T.G., Raghunath, J., and Benowitz, N.L. (1985). Altered methadone pharmacokinetics in methadone-maintained pregnant women. J. Pharmacol. Exp. Ther. *233*, 1–6.

Preskorn, S.H. (1983). Antidepressant response and plasma concentrations of bupropion. J. Clin. Psychiatry *44*, 137–139.

Preskorn, S., Patroneva, A., Silman, H., Jiang, Q., Isler, J.A., Burczynski, M.E., Ahmed, S., Paul, J., and Nichols, A.I. (2009). Comparison of the pharmacokinetics of venlafaxine extended release and desvenlafaxine in extensive and poor cytochrome P450 2D6 metabolizers. J. Clin. Psychopharmacol. *29*, 39–43.

Rajoli, R.K.R., Back, D.J., Rannard, S., Freel Meyers, C.L., Flexner, C., Owen, A., and Siccardi, M. (2014). Physiologically Based Pharmacokinetic Modelling to Inform Development of Intramuscular Long-Acting Nanoformulations for HIV. Clin. Pharmacokinet. *54*, 639–650.

Reese, M.J., Wurm, R.M., Muir, K.T., Generaux, G.T., St John-Williams, L., and McConn, D.J. (2008). An in vitro mechanistic study to elucidate the desipramine/bupropion clinical drug-drug interaction. Drug Metab. Dispos. Biol. Fate Chem. *36*, 1198–1201.

Reinoso, R.F., Telfer, B.A., Brennan, B.S., and Rowland, M. (2001). Uptake of teicoplanin by isolated rat hepatocytes: comparison with in vivo hepatic distribution. Drug Metab. Dispos. *29*, 453–459.

Rekic, D., Roshammar, D., Mukonzo, J., and Ashton, M. (2011). In silico prediction of efavirenz and rifampicin drug-drug interaction considering weight and CYP2B6 phenotype. Br. J. Clin. Pharmacol. *71*, 536–543.

Richter, T., Mürdter, T.E., Heinkele, G., Pleiss, J., Tatzel, S., Schwab, M., Eichelbaum, M., and Zanger, U.M. (2004). Potent Mechanism-Based Inhibition of Human CYP2B6 by Clopidogrel and Ticlopidine. J. Pharmacol. Exp. Ther. *308*, 189–197.

Rissmiller, D.J., and Campo, T. (2007). Extended-release bupropion–induced grand mal seizures. J. Am. Osteopath. Assoc. *107*, 441–442.

Robertson, S.M., Maldarelli, F., Natarajan, V., Formentini, E., Alfaro, R.M., and Penzak, S.R. (2008). Efavirenz induces CYP2B6-mediated hydroxylation of bupropion in healthy subjects. J. Acquir. Immune Defic. Syndr. 1999 *49*, 513–519.

Rodrigues, A.D., and Lu, P. (2004). IS 17α-ETHINYL ESTRADIOL AN INHIBITOR OF CYTOCHROME P450 2C19? Drug Metab. Dispos. *32*, 364–365.

Rytting, E., Wang, X., Vernikovskaya, D.I., Zhan, Y., Bauer, C., Abdel-Rahman, S.M., Ahmed, M.S., and Nanovskaya, T.N. (2014). Metabolism and Disposition of Bupropion in Pregnant Baboons (Papio cynocephalus). Drug Metab. Dispos. *42*, 1773–1779.

Sager, J.E., Lutz, J.D., Foti, R.S., Davis, C., Kunze, K.L., and Isoherranen, N. (2014). Fluoxetine- and Norfluoxetine-Mediated Complex Drug–Drug Interactions: In Vitro to In Vivo Correlation of Effects on CYP2D6, CYP2C19, and CYP3A4. Clin. Pharmacol. Ther. *95*, 653–662.

Sager, J.E., Choiniere, J.R., Chang, J., Stephenson-Famy, A., Nelson, W.L., and Isoherranen, N. (2016). Identification and Structural Characterization of Three New Metabolites of Bupropion in Humans. ACS Med. Chem. Lett.

Schroeder, D.H. (1983). Metabolism and kinetics of bupropion. J. Clin. Psychiatry *44*, 79–81.

Shardlow, C.E., Generaux, G.T., Patel, A.H., Tai, G., Tran, T., and Bloomer, J.C. (2013). Impact of Physiologically Based Pharmacokinetic Modeling and Simulation in Drug Development. Drug Metab. Dispos. *41*, 1994–2003.

Sherman, M.M., Ungureanu, S., and Rey, J.A. (2016). Naltrexone/Bupropion ER (Contrave). *41*.

Shirasaka, Y., Sager, J.E., Lutz, J.D., Davis, C., and Isoherranen, N. (2013). Inhibition of CYP2C19 and CYP3A4 by Omeprazole Metabolites and Their Contribution to Drug-Drug Interactions. Drug Metab. Dispos. *41*, 1414–1424.

Silverstone, P.H., Williams, R., McMahon, L., Fleming, R., and Fogarty, S. (2008). Convulsive liability of bupropion hydrochloride metabolites in Swiss albino mice. Ann. Gen. Psychiatry *7*, 19.

Skarydova, L., Tomanova, R., Havlikova, L., Stambergova, H., Solich, P., and Wsol, V. (2013). Deeper insight into the reducing biotransformation of bupropion in the human liver. Drug Metab. Pharmacokinet. *advpub*.

Slemmer, J.E., Martin, B.R., and Damaj, M.I. (2000). Bupropion Is a Nicotinic Antagonist. J. Pharmacol. Exp. Ther. *295*, 321–327.

Soldin, O.P., Guo, T., Weiderpass, E., Tractenberg, R.E., Hilakivi-Clarke, L., and Soldin, S.J. (2005). Steroid hormone levels in pregnancy and 1 year postpartum using isotope dilution tandem mass spectrometry. Fertil. Steril. *84*, 701–710.

Stahl, S.M., Pradko, J.F., Haight, B.R., Modell, J.G., Rockett, C.B., and Learned-Coughlin, S. (2004). A Review of the Neuropharmacology of Bupropion, a Dual Norepinephrine and Dopamine Reuptake Inhibitor. Prim. Care Companion J. Clin. Psychiatry *6*, 159–166.

Stringer, R.A., Strain-Damerell, C., Nicklin, P., and Houston, J.B. (2009). Evaluation of Recombinant Cytochrome P450 Enzymes as an in Vitro System for Metabolic Clearance Predictions. Drug Metab. Dispos. *37*, 1025–1034.

Taylor, L.C.E. (1995). The identification of in vitro metabolites of bupropion using ion trap mass spectrometry. Rapid Commun. Mass Spectrom. *9*, 902–910.

Templeton, I., Peng, C.-C., Thummel, K.E., Davis, C., Kunze, K.L., and Isoherranen, N. (2010). Accurate prediction of dose-dependent CYP3A4 inhibition by itraconazole and its metabolites from in vitro inhibition data. Clin. Pharmacol. Ther. *88*, 499–505.

Tong, V.T., Dietz, P.M., Morrow, B., D'Angelo, D.V., Farr, S.L., Rockhill, K.M., England, L.J., and others (2013). Trends in smoking before, during, and after pregnancy—Pregnancy Risk Assessment Monitoring System, United States, 40 sites, 2000–2010. MMWR Surveill Summ *62*, 1–19.

Totah, R.A., Sheffels, P., Roberts, T., Whittington, D., Thummel, K., and Kharasch, E.D. (2008). Role of CYP2B6 in Stereoselective Human Methadone Metabolism: Anesthesiology *108*, 363–374.

Tripathy, S., Chapman, J.D., Han, C.Y., Hogarth, C., Arnold, S.L., Onken, J., Kent, T., Goodlett, D.R., and Isoherranen, N. (2016). All-trans-retinoic acid Enhances Mitochondrial Function in Models of Human Liver. Mol. Pharmacol. mol.116.103697.

Turpeinen, M., Tolonen, A., Uusitalo, J., Jalonen, J., Pelkonen, O., and Laine, K. (2005). Effect of Clopidogrel and Ticlopidine on Cytochrome P450 2B6 Activity as Measured by Bupropion Hydroxylation*. Clin. Pharmacol. Ther. *77*, 553–559.

U.S. Department of Health and Human Services. (2014). The Health Consequences of Smoking: 50 Years of Progress. A Report of the Surgeon General. (Atlanta, Georgia: U.S. Department of Health and Human Services, Centers for Disease Control and Prevention, National Center for Chronic Disease Prevention and Health Promotion, Office on Smoking and Health).

U.S. Food and Drug Administration Center for Drug Evaluation (1985). Wellbutrin NDA 018644.

U.S. Food and Drug Administration Center for Drug Evaluation (1997). Zyban NDA 20-711 Approval Letter.

U.S. Food and Drug Administration Center for Drug Evaluation (2000). NDA 21-078 Malarone.

U.S. Food and Drug Administration Center for Drug Evaluation (2001). Wellbutrin SR Label 2001.

U.S. Food and Drug Administration Center for Drug Evaluation (2008). Guidance for Industry - Metabolites in Safety testing.

U.S. Food and Drug Administration Center for Drug Evaluation (2013a). Wellbutrin and Wellbutrin SR (bupropion hydrochloride) - NDA 020358.

U.S. Food and Drug Administration Center for Drug Evaluation (2013b). Wellbutrin and Welbutrin SR NDA 018644/S-041 and 02358/S-048 Approval Letter.

U.S. Food and Drug Administration Center for Drug Evaluation and Research (2003). Wellbutrin XL Clinical pharmacology and biopharmaceutics review.

U.S. Food and Drug Administration, Center for Drug Evaluation and Research (2014). Contrave NDA 20006Orig1s000 Approval Letter.

U.S. Food and Drug Administration Center for Drug Evaluation and Research (CDER) (2012). Guidance for Industry: Drug interaction studies- study design, data analysis, implications for dosing, and labeling.

Varma, M.V., Pang, K.S., Isoherranen, N., and Zhao, P. (2015a). Dealing with the complex drug–drug interactions: Towards mechanistic models. Biopharm. Drug Dispos. *36*, 71–92.

Varma, M.V.S., Lai, Y., Feng, B., Litchfield, J., Goosen, T.C., and Bergman, A. (2012). Physiologically Based Modeling of Pravastatin Transporter-Mediated Hepatobiliary Disposition and Drug-Drug Interactions. Pharm. Res. *29*, 2860–2873.

Varma, M.V.S., Lin, J., Bi, Y.-A., Rotter, C.J., Fahmi, O.A., Lam, J.L., El-Kattan, A.F., Goosen, T.C., and Lai, Y. (2013). Quantitative Prediction of Repaglinide-Rifampicin Complex Drug Interactions Using Dynamic and Static Mechanistic Models: Delineating Differential CYP3A4 Induction and OATP1B1 Inhibition Potential of Rifampicin. Drug Metab. Dispos. *41*, 966–974.

Varma, M.V.S., Lin, J., Bi, Y., Kimoto, E., and Rodrigues, D. (2015b). Quantitative Rationalization of Gemfibrozil Drug Interactions: Consideration of Transporters-Enzyme Interplay and the Role of Circulating Metabolite Gemfibrozil 1-O-β-Glucuronide. Drug Metab. Dispos. dmd.115.064303.

Venkatakrishnan, K. (2005). In vitro-in vivo Extrapolation of CYP2D6 Inactivation by Paroxetine; Prediction of Nonstationary Pharmacokinetics and Drug Interaction Magnitude. Drug Metab. Dispos. *33*, 845–852.

Vieira, M.L.T., Kirby, B., Ragueneau-Majlessi, I., Galetin, A., Chien, J.Y.L., Einolf, H.J., Fahmi, O.A., Fischer, V., Fretland, A., Grime, K., et al. (2014). Evaluation of Various Static In Vitro–In Vivo Extrapolation Models for Risk Assessment of the CYP3A Inhibition Potential of an Investigational Drug. Clin. Pharmacol. Ther. *95*, 189–198.

Wadden, T.A., Foreyt, J.P., Foster, G.D., Hill, J.O., Klein, S., O'Neil, P.M., Perri, M.G., Pi-Sunyer, F.X., Rock, C.L., Erickson, J.S., et al. (2011). Weight loss with naltrexone SR/bupropion SR combination therapy as an adjunct to behavior modification: the COR-BMOD trial. Obes. Silver Spring Md *19*, 110–120.

Wang, J.-S., and DeVane, C.L. (2003). Involvement of Cyp3a4, Cyp2c8, and Cyp2d6 in the Metabolism of (r)- and (s)-Methadone in Vitro. Drug Metab. Dispos. *31*, 742–747.

Watanabe, T., Kusuhara, H., Maeda, K., Shitara, Y., and Sugiyama, Y. (2009). Physiologically Based Pharmacokinetic Modeling to Predict Transporter-Mediated Clearance and Distribution of Pravastatin in Humans. J. Pharmacol. Exp. Ther. *328*, 652–662.

Weisler, R.H., Johnston, J.A.P., Lineberry, C.G., Samara, B., Branconnier, R.J., and Billow, A.A.B. (1994). Comparison of Bupropion and Trazodone for the Treatment of Major Depression. [Editorial]. J. Clin. Psychopharmacol. *14*, 170–179.

Welch, R.M., Lai, A.A., and Schroeder, D.H. (1987). Pharmacological significance of the species differences in bupropion metabolism. Xenobiotica Fate Foreign Compd. Biol. Syst. *17*, 287–298.

Wilkes, S. (2008). The use of bupropion SR in cigarette smoking cessation. Int. J. Chron. Obstruct. Pulmon. Dis. *3*, 45–53.

Wolff, K., Boys, A., Rostami-Hodjegan, A., Hay, A., and Raistrick, D. (2005). Changes to methadone clearance during pregnancy. Eur. J. Clin. Pharmacol. *61*, 763–768.

Woodcock, J., Khan, M., and Yu, L.X. (2012). Withdrawal of Generic Budeprion for Nonbioequivalence. N. Engl. J. Med. *367*, 2463–2465.

Yamada, H., Gohyama, N., Honda, S., Hara, T., Harada, N., and Oguri, K. (2002). Estrogen-Dependent Regulation of the Expression of Hepatic Cyp2b and 3a Isoforms: Assessment Using Aromatase-Deficient Mice. Toxicol. Appl. Pharmacol. *180*, 1–10.

Yamamoto, M., Sakuma, T., Ichimaru, H., and Nemoto, N. (2001). Localization of estradiol-responsive region in the phenobarbital-responsive enhancer module of mouse Cyp2b-10 gene. J. Biochem. Mol. Toxicol. *15*, 76–82.

Yannone, M.E., Mueller, J.R., and Osborn, R.H. (1969). Protein binding of progesterone in the peripheral plasma during pregnancy and labor. Steroids *13*, 773–781.

Yeung, C.K., Fujioka, Y., Hachad, H., Levy, R.H., and Isoherranen, N. (2011). Are Circulating Metabolites Important in Drug–Drug Interactions?: Quantitative Analysis of Risk Prediction and Inhibitory Potency. Clin. Pharmacol. Ther. *89*, 105–113.

Yu, H., and Tweedie, D. (2013). A Perspective on the Contribution of Metabolites to Drug-Drug Interaction Potential: The Need to Consider Both Circulating Levels and Inhibition Potency. Drug Metab. Dispos. *41*, 536–540.

Yu, H., Balani, S.K., Chen, W., Cui, D., He, L., Humphreys, W.G., Mao, J., Lai, W.G., Lee, A.J., Lim, H.-K., et al. (2015). Contribution of Metabolites to P450 Inhibition-Based Drug-Drug Interactions: Scholarship from the Drug Metabolism Leadership Group of the Innovation and Quality Consortium Metabolite Group. Drug Metab. Dispos. *43*, 620–630.

Zhang, L., Zhang, Y. (Derek), Zhao, P., and Huang, S.-M. (2009). Predicting Drug–Drug Interactions: An FDA Perspective. AAPS J. *11*, 300–306.

Zhao, Y., and Hu, Z.-Y. (2014). Physiologically based pharmacokinetic modelling and in vivo [I]/Ki accurately predict P-glycoprotein-mediated drug-drug interactions with dabigatran etexilate. Br. J. Pharmacol. *171*, 1043–1053.

Zhu, A.Z.X., Cox, L.S., Nollen, N., Faseru, B., Okuyemi, K.S., Ahluwalia, J.S., Benowitz, N.L., and Tyndale, R.F. (2012a). CYP2B6 and bupropion's smoking cessation pharmacology: the role of hydroxybupropion. Clin. Pharmacol. Ther. *92*, 771–777.

Zhu, A.Z.X., Cox, L.S., Nollen, N., Faseru, B., Okuyemi, K.S., Ahluwalia, J.S., Benowitz, N.L., and Tyndale, R.F. (2012b). CYP2B6 and bupropion's smoking cessation pharmacology: the role of hydroxybupropion. Clin. Pharmacol. Ther. *92*, 771–777.

Zhu, A.Z.X., Zhou, Q., Cox, L.S., Ahluwalia, J.S., Benowitz, N.L., and Tyndale, R.F. (2014). Gene Variants in CYP2C19 Are Associated with Altered In Vivo Bupropion Pharmacokinetics but Not Bupropion-Assisted Smoking Cessation Outcomes. Drug Metab. Dispos. *42*, 1971–1977.

VITA

Jennifer Sager was born in Redmond, Washington in 1985. She attended high school at Holy Names Academy in Seattle, Washington prior to pursuing her undergraduate degrees in Biochemistry and Microbiology at the University of Washington.